

ISSN : 2165-4069(Online)

ISSN : 2165-4050(Print)



IJARAI

International Journal of
Advanced Research in Artificial Intelligence

Volume 4 Issue 6

www.ijarai.thesai.org

A Publication of
The Science and Information Organization



INTERNATIONAL JOURNAL OF
ADVANCED RESEARCH IN ARTIFICIAL INTELLIGENCE



THE SCIENCE AND INFORMATION ORGANIZATION

www.thesai.org | info@thesai.org

OAlster



Editorial Preface

From the Desk of Managing Editor...

Artificial Intelligence is hardly a new idea. Human likenesses, with the ability to act as human, dates back to Geek mythology with Pygmalion's ivory statue or the bronze robot of Hephaestus. However, with innovations in the technological world, AI is undergoing a renaissance that is giving way to new channels of creativity.

The study and pursuit of creating artificial intelligence is more than designing a system that can beat grand masters at chess or win endless rounds of Jeopardy!. Instead, the journey of discovery has more real-life applications than could be expected. While it may seem like it is out of a science fiction novel, work in the field of AI can be used to perfect face recognition software or be used to design a fully functioning neural network.

At the International Journal of Advanced Research in Artificial Intelligence, we strive to disseminate proposals for new ways of looking at problems related to AI. This includes being able to provide demonstrations of effectiveness in this field. We also look for papers that have real-life applications complete with descriptions of scenarios, solutions, and in-depth evaluations of the techniques being utilized.

Our mission is to be one of the most respected publications in the field and engage in the ubiquitous spread of knowledge with effectiveness to a wide audience. It is why all of articles are open access and available view at any time.

IJARAI strives to include articles of both research and innovative applications of AI from all over the world. It is our goal to bring together researchers, professors, and students to share ideas, problems, and solution relating to artificial intelligence and application with its convergence strategies. We would like to express our gratitude to all authors, whose research results have been published in our journal, as well as our referees for their in-depth evaluations.

We hope that this journal will inspire and educate. For those who may be enticed to submit papers, thank you for sharing your wisdom.

Editor-in-Chief

IJARAI

Volume 4 Issue 6 June 2015

ISSN: 2165-4069(Online)

ISSN: 2165-4050(Print)

©2013 The Science and Information (SAI) Organization

Editorial Board

Peter Sapaty - Editor-in-Chief

National Academy of Sciences of Ukraine

Domains of Research: Artificial Intelligence

Alaa F. Sheta

Electronics Research Institute (ERI)

Domain of Research: Evolutionary Computation, System Identification, Automation and Control, Artificial Neural Networks, Fuzzy Logic, Image Processing, Software Reliability, Software Cost Estimation, Swarm Intelligence, Robotics

Antonio Dourado

University of Coimbra

Domain of Research: Computational Intelligence, Signal Processing, data mining for medical and industrial applications, and intelligent control.

David M W Powers

Flinders University

Domain of Research: Language Learning, Cognitive Science and Evolutionary Robotics, Unsupervised Learning, Evaluation, Human Factors, Natural Language Learning, Computational Psycholinguistics, Cognitive Neuroscience, Brain Computer Interface, Sensor Fusion, Model Fusion, Ensembles and Stacking, Self-organization of Ontologies, Sensory-Motor Perception and Reactivity, Feature Selection, Dimension Reduction, Information Retrieval, Information Visualization, Embodied Conversational Agents

Liming Luke Chen

University of Ulster

Domain of Research: Semantic and knowledge technologies, Artificial Intelligence

T. V. Prasad

Lingaya's University

Domain of Research: Bioinformatics, Natural Language Processing, Image Processing, Robotics, Knowledge Representation

Wichian Sittiprapaporn

Maharakham University

Domain of Research: Cognitive Neuroscience; Cognitive Science

Yaxin Bi

University of Ulster

Domains of Research: Ensemble Learning/Machine Learning, Multiple Classification Systems, Evidence Theory, Text Analytics and Sentiment Analysis

Reviewer Board Members

- **AKRAM BELGHITH**
University Of California, San Diego
- **ALAA F. SHETA**
Electronics Research Institute (ERI)
- **Albert Alexander S**
Kongu Engineering College
- **Alexandre Bou nard**
Sensopia
- **Amir HAJJAM EL HASSANI**
Universit  de Technologie de Belfort-Monb liard
- **Amitava Biswas**
Cisco Systems
- **Anshuman Sahu**
Hitachi America Ltd.
- **Antonio Dourado**
University of Coimbra
- **Appasami Govindasamy**
- **ASIM TOKGOZ**
Marmara University
- **Babatunde Opeoluwa Akinkunmi**
University of Ibadan
- **Badre Bossoufi**
University of Liege
- **BASANT KUMAR VERMA**
JNTU
- **Basim Almayahi**
UOK
- **Bestoun S. Ahmed**
College of Engineering, Salahaddin University - Hawler (SUH)
- **Bhanu Prasad Pinnamaneni**
Rajalakshmi Engineering College; Matrix Vision GmbH
- **Chien-Peng Ho**
Information and Communications Research Laboratories, Industrial Technology Research Institute of Taiwan
- **Chun-Kit (Ben) Ngan**
The Pennsylvania State University
- **Daniel Ioan Hunyadi**
Lucian Blaga University of Sibiu
- **David M W Powers**
Flinders University
- **Dimitris Chrysostomou**
Production and Management Engineering / Democritus University of Thrace
- **Ehsan Mohebi**
Federation University Australia
- **Fabio Mercorio**
University of Milan-Bicocca
- **Francesco Perrotta**
University of Macerata
- **Frank AYO Ibikunle**
Botswana Int'l University of Science & Technology (BIUST), Botswana.
- **Gerard Dumancas**
Oklahoma Baptist University
- **Goraksh Vithalrao Garje**
Pune Vidyarthi Griha's College of Engineering and Technology, Pune
- **Grigoras N. Gheorghe**
Gheorghe Asachi Technical University of Iasi, Romania
- **Guandong Xu**
Victoria University
- **Haibo Yu**
Shanghai Jiao Tong University
- **Harco Leslie Hendric SPITS WARNARS**
Surya university
- **Ibrahim Adepoju Adeyanju**
Ladoke Akintola University of Technology, Ogbomosho, Nigeria
- **Imran Ali Chaudhry**
National University of Sciences & Technology, Islamabad
- **ISMAIL YUSUF**
Lamintang Education & Training (LET) Centre
- **Jabar H Yousif**
Faculty of computing and Information Technology, Sohar University, Oman
- **Jatinderkumar Ramdass Saini**
Narmada College of Computer Application, Bharuch
- **Jos  Santos Reyes**
University of A Coru a (Spain)
- **Krasimir Yankov Yordzhev**

- South-West University, Faculty of Mathematics and Natural Sciences, Blagoevgrad, Bulgaria
- **Krishna Prasad Miyapuram**
University of Trento
 - **Le Li**
University of Waterloo
 - **Leon Andretti Abdillah**
Bina Darma University
 - **Liming Luke Chen**
University of Ulster
 - **Ljubomir Jerinic**
University of Novi Sad, Faculty of Sciences, Department of Mathematics and Computer Science
 - **M. Reza Mashinchi**
Research Fellow
 - **Malack Omae Oteri**
jkuat
 - **Marek Reformat**
University of Alberta
 - **Md. Zia Ur Rahman**
Narasaraopeta Engg. College, Narasaraopeta
 - **Mehdi Bahrami**
University of California, Merced
 - **Mohamed Najeh LAKHOUA**
ESTI, University of Carthage
 - **Mohammad Haghighat**
University of Miami
 - **Mokhtar Beldjehem**
University of Ottawa
 - **Nagy Ramadan Darwish**
Department of Computer and Information Sciences, Institute of Statistical Studies and Researches, Cairo University.
 - **Nestor Velasco-Bermeo**
UPFIM, Mexican Society of Artificial Intelligence
 - **Nidhi Arora**
M.C.A. Institute, Ganpat University
 - **Olawande Justine Daramola**
Covenant University
 - **Parminder Singh Kang**
De Montfort University, Leicester, UK
 - **Peter Sapaty**
National Academy of Sciences of Ukraine

- **PRASUN CHAKRABARTI**
Sir Padampat Singhanian University
- **Qifeng Qiao**
University of Virginia
- **Raja sarath kumar boddu**
LENORA COLLEGE OF ENGINEERING
- **Rajesh Kumar**
National University of Singapore
- **Rashad Abdullah Al-Jawfi**
Ibb university
- **Reza Fazel-Rezai**
Electrical Engineering Department, University of North Dakota
- **Said Ghoniemy**
Taif University
- **Secui Dinu Calin**
University of Oradea
- **Selem Charfi**
University of Pays and Pays de l'Adour
- **Shahab Shamshirband**
University of Malaya
- **Sim-Hui Tee**
Multimedia University
- **Simon Uzezi Ewedafe**
Baze University
- **SUKUMAR SENTHILKUMAR**
Universiti Sains Malaysia
- **T C.Manjunath**
HKBK College of Engg
- **T V Narayana rao Rao**
SNIST
- **T. V. Prasad**
Lingaya's University
- **Tran Xuan Sang**
IT Faculty - Vinh University - Vietnam
- **Urmila N Shrawankar**
GHRCE, Nagpur, India
- **V Baby Deepa**
M. Kumarasamy College of Engineering (Autonomous),
- **Visara Urovi**
University of Applied Sciences of Western Switzerland
- **Vitus S.W. Lam**
The University of Hong Kong
- **VUDA SREENIVASARAO**

PROFESSOR AND DEAN, St.Mary's
Integrated Campus,Hyderabad.

- **Wei Zhong**
University of south Carolina Upstate
- **Wichian Sittiprapaporn**
Mahasarakham University
- **Yaxin Bi**
University of Ulster
- **Yuval Cohen**
Tel-Aviv Afeka College of Engineering

- **Zhao Zhang**
Deptment of EE, City University of Hong
Kong
- **Zhigang Yin**
Institute of Linguistics, Chinese Academy of
Social Sciences
- **Zne-Jung Lee**
Dept. of Information management, Huafan
University

CONTENTS

Paper 1: Yahoo!Search and Web API Utilized Mashup based e-Learning Content Search Engine for Mobile Learning

Authors: Kohei Arai

PAGE 1 – 7

Paper 2: Psychological Status Monitoring with Cerebral Blood Flow: CBF, Electroencephalogram: EEG and Electro-Oculogram: EOG Measurements

Authors: Kohei Arai

PAGE 8 – 15

Paper 3: Relations between Psychological Status and Eye Movements

Authors: Kohei Arai

PAGE 16 – 22

Paper 4: Mobile Device Based Personalized Equalizer for Improving Hearing Capability of Human Voices in Particular for Elderly Persons

Authors: Kohei Arai, Takuto Konishi

PAGE 23 – 27

Paper 5: Iris Compression and Recognition using Spherical Geometry Image

Authors: Rabab M. Ramadan

PAGE 28 – 34

Paper 6: Gram–Schmidt Process in Different Parallel Platforms

Authors: Genci Berati

PAGE 35 – 39

Paper 7: A Heuristic Approach for Minimum Set Cover Problem

Authors: Fatema Akhter

PAGE 40 – 45

Yahoo!Search and Web API Utilized Mashup based e-Learning Content Search Engine for Mobile Learning

Kohei Arai 1

Graduate School of Science and Engineering
Saga University
Saga City, Japan

Abstract—Mashup based content search engine for mobile devices is proposed. Mashup technology is defined as search engine with plural different APIs. Mash-up has not only the plural APIs, but also the following specific features, (1) it enables classifications of the contents in concern by using web 2.0, (2) it may use API from the different sites, (3) it allows information retrievals from both sides of client and server, (4) it may search contents as an arbitrary structured hybrid content which is mixed content formed with the individual content from the different sites, (5) it enabling to utilize REST, RSS, Atom, etc. which are formed from XML conversions. The mash-up should be a flexible search engine for any purposes of content retrievals. The proposed search system allows 3D space display of search menus with these peculiarities on Android devices. The proposed search system featuring Yahoo!search BOSS and Web API is also applied for e-learning content retrievals. It is confirmed that the system can be used for search a variety of e-learning content in concern efficiently.

Keywords—Mashup; API; web 2.0; mobile devices; e-learning content; content retrieval; Yahoo!saerch BOSS; Web API

I. INTRODUCTION

E-learning content retrievals with mobile terminals have not been done easily due to the fact that display size is not good enough for search as well as there are a variety of contents types, video, document, etc. On the other hand, mashup technology [1], [2] supported web 2.0 [3] allows gathering information of e-learning contents efficiently and effectively. Meanwhile, visualization of web contents has been well developed. Therefore, e-learning content search engine can be improved in terms of efficiently and effectively based on the aforementioned mashup technology and visualization tools¹.

Web API [4] based e-learning content search engine is developed with Yahoo!search BOSS (Build your Own Search Service) [5] which is called ELDOXEA: E-Learning Content Search Engine [6]-[10]. Not only major keyword, but also minor keywords derived from the descriptions and keywords in the header information of URL which is hit by the first major keyword are used for search. The search engine proposed here is ELDOXEA for mobile devices. One of the

disadvantages of mobile devices is relatively small size of display. Therefore, in particular, representation method for search results has to be considered for fitting the search result contents efficiently and effectively.

There are many web visualization tools. In particular, UNIX software of Natto view [11] and mashup based search engine with www visualization of Flowser² are sophisticated tools. With the reference to these software tools, the proposed e-learning content search engine is designed.

E-learning content search engine with web API based approach is proposed in the following section. Bing and Google API are additionally featured. Furthermore, thesaurus based search results prioritized method is featured. Application software tool for the search engine is described followed by implementation and some experimental results. Then concluding remarks are described with some discussions.

II. PROPOSED METHOD AND SYSTEM

A. Mashup Technology

Mashup is defined as a method for providing web services and applications based on combination of more than two web APIs. It allows improve usability by combining search results which are obtained from the different web APIs separately. Search results from web APIs, in general, in the form of XML or JSON [12]. Therefore, it is easy to combine the search results into one. The following four web APIs are used for the proposed search engine,

1) Yahoo!search: web URL search API

<http://search.yahooapis.jp/PremiumWebSearchService/V1/webSearch>

2) Yahoo!search: Image retrieval API

<http://search.yahooapis.jp/PremiumImageSearchService/V1/imageSearch>

3) Youtube Data API developed by Google Inc.

<http://gdata.youtube.com/feeds/api/videos>

4) Product Advertising API developed by Amazon.com, Inc.

<http://ecs.amazonaws.jp/onca/xml>

¹
https://supportcenter.checkpoint.com/supportcenter/portal?eventSubmit_doGoviewsolutiondetails=&solutionid=sk30765

² <http://www.flowser.com/>

B. Search Result Display

In order to display search results in a comprehensive manner, the following four candidate models, helix, star, star helix and star slide are trade-off.

One of important roles of the displaying search results is to show the priority of the results. From the top to bottom priority, “helix model” of displaying method allows priority representation from the top to the bottom of the display positions in a spiral order. It, however, is not appropriate displaying method because there are many types of the search results, document, URL, image, etc. Therefore, it is complicated and overlapped so much among the search result types.

Another model of the search result representation is “star model”. This model is adopted by Flowser. The search results are classified by content types of nodes. From the top node to the node in concern, the length of link between both shows priority. It, however, is not so easy to see because the nodes are located in the 3D domain of the display positions.

Star-Helix model combines the aforementioned two models, star and helix models. It, however, is still difficult to see the priority. Star-Slide model of search result display method is the most appropriate model as shown in Fig.1.



Fig. 1. Star-Slide Model

In the Fig.1, star shows search result types while smile marks shows contents (URLs). From the top to bottom priority, “star-slide model” of displaying method allows priority representation from the top to the bottom of the display positions. It has to be displayed onto mobile device displays in a 3D CG representation. Away3D [9] is used for this purpose. There are a plenty of 3D CG representation software tools, OpenGL, ADOBE AIR, etc. under the programming language of Java, Objective-C, etc. In particular, Away3D is used on the ADOBE AIR (Stage3D) of Action Script as a library. The geometric relation between camera and object is shown in Figure 2 as well as rendering of object together with staging device.

C. LEDOXEA

LEDOXEA is mobile devices version of ELDOXEA: E-Learning Content Search Engine. After the activation of LEDOXEA, initial image of start-up is displayed onto mobile device display as shown in Fig.3 (a). Immediately after this, key-in is available with screen keyboard as shown in Fig.3 (b).

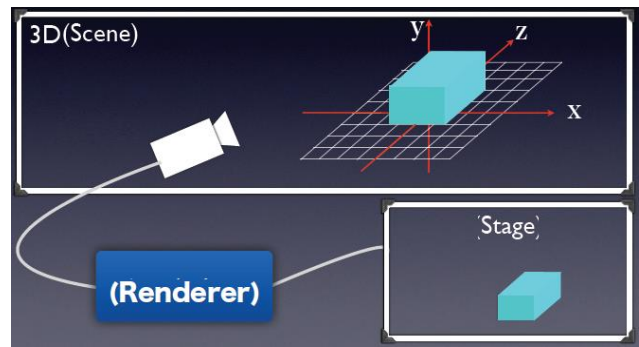


Fig. 2. Geometric relation among 3D view port, camera, object and 3D area definition for rendering



(a) Initial image



(b) Key-in image

Fig. 3. Display image

When users key-in their keyword in the dialog box as shown in Fig.4 (a), then users press the search button for retrievals. After that, users get their search results as shown in Fig.4 (b).



(a) Search initiate image

(b) Search results

Fig. 4. Display image

In this case, five content types and icons of search results of URLs appear in order of their priorities. Five content types

are (1) search engines such as Google, Yahoo search, (2) moving picture contents such as YouTube, (3) document contents, (4) image contents and (5) general purpose content search such as Amazon.com which are shown in Fig.5.



Fig. 5. Content types for search

Search results can be moved up and down when users swipe in the vertical direction as shown in Fig.6 (a). Therefore, search result content can be seen one by one. When users would like to see other types of search results of contents, they have to swipe the display in the horizontal direction as shown in Fig.6 (b).



Fig. 6. Move up and down as well as ration with vertical swipe and horizontal swipe

The icon sizes are different by content type for representation of the search results in 3D space on the display as shown in Fig.7. When users tap the title summary which is located the bottom of the display as shown in Fig.8, then users may take a look at the search result of contents through browser or external applications. There is “back button” for getting back to the previous display image after the referencing the search result contents.

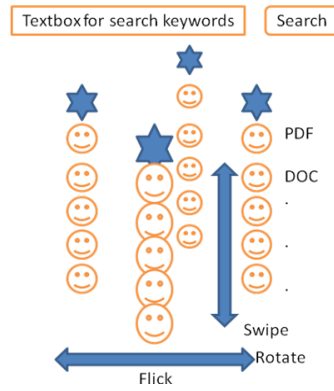


Fig. 7. 3D display of the icon during flick, swipe, and rotational operations

Search content types are rotated when users swipe the content type icons. These rotation angles can be calculated as shown in Fig.8.

Icon operations with swipe actions are illustrated in Fig.9. Swipe action in the vertical direction allows search results candidate selections. Meanwhile, swipe action in the horizontal direction allows content type selections. These can be done through camera position changes in 3D space in the CG space of Away 3D.

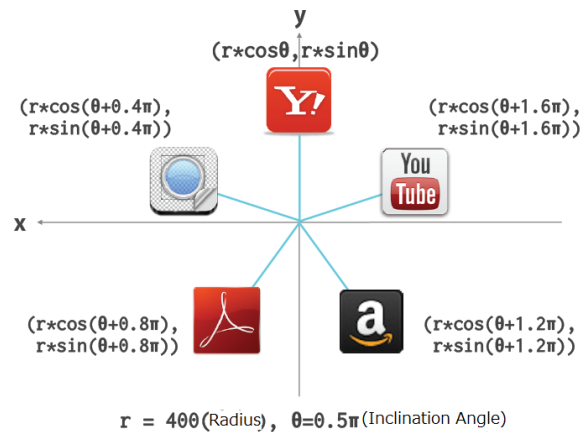


Fig. 8. Rotation angle of the five icons

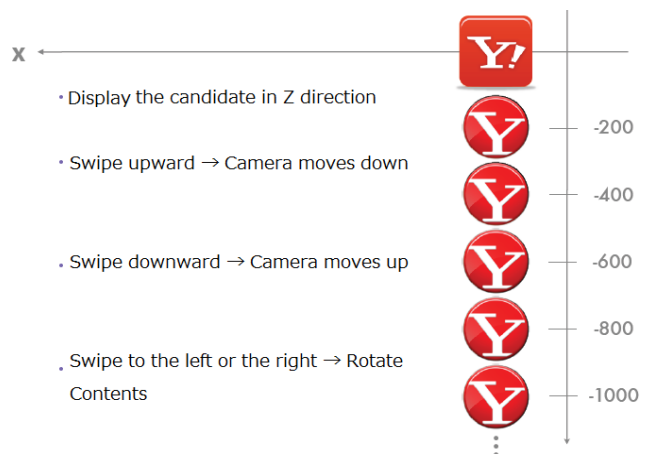


Fig. 9. icon manipulations utilizing swipe operations

A. LEDOXEA version 2

From the web site stability or availability points of view, the proposed search engine employed Bing API instead of Yahoo!Search. Display image layout is shown in Fig.10.



Fig. 10. Example of search result display with Bing API based LEDOXEA

YouTube (moving pictures), Amazon site, ADOBE content (documents), and Image contents are available for search. These are common to the previous LEDOXEA featuring Yahoo!Search. Search results are aligned in the order of their priority. When users choose one of the icon of search result, then the hyperlink of the search result appears on the bottom of the screen. Also, users get the contents when they click the hyperlinked search result. This is referred to the version 1 of LEDOXEA hereafter.

B. Thesaurus Approach

In order to improve effectiveness of search engine, not only major keyword but also minor keywords can be used for e-learning content search. In addition to the dialog box, thesaurus search is available for the LEDOXEA version 2. Example of the keyword input image display is shown in Fig.11 (a). There is the dialog box for thesaurus search which is situated just under the dialog box for the major keyword. Example of the image of thesaurus search results is shown in Fig.11 (b).



Fig. 11. Thesaurus search featured LEDOXEA

In this example, “Wikipedia” of thesaurus search engine is selected. Appropriate minor keywords are available as the thesaurus search results. Therefore, much appropriate e-learning content search can be done with major and minor keywords.

Fig.12 (a) shows the other thesaurus search result by keyword types abstract, history, word, footnote, reference, related site, other link are available for thesaurus search. Also, several languages are available for search by clicking the bottom button. Fig.12 (b) shows an example of e-learning content search with the major keyword of “Java”. When users key-in the minor keyword of “文法” (grammar in English) in the dialog box of thesaurus search engine, then they can get the much appropriate search results rather than LEDOXEA version 1 (without thesaurus engine).



(a)Thesaurus search keyword (b)Example for “Java”

Fig. 12. Search keyword types selection for thesaurus search and example of e-learning content search with the major keyword of “Java”

Fig.13 (a) shows an example of search image when users key-in the major keyword “Java” and the minor keyword “grammar” for the thesaurus search engine while Fig.13 (b) shows an example of search image when users key-in the major keyword “Java” and the minor keyword “question and answer” for the thesaurus search engine.



(a) minor keyword “grammar” (b) minor keyword “question and answer”

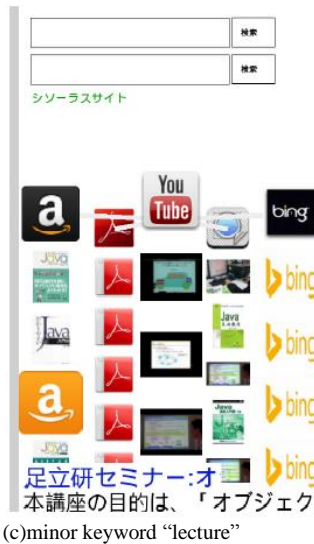


Fig. 13. Examples of e-learning content search results with major keyword of “Java” and minor keywords, “grammar” and “Question and answer” as well as “Lecture” for thesaurus search results

On the other hand, Fig.13 (c) shows an example of search image when users key-in the major keyword “Java” and the minor keyword “question and answer” for the thesaurus search engine.

Thus users can take a look at the search results from the top to the bottom priority of the search results by content type by type. Also, the highest priority of search result appears at the bottom of the image with hyperlink. In this example, the book on Java language specifically programming grammar is greatly featured is shown as search result. Users may input minor keywords on their own. Users also may use thesaurus search engine. It is totally up to users.

III. EXPERIMENTS

A. Implementation

Implementation of the proposed software is done with FlashProfessionalCS6 on Android 4.0.3. In order to publicize of the implemented source code based on Action Script, the following library, framework, image files are executed,

- 1) Away3D 4.1.0 Alpha (away3d-core-fp11 4 1 0 Alpha.swc)[8]
- 2) Bulk Loader (bulk loader.swc)[13]
- 3) As3 Crypto (as3crypto.swc)[14]
- 4) norm-top.png (128x128px of png file)
- 5) norm.png (128x128px of png file)
- 6) img-top.png (128x128px of png file)
- 7) img.png (128x128px of png file)
- 8) doc-top.png (128x128px of png file)
- 9) doc.png (128x128px of png file)
- 10)mv-top.png (128x128px of png file)
- 11)ama-top.png (128x128px of png file)
- 12)ama.png (128x128px of png file)
- 13)deflmgXML.xml (XML file which are acquired with Y! Image Retrieval API)

These source code package are provided by the URL of Github

<https://github.com/legnoh/ledoxea>

A.1 Main.as(ActionScript3.0)

```
package {
import flash.display.BitmapData;
import flash.display.Sprite;
import flash.display.SimpleButton;
import flash.events.*;
import flash.filesystem.StorageVolumeInfo;
import flash.geom.Matrix;
import flash.geom.Vector3D;
import flash.text.*;
import flash.utils.ByteArray;
import flash.utils.escapeMultiByte;
import flash.net.URLLoader;
import flash.net.URLRequest;
import flash.ui.Keyboard;
import flash.desktop.NativeApplication;
import away3d.containers.*;
import away3d.entities.*;
import away3d.materials.TextureMaterial;
import away3d.primitives.*;
```

On the other hand, XML file is created which is defined Android application software. Meanwhile, used APIs are Yahoo!JAPAN Web Retrieval API, Yahoo!JAPAN Image Retrieval API, YouTube Data API, and Amazon Product Advertising API.

B. Experiments

Fig.14 shows an example of display image of smartphone of which the proposed search engine is implemented (github.com/legnoh/ledoxea).

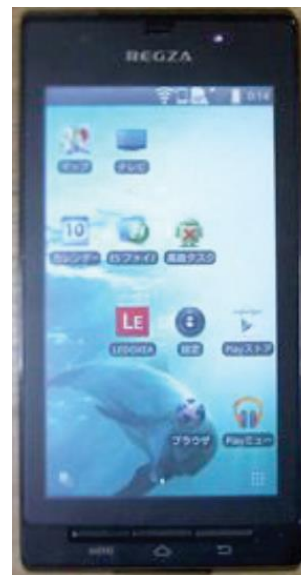


Fig. 14. Example of display image of smartphone of which the proposed search engine is implemented (github.com/legnoh/ledoxea)

“LE” of icon denotes LEDOXEA.



Fig. 15. Example of linked retrieved results (Merged contents of Yahoo search results with the other retrieved contents)

Twenty of university students (information science department) participate the experiments. They use the LEDOXEA and then they evaluate the LEDOXEA. Their comments and suggestions are as follows,

- 1) *It is comfortable to use the LEDOXEA because operability using swipe operations, smooth rendering, usability of Android tablet terminals, WWW visualizations are excellent,*
- 2) *Search results can be seen simultaneously,*
- 3) *PDF data and YouTube of search results can be accessible from the LEDOXEA directly,*
- 4) *Appropriate e-learning contents can be retrieved efficiently with a single keyword.*
- 5) *Prioritizing the search results is excellent because the most appropriate e-learning content can be found easily,*
- 6) *Five e-learning contents can be seen simultaneously with a single keyword,*
- 7) *Still pictures as well as moving pictures are displayed their thumbnail, it is comprehensive.*

IV. CONCLUSION

Mashup based content search engine with mobile terminals is proposed. Mashup technology is defined as search engine with plural different APIs. Mash-up has not only the plural APIs, but also the following specific features. it enables classifications of the contents in concern by using web 2.0, it may use API from the different sites, it allows information retrievals from both sides of client and server, it may search contents as an arbitrary structured hybrid contents which is mixed contents formed with the individual contents from the different sites, it enabling to utilize REST, RSS, Atom, etc. which are formed from XML conversions.

Although mashup allows content search which is same as portal, mashup has the aforementioned different features from portal. Therefore, mash-up is possible to create more flexible search engine for any purposes of content retrievals. The

search system which is proposed here is that make it possible to control the graph in the 3D space display with these peculiarity on Android devices. The proposed search system is applied for e-learning content retrievals. It is confirmed that the system enables to search a variety of content in concern efficiently.

It is found that users can take a look at the search results from the top to the bottom priority of the search results by content type by type. Also, the highest priority of search result appears at the bottom of the image with hyperlink. In this example, the book on Java language specifically programming grammar is greatly featured is shown as search result. Users may input minor keywords on their own. Users also may use thesaurus search engine. It is totally up to users.

ACKNOWLEDGMENT

The author would like to thank Mr. Ryoma Kai and Mr. Yohei Nishiguchi for their effort to the implementation and the experiment.

REFERENCES

- [1] Ahmet Soylu, Felix Mödritscher, Fridolin Wild, Patrick De Causmaecker, Piet Desmet. 2012. "Mashups by Orchestration and Widget-based Personal Environments: Key Challenges, Solution Strategies, and an Application." Program: Electronic Library and Information Systems 46 (4): 383-428.
- [2] Endres-Niggemeyer, Brigitte ed. 2013. Semantic Mashups. Intelligent Reuse of Web Resources. Springer. ISBN 978-3-642-36402-0
- [3] O'Reilly, T., 2005. What is Web 2.0. Design Patterns and Business Models for the Next Generation of Software, p. 30
- [4] Benslimane, D.; Dustdar, S.; Sheth, A. (2008). "Services Mashups: The New Generation of Web Applications". *IEEE Internet Computing* 10 (5): 13-15. doi:10.1109/MIC.2008.110
- [5] Tuesday, August 17th, 2010 (2010-08-17). "As Bing Takes Over Yahoo Search, SearchMonkey Dies, BOSS Is No Longer Free, But Site Explorer Still Works". TechCrunch. Retrieved 2012-09-18.
- [6] Kohei Arai, Mash-up based content search engine for mobile devices, International Journal of Advanced Research in Artificial Intelligence, 2, 5, 39-43, 2013.
- [7] Kohei Arai and Tolle Herman, Module based content adaptation of composite e-learning content for delivering to mobile learners, International Journal of Computer Theory and Engineering, 3, 3, 382-387, 2011.
- [8] Kohei Arai, Herman Tolle, Efficiency improvements of e-learning document search engine for mobile browser, International Journal of Research and Reviews on Computer Science, 2, 6, 1287-1291, 2011.
- [9] K.Arai, T.Herman, Efficiency improvement of e-learning document search engine for mobile browser, International Journal of Research and review on Computer Science, 2, 6, 1287-1291, 2012.
- [10] K.Arai, T.Herman, Video searching optimization with supplemental semantic keyword for e-learning video searching, International Journal of Research and Review on Computer Science, 3, 3, 1640-1644, 2012.
- [11] H. Shiozawa, K. Okada, Y. Matsushita: 3D Interactive Visualization for Inter-Cell Dependencies of Spreadsheets, Proc. IEEE InfoVis '99, pp. 79-82, Oct. 1999.
- [12] Douglas Crockford (July 2006). "IANA Considerations". *The application/json Media Type for JavaScript Object Notation (JSON)*. IETF. sec. 6. RFC 4627. <https://tools.ietf.org/html/rfc4627#section-6>. Retrieved October 21, 2009.

AUTHORS PROFILE

Kohei Arai He received BS, MS and PhD degrees in 1972, 1974 and 1982, respectively. He was with The Institute for Industrial Science and Technology of the University of Tokyo from April 1974 to December 1978 and also was with National Space Development Agency of Japan from

January, 1979 to March, 1990. During from 1985 to 1987, he was with Canada Centre for Remote Sensing as a Post Doctoral Fellow of National Science and Engineering Research Council of Canada. He moved to Saga University as a Professor in Department of Information Science on April 1990. He was a councilor for the Aeronautics and Space related to the Technology Committee of the Ministry of Science and Technology during from 1998 to

2000. He was a councilor of Saga University for 2002 and 2003. He also was an executive councilor for the Remote Sensing Society of Japan for 2003 to 2005. He is an Adjunct Professor of University of Arizona, USA since 1998. He also is Vice Chairman of the Commission-A of ICSU/COSPAR since 2008. He wrote 33 books and published 500 journal papers.

Psychological Status Monitoring with Cerebral Blood Flow: CBF, Electroencephalogram: EEG and Electro-oculogram: EOG Measurements

Kohei Arai 1

Graduate School of Science and Engineering
Saga University
Saga City, Japan

Abstract—Psychological status monitoring with cerebral blood flow (CBF), EEG and EOG measurements are attempted. Through experiments, it is confirmed that the proposed method for psychological status monitoring is valid. It is also found correlations among the amplitudes of peak alpha and beta as well as gamma frequency of EEG signals and EOG as well as cerebral blood flow. Therefore, psychological status can be monitored with either EEG measurements or cerebral blood flow and EOG measurements.

Keywords—Cerebral Blood Flow; CBF; EEG; EOG; psychological status

I. INTRODUCTION

Psychological status monitoring is getting much important for health care. Eye based psychological status monitoring is proposed and applied to a variety of fields such as Electric Wheel Chair control, e-learning system, etc.[1]-[22].

The methods and measuring instruments are proposed and well developed now a day. Relations among the psychological status monitored with cerebral blood flow (CBF), EEG (Electroencephalogram: EEG) and EOG (Electro-oculogram: EOG) measurements are not clarified. EEG sensor used to be affected by sounding noises. In such case EOG or CBF is useful. Furthermore, CBF is very expensive compared to the other two. If relations among CBF, EEG and EOG are clarified, then EEG and EOG can be used instead of CBF. There is no previous paper which deals with the relation among CBF, EEG and EOG.

In order to clarify the relations, experiments are conducted with patients through rhythm gaming and adding gaming. When the patients play rhythm game, in general, psychological statuses of the patients are calm and relax while psychological statuses of the patients are severe and irritated when they play adding game. Through the experiments, this paper intends to clarify the relations. Furthermore, appropriate monitoring method and system as well as measuring instruments for psychological status is clarified.

The paper is organized as follows. First, the method and procedure for psychological status monitoring is described followed by some experimental methods and procedures together with experimental results. Then some concluding remarks are described with some discussions.

II. METHOD AND PROCEDURE FOR PSYCHOLOGICAL STATUS MONITORING

EEG and EOG sensors of ZA¹ manufactured by Pro-Assist Co. Ltd. is used in experiments together with Near Infrared: NIR Spectroscopy (NIRS) of HOT 121-B manufactured by Hitachi Co. Ltd. for cerebral blood flow measurements. Table 1 and 2 show the major specifications of the EEG and EOG sensors of ZA and HOT 121-B of NIRS.

TABLE I. MAJOR SPECIFICATION OF EEG AND EOG MEASURING INSTRUMENT NAMED "ZA"

Electrodes	EEG and EOG
AD_converter	12_bit
Sampling_Frequency	128(kHz)
Band_Width	Brain_Wave:0.5-40Hz&Eye_Vol.:0.5-10Hz

TABLE II. MAJOR SPECIFICATION OF CEREBRAL BLOOD FLOW (CBF) MEASURING INSTRUMENT, HOT 121B

Sampling	100ms
Wave_Length	810nm
Repetition_Cycle	2kHz
Temp.Sensor	±1 degree C
Acceleration_Sensor	±2G
EMI	VCC-1_Class B
Application	Cerebral blood flow (left and &right), heart rate, LF/HF, Attitude

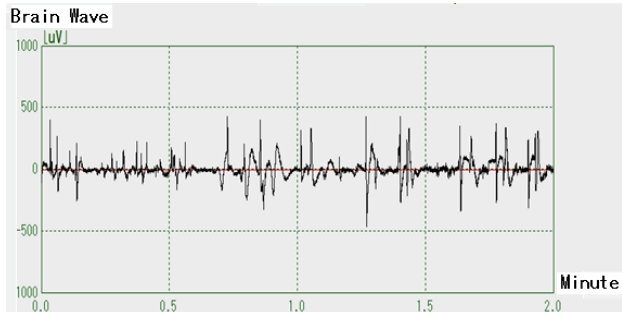
In Table 2, LF/HF denotes the ratio of Sympathetic to Parasympathetic which is called heart rate changing index. Sympathetic is dominant when patients are in irritated, active and having stress status. Therefore, LF/HF is increased in such time period. On the other hand, LF/HF is decreased when patients are in relaxing, taking a rest, and sleeping status because parasympathetic is dominant in such time period.

The experiments are conducted with 5 patients. In the experiments, each patient takes a rest for 1 minute and then plays for 1 minute with three games; adding game, rhythm game and breakout destroy game separately. It is suspected that most of patients are in relax status when they playing with rhythm game while are in irritating status when they plays with adding game and breakout destroy game. They have to have an instruction on how to play the games before getting start a set of experiment (1 minute for a rest and then 1 minute

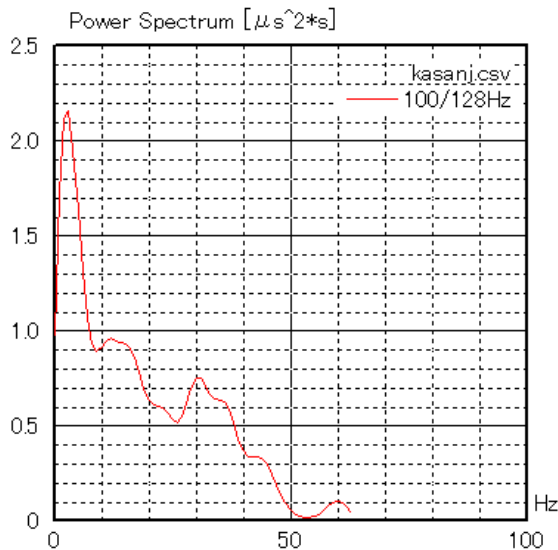
¹ ZA is the type name of the measuring instrument.

for gaming). They have to have 15 sets of experiment each. All sets of experiment is finished within a hour.

EEG data is filtered by low pass filter with cut off frequency of 50 Hz (6dB octave) for noise removals. After that FFT is applied to the filtered EEG. One of the examples is shown in Figure 1.



(a)Original EEG data
Data 128 (11648 - 11775) Smooth 10
Unfiltered



(b)Frequency component

Fig. 1. Examples of EEG and its frequency component

Usually, frequency components of 0-4 Hz, 4-8 Hz, 8-12 Hz, 12-40 Hz are named delta, theta, alpha and beta frequencies. In particular, alpha frequency component is dominant when users are in relaxing status while beta frequency component is large when they are in irritating status. When their EEG data is acquired, they have to attach electrodes on their forehead. This is the same thing for EOG measurements. They have to attach electrodes at the end of their eyes.

EOG data, on the other hand, show eye movement behavior which is reflected users' psychological status. Namely, EOG data is calm when they are in relaxing status while EOG data varied rapidly and quickly when they are in irritating status. Figure 2 shows an example of EOG data. From the data, eye movement speed can be analyzed.

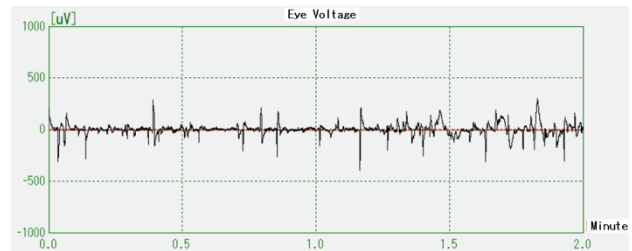


Fig. 2. Example of EOG data

Meanwhile, cerebral blood flow data shows varied rapidly and quickly when they are in irritating status while cerebral blood flow data shows calm when they are in relaxing status. It is expected that then they play with adding game, they are used to in an irritating status while they are in relaxing status when they play with rhythm game.

Figure 3 shows an example of acquired cerebral blood flow data. There are two data of cerebral blood flows, left brain (Red colored line in Figure 3) and right brain (Blue colored line in Figure 3). Also, left and right heart rate is acquired with HOT 121-B sensor. In meantime, LF/HF of right brain and left brain are also measured.

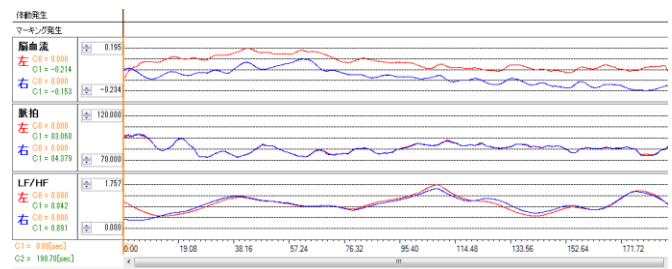
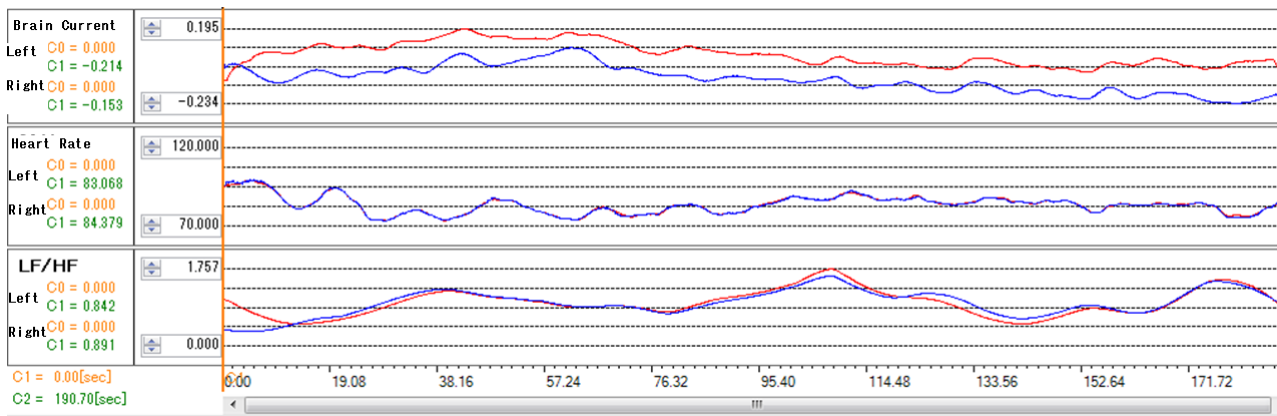


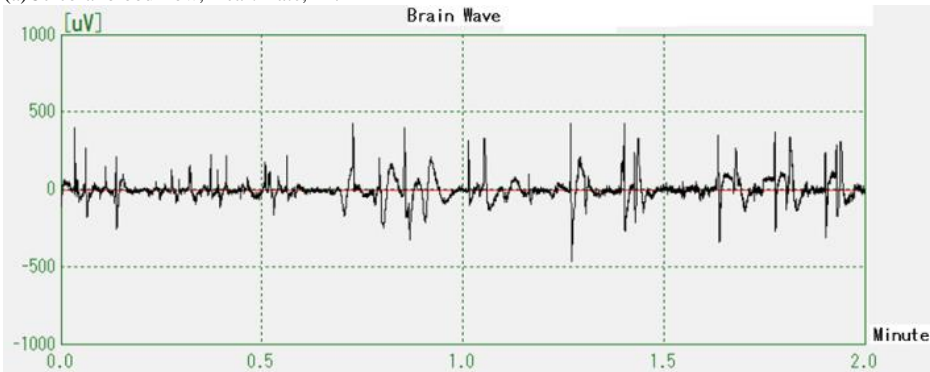
Fig. 3. shows an example of acquired cerebral blood flow data

III. EXPERIMENTAL RESULTS

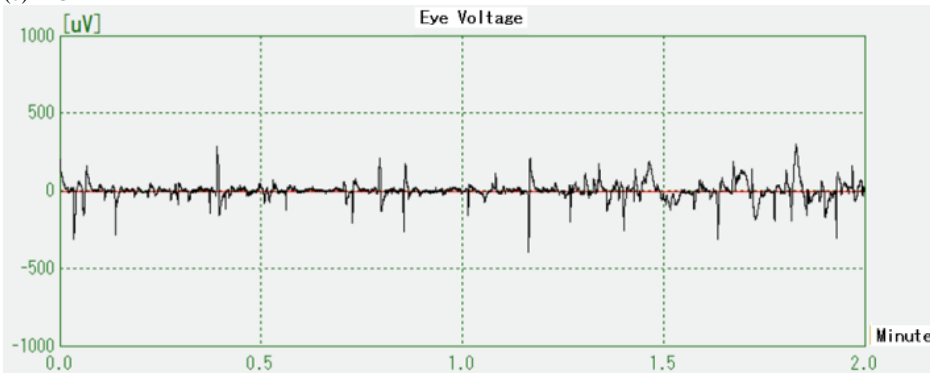
One of the typical measured data of cerebral blood flow, heart rate, LF/HF of one of the patients is shown in Figure 4 (a) together with EEG in Figure 4 (b) and EOG in Figure 4 (c). During the first half time, the patient takes a rest and plays rhythm game during the second half time period. As shown in Figure 4, there is not so large difference of the measured data between the first and the second half time periods. Therefore, most of the patients are in relaxing status when they play rhythm game.



(a) Cerebral blood flow, Heart Rate, LF/HF



(b) EEG



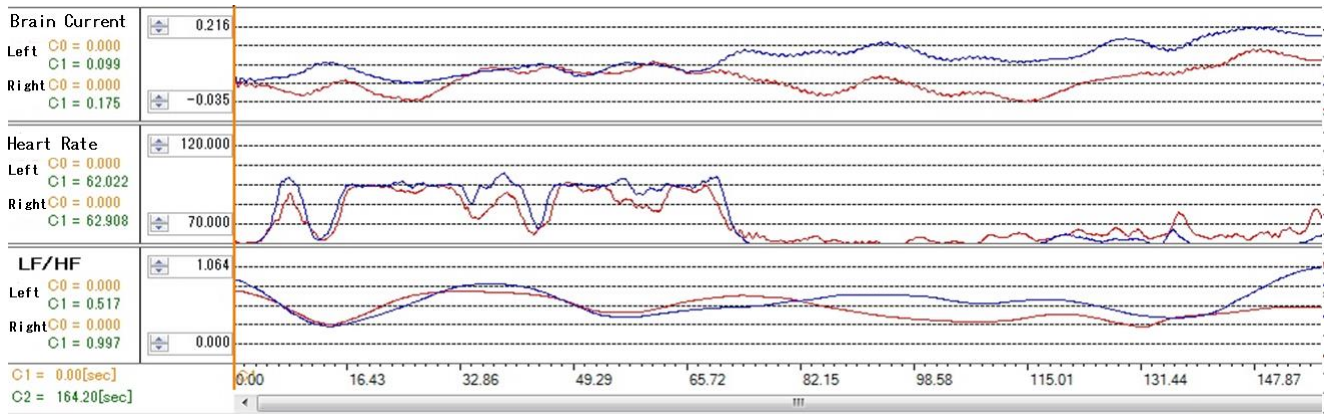
(c) EOG

Fig. 4. Measured data when the typical patient plays Rhythm Game

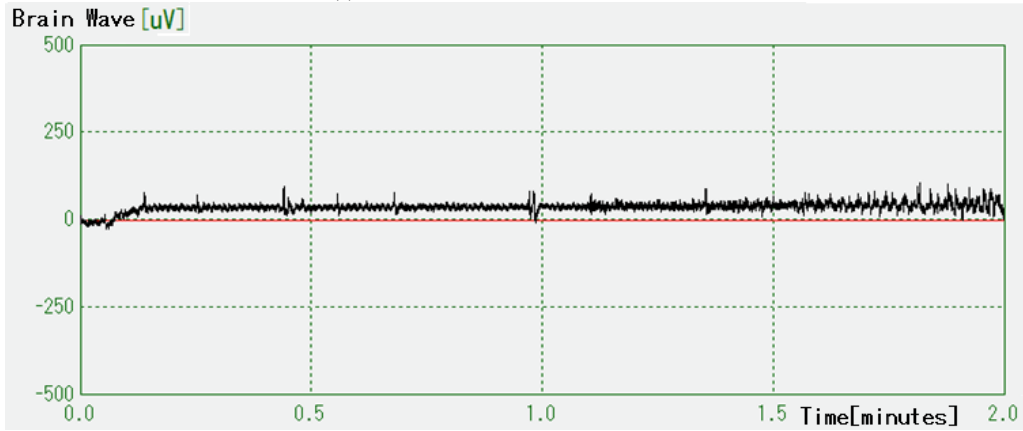
One of the typical measured data of cerebral blood flow, heart rate, LF/HF of one of the patients is shown in Figure 5 (a) together with EEG in Figure 5 (b) and EOG in Figure 5 (c). During the first half time, the patient takes a rest and plays adding game during the second half time period. As shown in Figure 5, there is relatively large difference of the measured

data between the first and the second half time periods. Therefore, most of the patients are in irritating status when they play adding game.

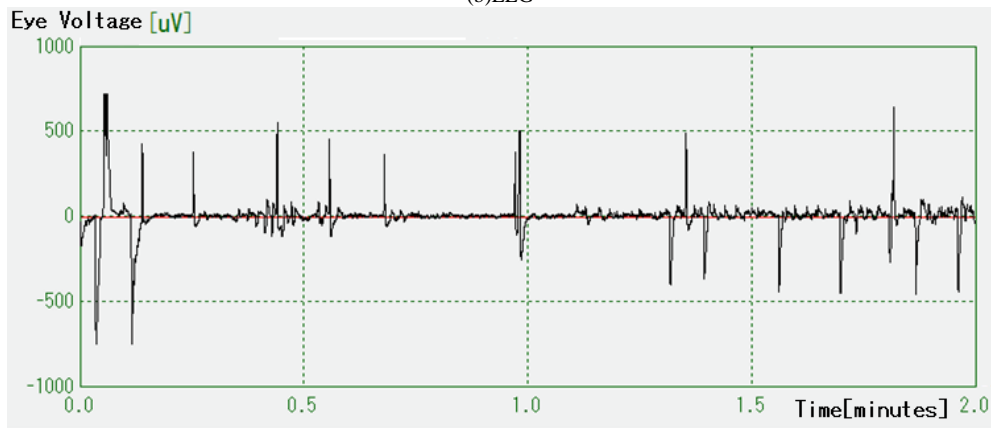
Meanwhile, frequency component of the measured EEGs when the patient plays rhythm game is shown in Figure 6 (a) while that for adding game is shown in Figure 6 (b).



(a)Cerebral blood flow, Heart Rate, LF/HF



(b)EEG



(c)EOG

Fig. 5. Measured data when the typical patient plays Adding Game

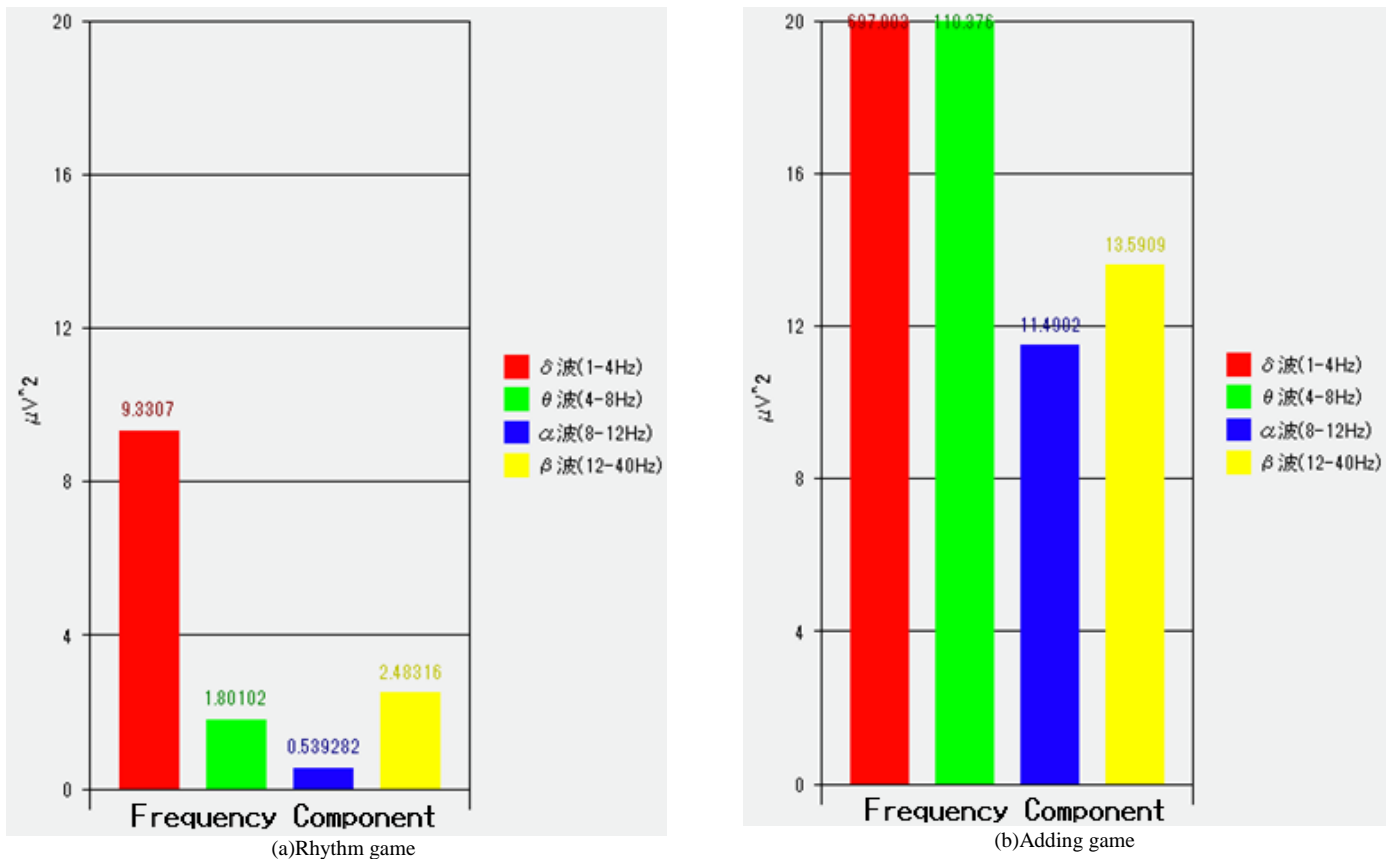


Fig. 6. Frequency component of EEGs when the patient plays rhythm game and adding game

TABLE III. FREQUENCY COMPONENTS OF THE MEASURED EEGS WHEN THE PATIENT PLAYS RHYTHM GAME AND ADDING GAME

Game	Rhythm	Adding
δ	697.003	9.3307
θ	110.376	1.80102
α	11.4002	0.53928
β	13.5909	2.48316

As shown in Table 3, alpha wave is relatively small in comparison to beta wave when the patient plays adding game rather than rhythm game.

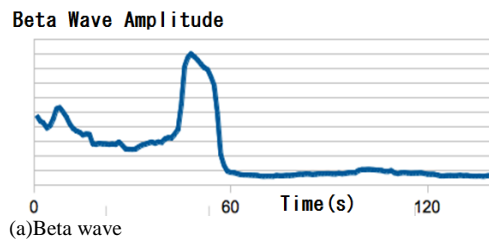
The amplitudes of peak alpha frequency, peak beta frequency, as well as peak gamma frequency (more than 30Hz) are used to be evaluated as psychological status indexes. These are used to be highly correlated to cerebral blood flow, heart rate, and LF/HF. The amplitudes of peak beta frequency and peak gamma frequency together with EOG of the patient when he plays rhythm game are plotted in Figure 7 (a), (b), and (c), respectively. EOG is highly correlated to the amplitudes of beta wave and gamma wave as shown in Figure 8. Correlation coefficients between EOG and beta wave amplitude is around 0.77 while that between EOG and gamma wave is 0.89, respectively. Therefore, it implies that the patient is irritated and stressed because his eyes move so rapidly and quickly.

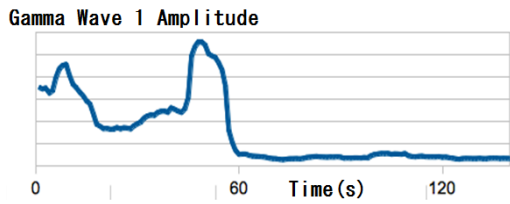
On the other hand, the amplitudes of peak beta frequency and right cerebral blood flow of the patient when he plays

rhythm game are plotted in Figure 9 (a), and (b), respectively. Right cerebral blood flow is correlated to the amplitudes of beta wave as shown in Figure 9 (c). Correlation coefficients between right cerebral blood flow and beta wave amplitude is around 0.45.

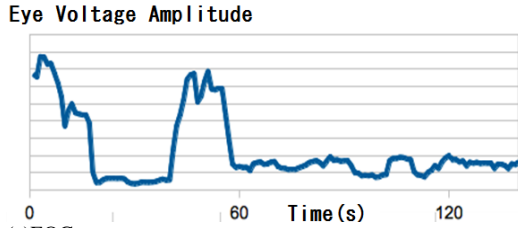
Meanwhile, Figure 10 (a) and (b) shows amplitudes of EEG of gamma frequency components and cerebral blood flow when the patient plays breakout game as well as correlations between cerebral blood flow and EEG of gamma frequency (Figure 10 (c)). Correlation coefficients between right cerebral blood flow and beta wave amplitude of EEG is around 0.81.

For the breakout game, in general, CBF is increased together with beta and gamma waves while EOG signal amplitude is relatively large. For the adding game, beta wave is increased while EOG signal amplitude is relatively small. On the other hand, CBF is decreased together with gamma wave while EOG signal amplitude is comparatively small for the rhythm game.



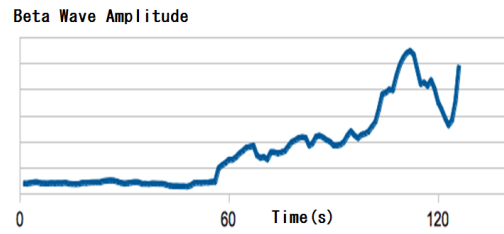


(b)Gamma wave

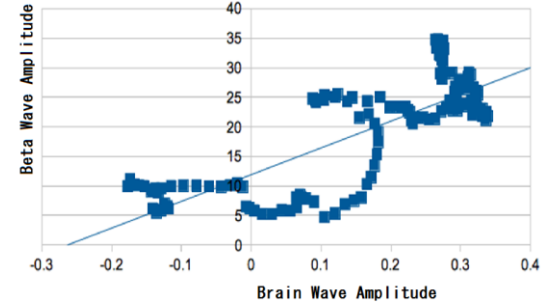


(c)EOG

Fig. 7. Amplitudes of EEG of beta and gamma frequency components when the patient plays rhythm game

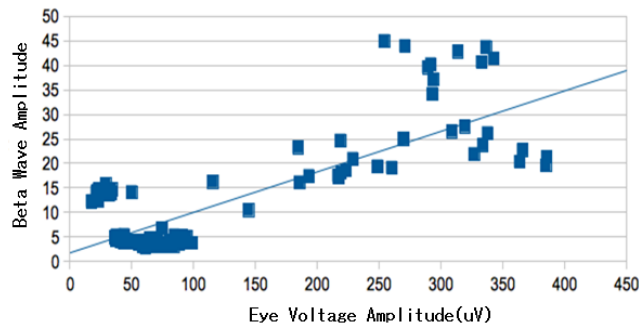


(b)Beta wave

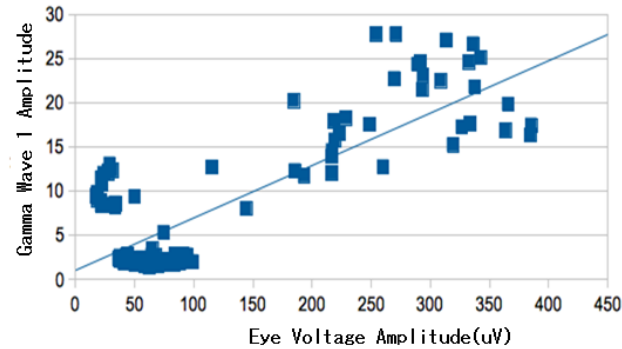


(c)Correlation

Fig. 9. Amplitudes of EEG of beta frequency components and cerebral blood flow when the patient plays adding game as well as correlations between cerebral blood flow and EEG of beta frequency

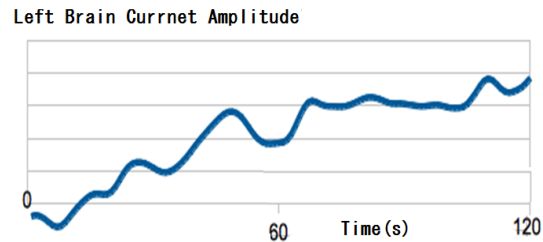


(a)Beta wave

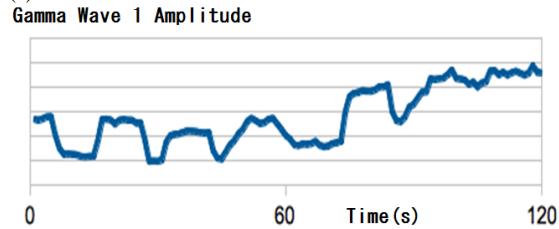


(b)Gamma wave

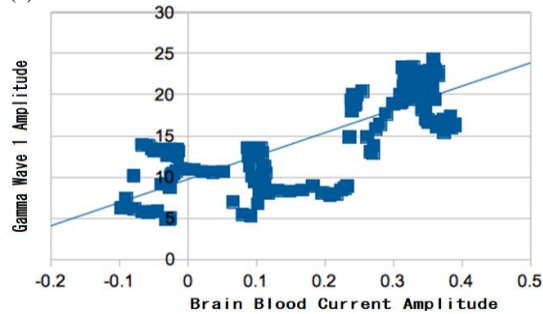
Fig. 8. Correlations between EOG and EEG of beta wave as well as gamma wave



(a)Left CBF

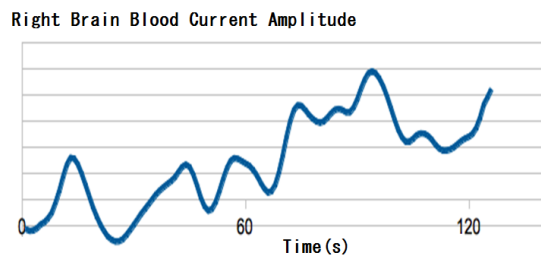


(b)Gamma wave



(c)Correlation between CBF and gamma wave of EEG

Fig. 10. Amplitudes of EEG of gamma frequency components and cerebral blood flow when the patient plays breakout game as well as correlations between cerebral blood flow and EEG of gamma frequency



(a)Cerebral blood flow

As the experimental results, it is found that the followings,

REFERENCES

A. Breakout game:

1) three patients out of five patients show high correlations between CBF and gamma wave of frequency component of EEG signals

2) two patients out of five patients show relatively high correlation between CBF and beta wave of frequency component of EEG signals

B. Adding game:

1) Two patients out of five patients show comparatively high correlation between CBF and beta wave of frequency component of EEG signals

C. Rhythm game:

1) Three patients out of four patients show high correlation between EOG signal amplitude and beta/gamma frequency component of EEG signals

2) Two patients out of four patients show relatively high correlation between CBF and gamma wave of frequency component of EEG

IV. CONCLUSION

Psychological status monitoring with cerebral blood flow (CBF), EEG (EEG) and EOG (EOG) measurements are attempted. Through experiments, it is confirmed that the proposed method for psychological status monitoring is valid. It is also found correlations among the amplitudes of peak alpha and beta EEGs and EOG as well as cerebral blood flow. Therefore, psychological status can be monitored with either EEG measurements or cerebral blood flow and EOG measurements.

It is found that three patients out of five patients show high correlations between CBF and gamma wave of frequency component of EEG signals for breakout game, two patients out of five patients show relatively high correlation between CBF and beta wave of frequency component of EEG signals for breakout game, two patients out of five patients show comparatively high correlation between CBF and beta wave of frequency component of EEG signals for adding game, three patients out of four patients show high correlation between EOG signal amplitude and beta/gamma frequency component of EEG signals for rhythm game, two patients out of four patients show relatively high correlation between CBF and gamma wave of frequency component of EEG for rhythm game.

From these experimental results, it may conclude that these EEG, EOG, and CBF are highly correlated. Therefore, these measurements can be used alternatively. CBF measuring instruments are relatively expensive than the others. EEG and EOG sensors are very sensitive to the surrounding noises rather than the others.

ACKNOWLEDGMENT

The author would like to thank Mr. Tsuyoshi Miyazaki for his effort to the experiment.

- [1] Djoko Purwanto, Ronny Mardiyanto and Kohei Arai, Electric wheel chair control with gaze detection and eye blinking, *Artificial Life and Robotics*, AROB Journal, 14, 694,397-400, 2009.
- [2] Kohei Arai and Makoto Yamaura, Computer input with human eyes only using two Purkinje images which works in a real time basis without calibration, *International Journal of Human Computer Interaction*, 1,3, 71-82,2010
- [3] Kohei Arai, Ronny Mardiyanto, A prototype of electric wheel chair control by eye only for paralyzed user, *Journal of Robotics and Mechatronics*, 23, 1, 66-75, 2010.
- [4] Djoko Purwanto, Ronny Mardiyanto, Kohei Arai, Electric wheel chair control with gaze detection and eye blinking, *Proceedings of the International Symposium on Artificial Life and Robotics*, GS9-4, 2009.
- [5] Kohei Arai and Kenro Yajima, Communication Aid and Computer Input System with Human Eyes Only, *Electronics and Communications in Japan*, Volume 93, Number 12, 2010, pages 1-9, John Wiley and Sons, Inc., 2010.
- [6] Kohei Arai, Ronny Mardiyanto, Evaluation of users' impact for using the proposed eye based HCI with moving and fixed keyboard by using eeg signals, *International Journal of Research and Reviews on Computer Science*, 2, 6, 1228-1234, 2011.
- [7] Kohei Arai, Kenro Yajima, Robot arm utilized having meal support system based on computer input by human eyes only, *International Journal of Human-Computer Interaction*, 2, 1, 120-128, 2011.
- [8] Kohei Arai, Ronny Mardiyanto, Autonomous control of eye based electric wheel chair with obstacle avoidance and shortest path finding based on Dijkstra algorithm, *International Journal of Advanced Computer Science and Applications*, 2, 12, 19-25, 2011.
- [9] Kohei Arai, Ronny Mardiyanto, Eye-based human-computer interaction allowing phoning, reading e-book/e-comic/e-learning, Internet browsing and TV information extraction, *International Journal of Advanced Computer Science and Applications*, 2, 12, 26-32, 2011.
- [10] Kohei Arai, Ronny Mardiyanto, Eye based electric wheel chair control system-(eye) can control EWC-, *International Journal of Advanced Computer Science and Applications*, 2, 12, 98-105, 2011.
- [11] Kohei Arai, Ronny Mardiyanto, Electric wheel chair controlled by human eyes only with obstacle avoidance, *International Journal of Research and Reviews on Computer Science*, 2, 6, 1235-1242, 2011.
- [12] Kohei Arai, Ronny Mardiyanto, Evaluation of users' impact for using the proposed eye based HCI with moving and fixed keyboard by using eeg signals, *International Journal of Research and Reviews on Computer Science*, 2, 6, 1228-1234, 2011.
- [13] K.Arai, R.Mardiyanto, Evaluation of users' impact for using the proposed eye based HCI with moving and fixed keyboard by using eeg signals, *International Journal of Research and review on Computer Science*, 2, 6, 1228-1234, 2012.
- [14] K.Arai, R.Mardiyanto, Electric wheel chair controlled by human eyes only with obstacle avoidance, *International Journal of Research and review on Computer Science*, 2, 6, 1235-1242, 2012.
- [15] R.Mardiyanto, K.Arai, Eye-based Human Computer Interaction (HCI) A new keyboard for improving accuracy and minimizing fatigue effect, *Scientific Journal Kursor*, (ISSN 0216-0544), 6, 3, 1-4, 2012.
- [16] K.Arai, R.Mardiyanto, Moving keyboard for eye-based Human Computer Interaction: HCI, *Journal of Image and Electronics Society of Japan*, 41, 4, 398-405, 2012.
- [17] Kohei Arai, Ronny Mardiyanto, Eye-based domestic robot allowing patient to be self-services and communications remotely, *International Journal of Advanced Research in Artificial Intelligence*, 2, 2, 29-33, 2013.
- [18] Kohei Arai, Ronny Mardiyanto, Method for psychological status estimation by gaze location monitoring using eye-based Human-Computer Interaction, *International Journal of Advanced Computer Science and Applications*, 4, 3, 199-206, 2013.
- [19] Kohei Arai, Kiyoshi Hasegawa, Method for psychological status monitoring with line of sight vector changes (Human eyes movements) detected with wearing glass, *International Journal of Advanced Research in Artificial Intelligence*, 2, 6, 65-70, 2013.

- [20] Kohei Arai, Wearable computing system with input output devices based on eye-based Human Computer Interaction: HCI allowing location based web services, *International Journal of Advanced Research in Artificial Intelligence*, 2, 8, 34-39, 2013.
- [21] Kohei Arai Ronny Mardiyanto, Speed and vibration performance as well as obstacle avoidance performance of electric wheel chair controlled by human eyes only, *International Journal of Advanced Research in Artificial Intelligence*, 3, 1, 8-15, 2014.
- [22] Kohei Arai Ronny Mardiyanto, Speed and vibration performance as well as obstacle avoidance performance of electric wheel chair controlled by human eyes only, *International Journal of Advanced Research in Artificial Intelligence*, 3, 1, 8-15, 2014.

AUTHORS PROFILE

Kohei Arai He received BS, MS and PhD degrees in 1972, 1974 and 1982, respectively.

He was with The Institute for Industrial Science and Technology of the University of Tokyo from April 1974 to December 1978 and also was with National Space Development Agency of Japan from January, 1979 to March, 1990. During from 1985 to 1987, he was with Canada Centre for Remote Sensing as a Post Doctoral Fellow of National Science and Engineering Research Council of Canada. He moved to Saga University as a Professor in Department of Information Science on April 1990.

He was a councilor for the Aeronautics and Space related to the Technology Committee of the Ministry of Science and Technology during from 1998 to 2000. He was a councilor of Saga University for 2002 and 2003. He also was an executive councilor for the Remote Sensing Society of Japan for 2003 to 2005. He is an Adjunct Professor of University of Arizona, USA since 1998. He also is Vice Chairman of the Commission-A of ICSU/COSPAR since 2008. He wrote 33 books and published 500 journal papers.

Relations between Psychological Status and Eye Movements

Kohei Arai

Graduate School of Science and Engineering
Saga University
Saga City, Japan

Abstract—Relations between psychological status and eye movements are found through experiments with readings of different types of documents as well as playing games. Psychological status can be monitored with Electroencephalogram: EEG sensor while eye movements can be monitored with Near Infrared: NIR cameras with NIR Light Emission Diode: LED. EEG signals are suffered from noises while eye movement can be acquired without any influence from noise. Therefore, psychological status can be monitored with eye movement detection instead of EEG signal acquisition if there is relation between both. Through the experiments, it is found strong relation between both. In particular, relation between the number of rapid changes of line of sight directions and relatively high frequency components of EEG signals is found. It is also found that the number of rapid eye movement is counted when the users are reading the documents. The rapid eye movement is defined as 10 degrees of look angle difference for one second. Not only when the users change the lines in the document, but also when the users feel a difficulty for reading words in the document, the users' line of sight direction moves rapidly.

Keywords—EEG; eye movement; psychological status; alpha wave; beta wave

I. INTRODUCTION

Nowadays, the eye-based HCI has been widely used to assist not only handicap person but also for a normal person. In handicap person, especially paraplegic, they use eye-based HCI for helping them to self-sufficient in the daily life such as input text to compute [1], communication aids [2], controlling wheelchair [3], [4], fetch a meal on table using robot arm [5], etc. The eye key-in system has been developed by many researchers [1]. The commercial available system provided by Tobii Tracker Company has been used by many researchers for developing text input, customer interest estimator on the business market, etc. [6]. Technology has been successful in rehabilitating paraplegics' personal lives. Prof Stephen Hawking, who was diagnosed with Amyotrophic Lateral Sclerosis (ALS), uses an electronic voice synthesizer to help him communicate with others [7]. By typing the text through aid of a predictive text entry system, approximating his voice, he is able to make coherent speech and present at conferences. To give another example, a paraplegic patient wearing a head-mounted camera is able to draw figures, lines, and play computer games [1]. Clearly, through the use of assistive technology, handicapped people are able to do feats on par with non-handicapped people.

The published papers discussing eye-based HCI system are categorized into: (1) vision-based and (2) bio-potential-based. The vision-based method utilized camera to capture an image and estimate the user sight. The key issue here is how the method/system could be deal with environment changing. Lighting changing, user movement, various types of user, etc have to cooperate with the system. The vision-based system could be explained as follow.

Eye mouse based on sight is developed [8]. The method searches and tracks the eye by using projection of difference left-right eye after it is success to detect the face. It obtains left and right direction that could be used for controlling mouse pointer without upward and downward directions. They implemented the method for controlling application such as "Block Escape" game and spelling program. Eye mouse by utilizing sight obtained from pupil location and detected by using Haar Classifier (OpenCv function) is developed [9]. It used blinking for replacing left click of mouse event. The system enabling it to control mouse by utilizing face movement and blinking is developed [10]. The Adaboost face detection method detects center position of face and tracks it by using Lucas-Kanade Optical flow. The user used the resulted location for controlling mouse cursor and will execute left mouse click by detecting the blinking. Human-computer interface by integrating eye and head position monitoring devices is developed [11]. It controlled the interface based on sight and blinking. The user command could be translated by system via sight and blinking. Also, they modified calibration method for reducing visual angle between the center of target and the intersection point (derived by sight). They reported that the modification allowed 108 or higher number of command blocks to be displayed on 14 inch monitor. Also, they reported that it has hit rate of 98% when viewed at the distance of 500mm. For triggering, the blinking invokes commands.

The bio-potential-based method estimated user behavior (eye behavior) by measuring user's bio-potential. The bio-potential measurement instrument such as Electrooculograph (EOG), Electroencephalograph (EEG), etc could be used for measuring eye behaviors. The example of bio-potential-based has been applied in application of electric wheelchair controlled using EOG analyzed user eye movement via electrodes directly on the eye to obtain horizontal and vertical eye-muscle activity.

Signal recognition analyzed Omni directional eye movement patterns [12]. I search pupil location on an eye image by using the proposed method that has been published [13]. I estimate the sight by converting the obtained position of pupil to sight angle. After the sight angle is estimated, I control the mouse cursor by using this sight.

In the following section, eye movement detection method is described followed by psychological status monitoring with EEG sensor. Then relations between eye movement and psychological status are described followed by conclusion with discussions.

II. EYE MOVEMENT DETECTION SYSTEM

A. Hardware Configuration

The system utilizes Infrared Camera NetCowBoy DC NCR-131 to acquire user image. I modified the position of 8 IR LED for adjusting illumination and obtaining stable image even illumination of environment changes as shown in Fig. 1.

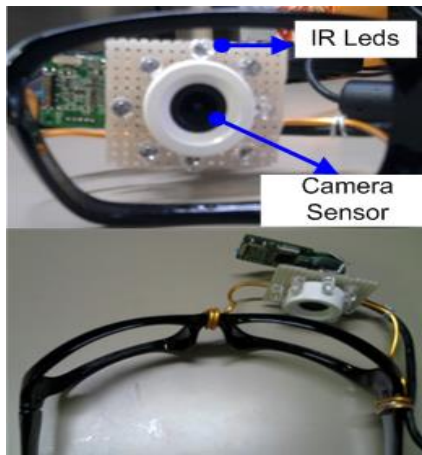


Fig. 1. Modified Camera Sensor

The use of IR camera will solve problem of illumination changes. I put the camera on user's glasses. Distance between camera and eye is 2 cm. I use Netbook Asus Eee PC 1002 HA with Intel Atom N270 CPU (1.6 GHz), 1GB Memory, 160 GB SATA HDD, and have small screen display 10 inch as main processing device. The software is developed under C++ language of Visual Studio 2005 and OpenCv, image processing library, which can be downloaded as free at their website. The hardware configuration is shown in Fig.2.

B. Eye Detection

The eye detection is handled by adaptive thresholds and pupil knowledge. I do not need the tracking method because the camera is on the user's glasses, so the next eye location has the same position as the previous one. Pupil location is detected by using pupil knowledge such as color, size, shape, sequential location, and movement.

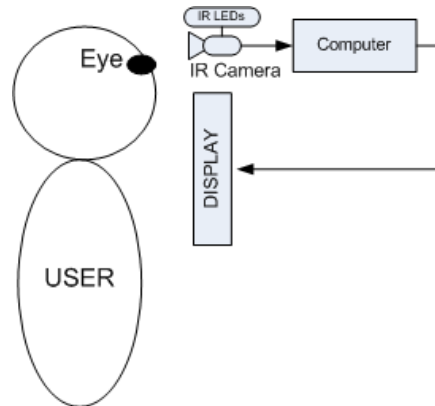


Fig. 2. Hardware Configuration

In pupil detection, pupil location is estimated as stated earlier using pupil knowledge extracted using an adaptive threshold to separate the pupil from other eye components. The threshold value T is 0.27% below the mean μ of eye image I and is derived from adjusting illumination intensity of 150 lux. The proposed threshold is suitable only for this condition but enables the camera to automatically adjust illumination as it changes.

$$\mu = \frac{1}{N} \sum_{i=0}^{N-1} I_i \quad (1)$$

$$T = 0.27\mu \quad (2)$$

Output from the adaptive threshold is black pixels representing the pupil in the image. To eliminate noise, I use a median filter. Widely adaptive threshold output is divided into three categories: (1) case 1, in which noise free black pixels clearly represent the pupil, (2) case 2, in which noise appears and is the same size and shape as pupil, and (3) case 3, when no pupil properties can be used to locate pupil. Cases are shown in Fig. 3.

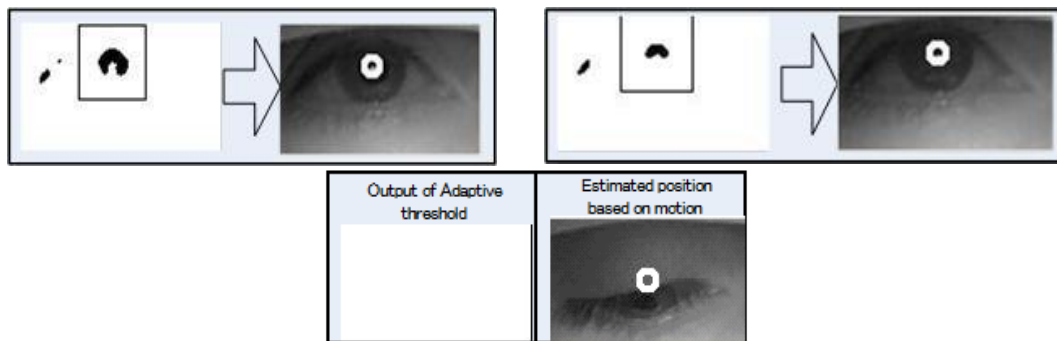


Fig. 3. Three cases in pupil detection that to be solved by using pupil knowledge

Once adaptive threshold output is classified, I estimate pupil location in three steps based on pupil knowledge. In case 1, the pupil is easily located by shape and size, even with noise in the image. In case 2, noise appears as almost the same size and shape as the pupil, e.g., when the adaptive threshold cannot be separated from other eye components such as the eyelid or the corner of the eye. To minimize these problems I recorded pupil movement histories assuming that the true pupil is closest to its previous location.

$$P(t-1) - C < P(t) < P(t-1) + C \quad (3)$$

Reasonable pupil location $P(t)$ is within the surrounding of previous location $P(t-1)$ with area C . In case 3, when features cannot be found to locate the pupil as when the user is looking from the corner of the eye, I estimate pupil location based on the movement.

C. EEG Sensor

The EEG sensor used for getting EEG signal from users' forehead in the experiment is Brain Catcher BCG-1S manufactured by TECHNOS Co. Ltd. Outlook of the sensor is shown in Fig.4. The sensor consists of two subsystems, EEG sensor and EEG signal receiver. Major specification is shown in Table 1.



Fig. 4. Outlook of the EEG sensor used

TABLE I. SPECIFICATION OF BRAIN CATCHER BCG-1S MANUFACTURED BY TECHNOS CO. LTD.

Size	W:23 × D:79 × H:15(mm)
Weight	16g

(a)EEG signal receiver (USB terminal)

Size	W:160 × D:180 × H:37(mm)
Weight	85g

(b)EEG sensor

III. EXPERIMENTS

A. Eye detection Accuracy

In order to measure performance of pupil detection, I involved five different users who have different race and nationality (Indonesian, Japanese, Sri Lankan, and Vietnamese). The uses of many samples will prove that the proposed method work when it is used for all types of users. The eye movement data was collected from each user while was making several eye movement.

Eye images of three Indonesian show that even though images were taken from same country, each person has different eye shape. The number of one of the Indonesian images 882 samples. One of them has slated eye and the other two Indonesians have narrow eye and clear pupil. The number of samples of these two Indonesian is 552 and 668, respectively. The collected data from Sri Lankan consists of the number of images is 828 samples. His skin color is black and eyelid is thick. Collected data from Japanese consists of the number of images is 665 samples. His skin color is bright and eye is slant. The collected data from Vietnamese is almost same of the other five.

This experiment evaluates pupil detection accuracy and variance against different user by counting the success sample and the fail one. After accuracy of pupil detection has been counted, I compared the proposed method with adaptive threshold method and also template matching method. The compared adaptive threshold method uses combination between adaptive threshold itself and connected labeling method. Also, another compared method uses pupil template as reference and matched with the pupil images. The accuracy of the proposed pupil detection method against different users is shown in TABLE II. . The result data show that the proposed pupil detection method is accurate and robust against different users with variance value is 16.27.

TABLE II. ACCURACY OF THE PROPOSED PUPIL DETECTION METHOD AGAINST DIFFERENT USERS, THIS TABLE SHOWS THAT THE PROPOSED METHOD IS ROBUST AGAINST DIFFERENT USER AND ACCURATE

User Types	Nationality	Adaptive Threshold (%)	Template Matching (%)	Proposed Method (%)
1	Indonesian	99.85	63.04	99.99
2	Indonesian	80.24	76.95	96.41
3	Sri Lankan	87.8	52.17	96.01
4	Indonesian	96.26	74.49	99.77
5	Japanese	83.49	89.1	89.25
6	Vietnamese	98.77	64.74	98.95
Average		91.07	70.08	96.73
Variance		69.75	165.38	16.27

Line of sight direction is detected with NIR camera and NIR LED. Therefore, eye color and skin color are not matter for the eye movement detections.

B. Relation between Eye Movements and EEG Signals

Four Japanese users are selected for the experiment of eye movement detections and EEG signal acquisitions. Through the experiment, two documents (simple document¹ and complicated document² which are shown in Fig.5) are read by the users. It is expected that brain is in very active for the complicated document while users are in relax status for the simple document.

むかし、あるところに、おじいさんがひとりですんでいました。
あるひ、ひるごはんのあとに、つばめがいちわどまにおちてきました。
つばめは、はねをバタバタさせて、まいあがろうとするのですが、すぐにまた、どまにおちて、もがいています。

おじいさんが、どうしたのかとおもってしてみると、あしがおれていました。
「おおお、かわいそうに。これでは、とぶことはできんな。わしがなおしてやろうなあ」と、くすりをつけて、こえだをそえてほつたいをまいてやりました。
おじいさんは、まいにち、つばめをかいほうしてやりました。

しばらくしてつばめのあしは、なあって、とべるようになりました。
おじいさんは、「よかった、よかった、もうだいじょうぶ!」と、いってはなしてやりました。
つばめは、おじいさんのいえのうえを、ぐるりととんでから、とおくのそらへとんでいきました。
「これから、きをつけて、げんきでぐらせよー。そうして、らいねんもまた、こいよー」つばめがみえなくなっても、おじいさんは、こえをかけつづきました。

それから、いちねんたちました。
おじいさんが、まえにわでいぶくしていると、つばめがやってきました。
「お、きたかや。おまえはきよねん、たすけてやったやつか。ようきたなあ」と、はなしかけました。

つばめは、しばらくおじいさんのあたまのうえをとびまわっていましたが、まっくらけなのおおきなつづを、ひとつづポテンとおとして、とんでいってしまいました。

「なんだこれは! フンをおとしていったのかい」と、いいながらよくみると、おおきなすいかのたねでした。
「あれあれ、すいかのたねを、おとしていったのか。そうか、おれにこれをうえて、すいかになったらたべるといふことかな。きよねん、たすけてやったおまえに、すいかのたねを、もってきたというわけか」

おじいさんは、つばめがもってきたすいかのたねを、はたけにまきました。
みずをやったり、こやしをやったり、だいにせわをしていると、やがておおきなつるがのびてきて、みがひとつになりました。
おじいさんは、まいにちはたけにいって、すいかをなでてやりました。

すいかのみは、どんどんどんどんおおきくなっていきました。
あるひ、おじいさんが、すいかをたたくと、ちょうどたべごろのおとがしました。
おじいさんは、おおきなすいかをうんとこしょどっこいしょと、やつのことで、いえにもちかえりました。

おじいさんが、すいかをまっぶたつにわたしたたん、たねのひとつづひとつづが、だいきんやこびきさんになって、どつとでてきました。

(a)Simple document

脳波 (のうは、Electroencephalogram : EEG) は、ヒト・動物の脳から生じる電気活動を、頭皮上、蝶形骨底、鼓膜、脳表、脳深部などに置いた電極で記録したものである。

英語のElectroencephalogramの忠実な訳語として、脳電図、EEGという呼び方もあり、中国語ではこちらの表現法を取っている。

本来は、脳波図と呼ぶべきであるが、一般的には「脳波」と簡略化して呼ばれることが多い。

脳波を測定、記録する装置を脳波計(Electroencephalograph : EEG)と呼び、それを用いた脳波検査(Electroencephalography : EEG)は、医療での臨床検査として、また医学、生理学、心理学、工学領域での研究方法として用いられる。

検査方法、検査機械、検査結果のどれも略語はEEGとなるので、使い分けに注意が必要である。

個々の神経細胞の発火を観察する単一細胞電極とは異なり、電極近傍あるいは遠隔部の神経細胞集団の電気活動の総和を観察する(少数の例外を除く)。近縁のものに、神経細胞の電気活動に伴って生じる磁場を観察する脳磁図(のうじず、Magnetoencephalogram : MEG)がある。

直接記録する方法はしばしば臨床検査として用いられる。背景脳波(基礎律動)や突発活動(てんかん波形など)を観察する。

各種のてんかん、ナルコレプシー、変性疾患、代謝性疾患、神経系の感染症、脳器質的疾患、意識障害、睡眠障害、精神疾患などの診断の補助・状態把握などに用いられる。

波形の加工の方法として、主なものに加算平均法、双極子推定法、周波数解析、コヒーレンス法、主成分分析、独立成分分析などがあり、一部は臨床でも用いられている。

脳波を直接記録する方法はしばしば臨床検査として用いられる。背景脳波(基礎律動)や突発活動(てんかん波形など)を観察する。

各種のてんかん、ナルコレプシー、変性疾患、代謝性疾患、神経系の感染症、脳器質的疾患、意識障害、睡眠障害、精神疾患などの診断の補助・状態把握などに用いられる。

波形の加工の方法として、主なものに加算平均法、双極子推定法、周波数解析、コヒーレンス法、主成分分析、独立成分分析などがあり、一部は臨床でも用いられている。

(b)Complicated document

Fig. 5. Documents used for the experiment

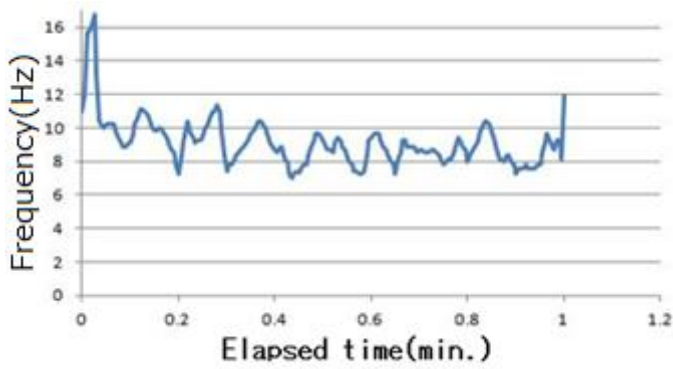
Fig.6 shows EEG signals when the users read the simple document.

Superimposed EEG signals for four users are shown in Fig.7 (The simple document).

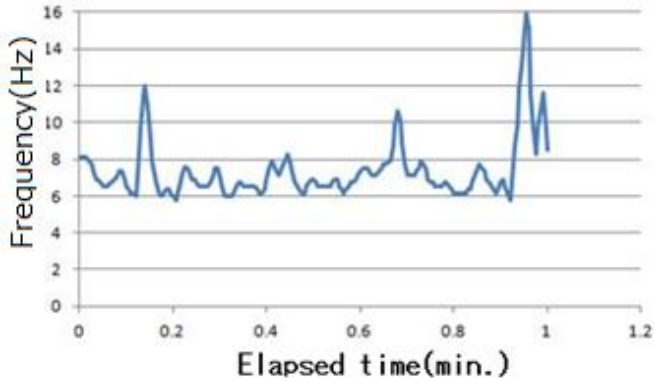
Meanwhile, Fig.8 shows those when the users read the complicated document.

¹ Simple document in Japanese is written in "Hiragana" character only. The content of the document is story for children. Therefore, it is very easy to read.

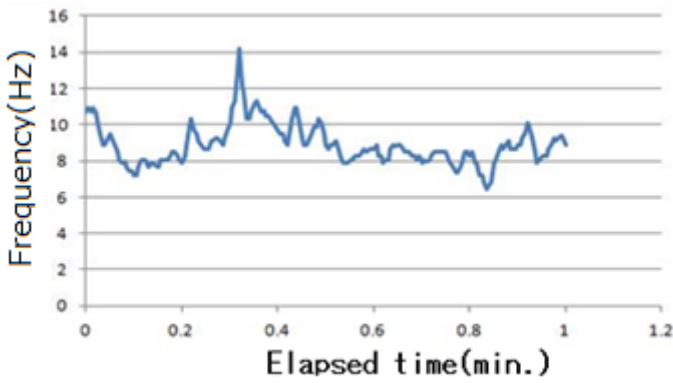
² Complicated document in Japanese is written in "Kanji" and "Hiragana" characters. The content of the document is text book for psychology for university students. Therefore, it is rather difficult to read.



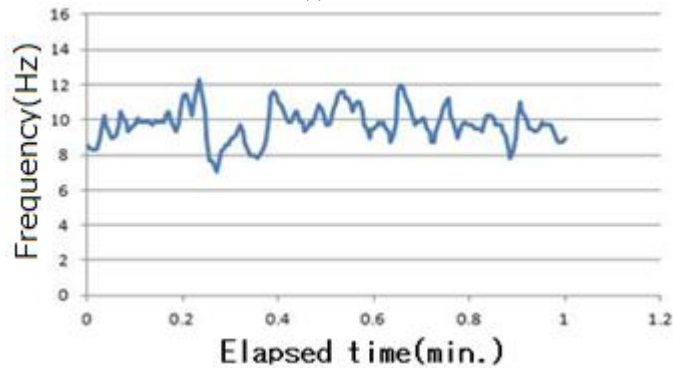
(a)A user



(b)B user



(c)C user



(d)D user

Fig. 6. EEG signals when the users read the simple document

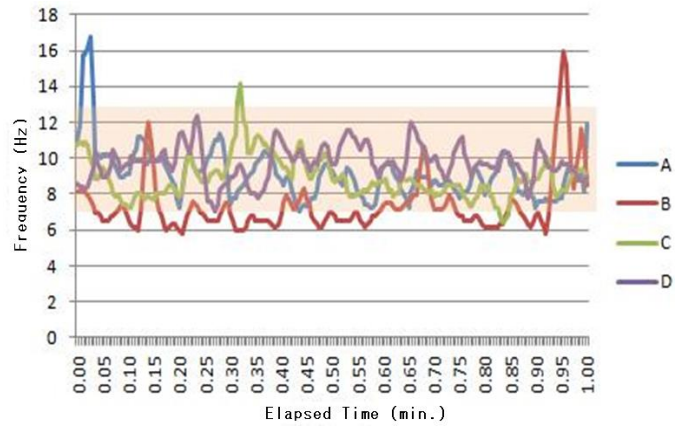
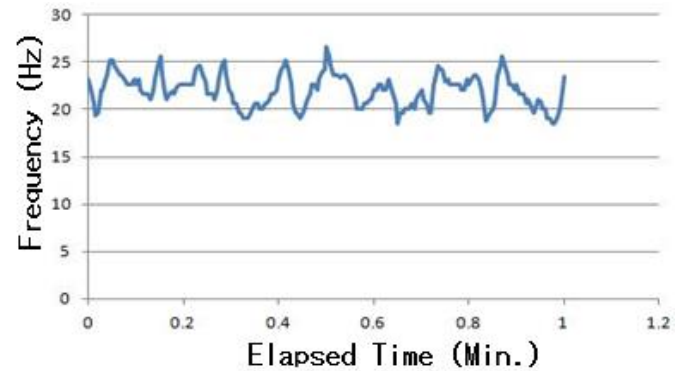
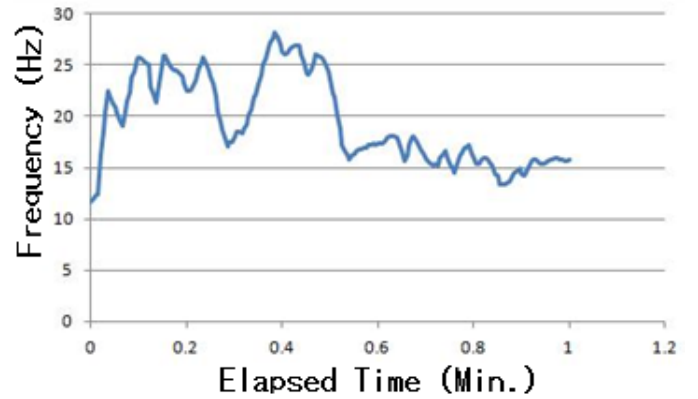


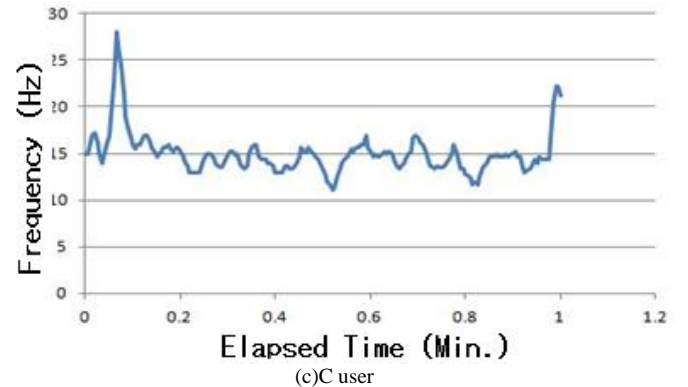
Fig. 7. Superimposed EEG signals for four users (The simple document)



(a)A user



(b)B user



(c)C user

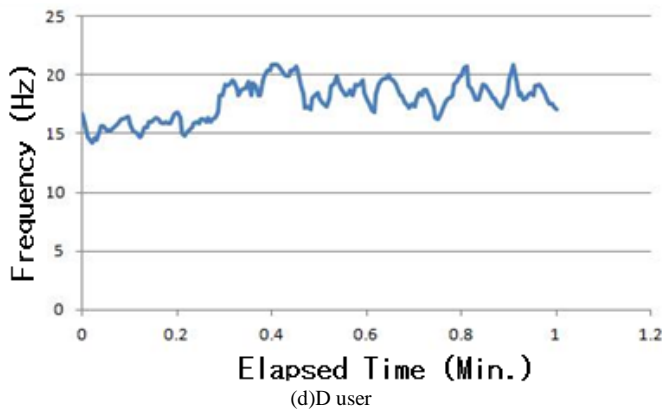


Fig. 8. EEG signals when the users read the complicated document

Superimposed EEG signals for four users are shown in Fig.9 (The complicated document).

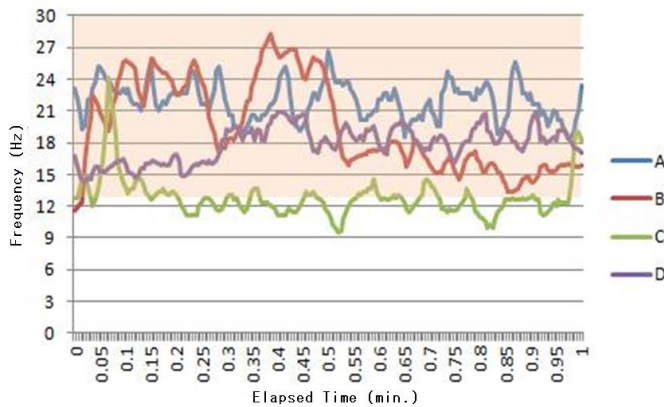


Fig. 9. Superimposed EEG signals for four users (The complicated document)

It is found that the frequency components for the simple document are much lower than those for the complicated document through a comparison between Fig.7 and Fig.9. The time variation is not so large. Also, there is not so large discrepancy among four users except user C. The user C is good at reading documents and has a plenty of knowledge and experiences on the contents of the documents.

From time to time, frequency component is getting high when users are reading complicated portions of the documents while is getting down when users are reading simple portions of the documents as shown in Fig.7 and Fig.9.

On the other hand, the number of rapid eye movement is counted when the users are reading the documents. The rapid eye movement is defined as 10 degrees of look angle difference for one second. Not only when the users change the lines in the document, but also when the users feel a difficulty for reading words in the document, the users' look direction moves rapidly. The number of the rapid eye movements is shown in Fig.10. The timing of the rapid eye movements is synchronized to raising the EEG frequency component. Namely, when the users feel a difficulty of reading the documents and line changes of the documents, EEG frequency components are raising and eye moves rapidly as shown in Fig.11 (Red circle indicates such moments).

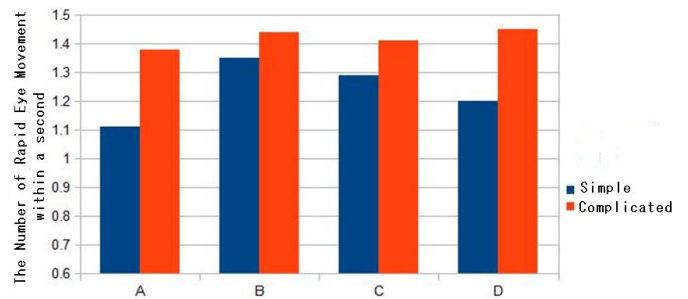


Fig. 10. The number of rapid eye movements

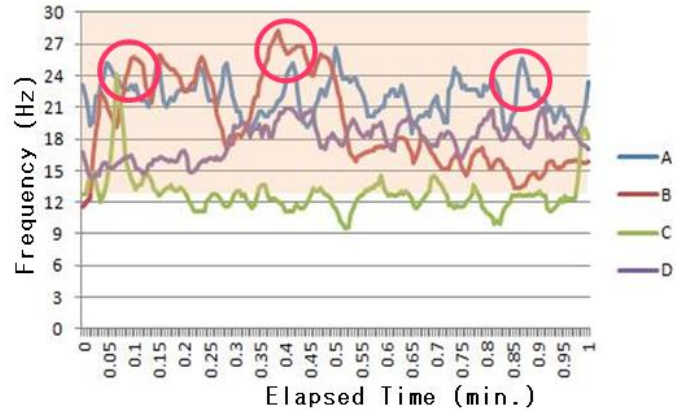


Fig. 11. EEG frequency components are raised when look direction changes rapidly

IV. CONCLUSION

Relations between psychological status and eye movements are found through experiments with readings of different types of documents as well as playing games. Psychological status can be monitored with Electroencephalogram: EEG sensor while eye movements can be monitored with Near Infrared: NIR cameras with NIR Light Emission Diode: LED. It is found that strong relation between both. In particular, the number of rapid changes of looking directions and relatively high frequency components of EEG signals. Therefore, it is possible to detect psychological status with monitoring eye movements. Due to the fact that EEG signals used to be affected by surrounding noises, eye movement detection is much useful for psychological status monitoring instead of EEG signals.

It is found that the number of rapid eye movement is counted when the users are reading the documents. The rapid eye movement is defined as 10 degrees of look angle difference for one second. Not only when the users change the lines in the document, but also when the users feel a difficulty for reading words in the document, the users' look direction moves rapidly. It is also found that the timing of the rapid eye movements is synchronized to raising the EEG frequency component. Namely, when the users feel a difficulty of reading the documents and line changes of the documents, EEG frequency components are raising and eye moves rapidly.

Future research works are required for typical psychological status monitoring, hatred, beloved, joy, anger, happy, surprise etc. with eye movement detection. Then the patients without mimic muscle function can represent their

emotions. Also, psychological status monitored with the proposed eye movement detection is useful for triage of victims when they evacuate from disaster occurred areas to safe areas. Because vital sign which consist heart rate, blood pressure, the number of breath, body temperature and copiousness is required for triage. If patients in hospitals, group homes, etc. wear the glass with eye movement detection function and physical status monitoring sensor and network system for transmission of these data, then the patients can be saved their life because their status are known together with their location and attitude.

ACKNOWLEDGMENT

The author would like to thank Dr. Ronny Mardiyanto for his effort to the experiment on eye detection accuracy evaluation.

REFERENCES

- [1] EYEWRIER: low-cost, open-source eye-based drawing system. Disponivel em: <<http://www.crunchgear.com/2009/08/25/%20eyewriter-low-cost-%20open-source-eye-%20based-drawing-system/>>. Acesso em: 7 October 2011.
- [2] LEFF, R. B.; LEFF, A. N. 4.954.083, 1990.
- [3] ARAI, K.; MARDIYANTO, R. A Prototype of Electric Wheelchair Controlled by Eye-Only for Paralyzed User. *Journal of Robotic and Mechatronic*, p. 66-74, 2011.
- [4] DJOKO PURWANTO, R. M. A. K. A. Electric wheel chair control with gaze detection and eye blinking. *Artificial Life and Robotics, AROB Journal*. 2009. p. 397-400.
- [5] ARAI, K.; YAJIMA, K. Robot Arm Utilized Having Meal Support System Based on Computer Input by Human Eyes Only. *International Journal of Human Computer Interaction (IJHCD)*, p. 1-9, 2011
- [6] JOHN J, M. et al. EyeKeys: A Real-Time Vision Interface Based on Gaze Detection from a Low-Grade Video Camera. 2004 Conference on Computer Vision and Pattern Recognition Workshop. 2004. p. 159.
- [7] ARAI, K.; YAJIMA, K. Robot Arm Utilized Having Meal Support System Based on Computer Input by Human Eyes Only. *International Journal of Human Computer Interaction (IJHCD)*, p. 1-9, 2011
- [8] JOHN J, M. et al. EyeKeys: A Real-Time Vision Interface Based on Gaze Detection from a Low-Grade Video Camera. 2004 Conference on Computer Vision and Pattern Recognition Workshop. 2004. p. 159.
- [9] CHANGZHENG, L.; CHUNG-KYUE, K.; JONG-SEUNG, P. The Indirect Keyboard Control System by Using the Gaze Tracing Based on Haar Classifier in OpenCV. 2009 International Forum on Information Technology and Applications.. 2009. p. 362-366.
- [10] ZHU, H.; QIANWEI, L. Vision-Based Interface: Using Face and Eye Blinking Tracking with Camera. 2008 Second International Symposium on Intelligent Information Technology Application. 2008. p. 306-310.
- [11] PARK K.S., L. K. T. Eye-controlled human/computer interface using the line-of-sight and the intentional blink. *Computers and Industrial Engineering*. 1993. p. 463-473.
- [12] BAREA, R. et al. System for Assisted Mobility using Eye Movements based on Electrooculography. *IEEE Transaction on Neural System and Rehabilitation Engineering*, v. 10, p. 209-218, 2002.
- [13] ARAI, K.; MARDIYANTO, R. Improvement of gaze estimation robustness using pupil knowledge. *Proceedings of the International Conference on Computational Science and Its Applications (ICCSA2010)*. 2010. p. 336-350.

AUTHORS PROFILE

Kohei Arai, He received BS, MS and PhD degrees in 1972, 1974 and 1982, respectively. He was with The Institute for Industrial Science, and Technology of the University of Tokyo from 1974 to 1978 also was with National Space Development Agency of Japan (current JAXA) from 1979 to 1990. During from 1985 to 1987, he was with Canada Centre for Remote Sensing as a Post Doctoral Fellow of National Science and Engineering Research Council of Canada. He was appointed professor at Department of Information Science, Saga University in 1990. He was appointed councilor for the Aeronautics and Space related to the Technology Committee of the Ministry of Science and Technology during from 1998 to 2000. He was also appointed councilor of Saga University from 2002 and 2003 followed by an executive councilor of the Remote Sensing Society of Japan for 2003 to 2005. He is an adjunct professor of University of Arizona, USA since 1998. He also was appointed vice chairman of the Commission "A" of ICSU/COSPAR in 2008. He wrote 30 books and published 500 journal papers

Mobile Device Based Personalized Equalizer for Improving Hearing Capability of Human Voices in Particular for Elderly Persons

Kohei Arai 1

Graduate School of Science and Engineering
Saga University
Saga City, Japan

Takuto Konishi 1

Graduate School of Science and Engineering
Saga University
Saga City, Japan

Abstract—Mobile device based personalized equalizer for improving the hearing capability of human voices in particular for elderly persons are proposed. Through experiments, it is found that the proposed equalizer does work well for improving hearing capability by 2 to 55 % of voice Recognition success ratio. According to the investigation of the frequency component analysis and *formant* detections, most of the voice sounds have the formant frequencies for the first to third frequencies within the range of 3445 Hz. Therefore, a nonlinear equalizing multiplier is better to enhance the frequency components for the first to third formants in particular. The experimental results with the voice above input experiments show that a good Percent Correct Recognition: PCR is required for 0 to more than 8000 Hz of frequency components. Also, 8162 Hz cut off frequency would be better for both noise suppressions and keeping a good PCR

Keywords—Frequency response equalization; mobile devices; formant frequency; hearing capability; hearing aids

I. INTRODUCTION

In general, hearing capability of human voices is getting bad for elderly persons due to the fact that a high-frequency response of elderly persons' ears is getting poor. Hearing capability is defined with the well-known averaged hearing capability level that is defined as Averaged value of hearing capability for human voices regarding frequency components ranged from 500 Hz to 4000 Hz. In accordance with the definition, 25-40 dB of loudness of human voices are difficult to hear slightly when human voice is not loud while 40-70 dB of loudness of human voices are difficult to hear when human voice is normal level.

Earlier devices, known as ear trumpets or ear horns [1], [2], were passive funnel-like amplification cones designed to gather sound energy and direct it into the ear canal. After that not so small number of methods have been proposed so far [3] – [10]

Although general purpose of frequency equalizer which allows compensation of hearing capability is used for that purpose (improvement of hearing capability), degradation of high frequency response depends on person. Therefore, customization is highly required for the frequency equalization devices. On the other hand, such customized frequency equalization devices are not so cheap and also are

not so good looking. Therefore, frequency equalizing devices are not so popular.

The human voice has base frequency sounds and overtone sounds. Frequency components of human voices consist of formant¹ (peaks of frequency components which are used for characterization of personal human voices). Lower-frequency components are dominant for vowels, in general, while relatively higher-frequency components are dominant for consonants. For elderly persons, high-frequency components are getting difficult to hear which results in the consonants are getting difficult to hear. Such difficulties are depending on persons by persons. Therefore, it is not so easy to customize frequency equalizers which allow improvement of hearing capability, in particular, for elderly persons.

There are several ways of evaluating how well a hearing aid compensates for hearing loss. One approach is audiometry which measures a subject's hearing levels in laboratory conditions. The threshold of audibility for various sounds and intensities is measured in a variety of conditions. Although audiometric tests may attempt to mimic real-world conditions, the patient's experiences may differ. An alternative approach is self-report assessment of which the patient reports their experiences with the hearing aid in concern. The evaluation method proposed here is based on using Electroencephalogram : EEG sensor. Namely, in accordance with hearing quality, Peak Alpha Frequency: PAF amplitude is getting large while it is getting small when hearing quality is getting poor.

The following section describes the proposed method and implementation of the compensation filter including mobile devices followed by some experiments for a specific person. Then a conclusion is described together with some discussions.

II. PROPOSED METHOD AND IMPLEMENTATION

In order to create a new personalized frequency equalizer, mobile devices are used. Mobile devices with headsets or ear phones are getting cheap and are good looking as well. Therefore, users can carry the proposed personalized equalizer.

In order to characterize hearing capability degradation, a specific user has to try to hear some sentences which cover the

¹ <http://newt.phys.unsw.edu.au/jw/formant.html>

spectral range from zero (Direct Current: DC) to around 20 KHz includes all the vowels and the consonants together with their overtones. Then a spectral response of a compensation filter for the specific user is designed. The compensation filter is implemented in a mobile device such as Android tablet terminal, i-phone, smart phone, etc.

Frequency responses of ears against human voices are, in general, characterized with formants which are shown in Fig.1. Namely, human voice spectra have peaks which are named as formants.

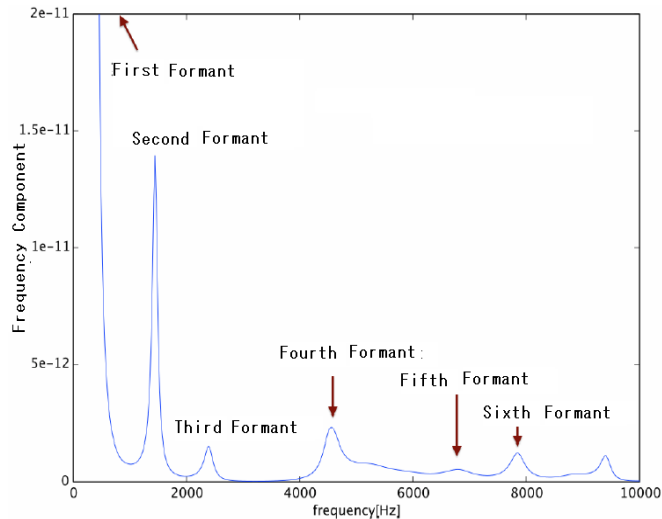


Fig. 1. Example of formants of human voices

According to the frequencies of the peaks, they are named the first formant, the second formant and so on. The proposed method detect formants through Fourier Transformation first. In the mean time, input voice signals are decomposed with 32 of filter bank. Degraded formants can be found by comparing the input voice signals with the synthesized voice signals derived from Auditory Toolbox, for instance. Then the degraded formants can be compensated in accordance with the difference between actual voice and synthesized voice signals.

After that, reconstruction is applied to the degraded voice signals with 32 filter bank as shown in Fig.2. Delay time which is caused by the nonlinear equalizing multiplier can be compensated with deley element of which delay time is totally corresponding to the delay time caused by the nonlinear equalizing multiplier as shown in Fig.3

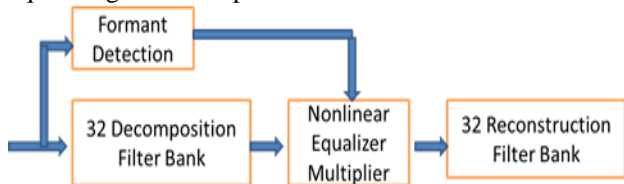


Fig. 2. Proposed method for degraded formant corrections with the consideration of formant ballunce

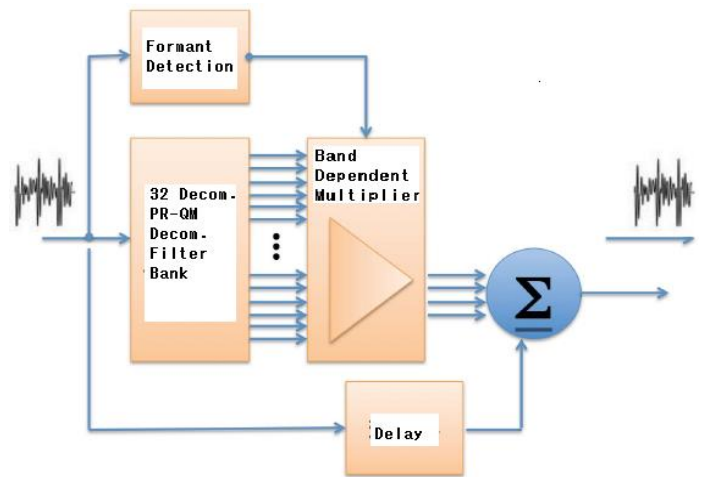


Fig. 3. Alternative of nonlinear equalizing multiplier with delay element

The correction filter is composed with high shelving filter of which the Frequency Transfer Function in analog filter function is expressed as follows,

$$H(s) = A \frac{As^2 + \frac{\sqrt{A}}{Q}s + 1}{S^2 + \frac{\sqrt{A}}{Q}s + A} \quad (1)$$

This can be re-written as follows,

$$H(z) = \frac{b_0 + b_1z^{-1} + b_2z^{-2}}{a_0 + a_1z^{-1} + a_2z^{-2}}$$

$$\begin{cases} b_0 = A((A + 2) + (A - 2) \cos \omega_0 + 2\sqrt{A} \alpha) \\ b_1 = 2A((A - 2) + (A + 2) \cos \omega_0) \\ b_2 = A((A + 2) + (A - 2) \cos \omega_0 - 2\sqrt{A} \alpha) \\ a_0 = (A + 2) - (A - 2) \cos \omega_0 + 2\sqrt{A} \alpha \\ a_1 = -2((A - 2) - (A + 2) \cos \omega_0) \\ a_2 = (A + 2) + (A - 2) \cos \omega_0 - 2\sqrt{A} \alpha \end{cases} \quad (2)$$

where $\alpha = \sin \omega_0/Q$, $\omega_0 = 2 \pi f_0/F_s$

The high shelving filter allows enhancement of arbitrary higher frequency components without suppression of low frequency components as shown in Fig.4. Also, the modulation transfer function of the high shelving filter is easy to design. Therefore, it is applicable for nonlinear equalizing multiplier.

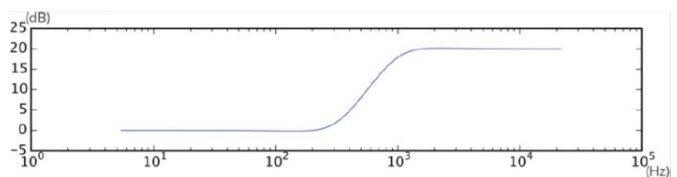


Fig. 4. Modulation Transfer Function of the high shelving filter

When the high shelving filter is applied to the input voice signals, high frequency components are enhanced as shown in Fig.5.

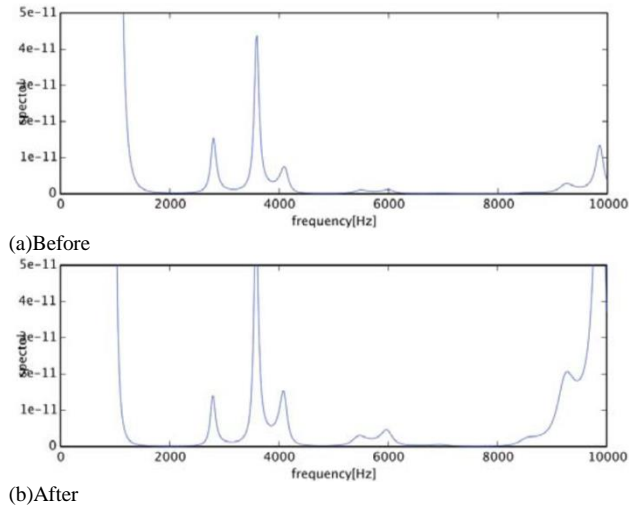


Fig. 5. High frequency component enhancing nonlinear equalizing multiplier

Lastly, low pass filter is applied to the nonlinear equalizing multiplier applied voice signals for noise removal as shown in Fig.6.

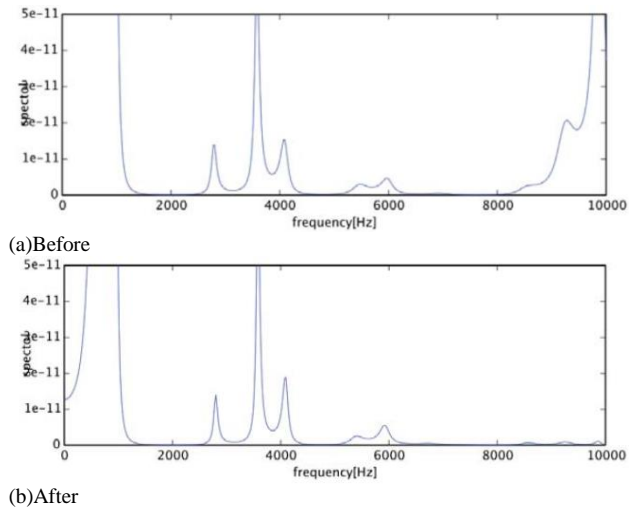


Fig. 6. Before and after the low pass filter is applied to the nonlinear equalization multiplier applied voice signals

Also, digital filter featuring wavelet transformation is used for the correction filter. Haar base function of wavelet transformation is used for the first attempt. Haar wavelet transformation is illustrated in Fig.7. The original voice signals in time domain can be converted in high (H1) and low (L1) frequency components as shown in Fig.7. Then L1 component can also be converted in high (H2) and low (L2) components and so on. These components are called as wavelet coefficients (frequency components). Using the wavelet coefficients, H_n and L_n , L_{n-1} can be reconstructed perfectly because Haar wavelet function is bi-orthogonal function.

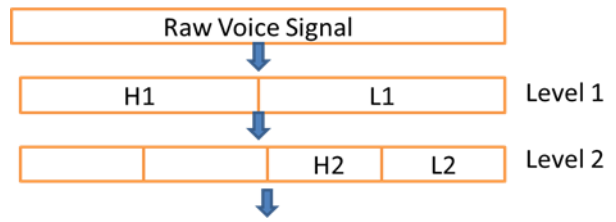


Fig. 7. Haar wavelet transformation

Then raw input voice signal is converted through Haar wavelet transformation with level 5 which corresponds to the third formant frequency. After that nonlinear multiplication is applied to the converted wavelet coefficients as shown in Fig.8. Also, the nonlinear multiplication is applied to the converted wavelet coefficients with the previously designed *cut off* frequency. In particular, high frequency components sounds so noisy that the frequency components higher than *cut off* frequency is better to suppressed.

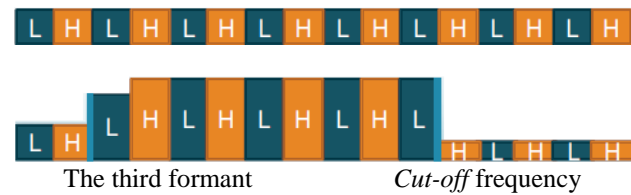


Fig. 8. Concept for the nonlinear equalizer multiplier

It is possible to construct low pass filter based on Haar wavelet transformation. Through reconstruction with the extracted low frequency component only derived from the decomposed voice signals, low pass filter can be realized as shown in Fig.9.



Fig. 9. Low pass filter based on Haar wavelet transformation

Therefore, arbitrary frequency components can be extracted from the level a of the wavelet coefficients. Haar wavelet transformation can be considered as filter bank which allows extraction of arbitrary frequency components. Also, it is possible to reconstruct arbitrary frequency component enhancing voice signals by adding wavelet coefficients. This is the method for frequency component equalization.

Through experiments, the following EEG sensor of ZA-9 + SleepSign-Lite manufactured by Kissei ComTec is used for evaluation of hearing quality. This EEG sensor allows measurements of EEG and electro - oculo-gram; EOG. Also, voice volume level meter of LM-8102 manufactured by Mother Tool Co. Ltd. is used for the experiments. Outlooks of the EEG and EOG sensor as well as voice volume level meter are shown in Fig.10 while the major specifications of the EEG and EOG sensors are shown in Table 1.



(a) EEG and EOG sensors



(b) Voice volume level meter

Fig. 10. Outlook of the EEG and EOG sensor as well as voice volume level meter used for the experiments

TABLE I. MAJOR SPECIFICATION OF EEG AND EOG SENSOR OF ZA-9 MANUFACTURED BY KISSEI COMTEC

Band Width	0.5~40Hz
Sampling Frequency	128Hz
AD Converter	12 bit

Meanwhile, the major specification of voice volume level meter is shown in Table 2.

TABLE II. MAJOR SPECIFICATION OF VOICE VOLUME LEVEL METER OF LM-8102 MANUFACTURED BY MOTHER TOOL CO. LTD

Auto range : 30~130dB
Manual range : L=30~80dB/M=50~100dB/H=80~130dB
Resolution : 0.1dB Frequency range : 31.5~130dB

III. EXPERIMENTS

Example of input voice signals is shown in Fig.9. From these input voice signals and synthetic voicesignals, formant

detection is performed together with creation of characteristics of nonlinear equalizer multiplier for correction of hearing capability compensation.



Fig. 11. Example of the input voice signal

The followings are examples of frequencies of the actual and the synthetic formants for “a”, “i” and “u”, respectively.

“a”
F1 : 718.75 F2 : 1093.75 F3 : 2437.5
 (F1=730; F2=1090; F3=2440)

“i”
F1 : 289.062 F2 : 2296.875 F3 : 3000
 (F1=270; F2=2290; F3=3010)

“u”
F1 : 304.688 F2 : 882.812 F3 : 2226.562
 (F1=300; F2=870; F3=2240)

The differences between actual and synthetic formants are very small. Therefore, formants are detected almost perfectly.

In order to determine *cut off* frequency for noise suppression, the following 67 voice sounds are used.

- “a”, “i”, “u”, “e”, “o”
- “ka”, “ki”, “ku”, “ke”, “ko”
- “sa”, “si”, “su”, “se”, “so”
- “ta”, “ti”, “tu”, “te”, “to”
- “na”, “ni”, “nu”, “ne”, “no”
- “ha”, “hi”, “hu”, “he”, “ho”
- “ma”, “mi”, “mu”, “me”, “mo”
- “ya”, “yu”, “yo”
- “ra”, “ri”, “ru”, “re”, “ro”
- “wa”
- “ga”, “gi”, “gu”, “ge”, “go”
- “za”, “zi”, “zu”, “ze”, “zo”
- “da”, “di”, “du”, “de”, “do”
- “ba”, “bi”, “bu”, “be”, “bo”
- “pa”, “pi”, “pu”, “pe”, “po”

Percent Correct Recognition of these voice sounds are evaluated with the different *cut off* frequencies. Nonlinear equalizing multiplier is created depending on the characteristics of hearing capabilities evaluated with EEG and EOG sensors. The results of PCR evaluation is shown in Table 3.

TABLE III. PERCENT CORRECT RECOGNITION: PCR WITH THE DIFFERENT CUT OFF FREQUENCIES

Frequency(Hz)	689	1378	2067	2756	3445
PCR(%)	45	79	90	98	100

If the *cut off* frequency is set at 689 Hz, then 55% of input voice sounds are not recognized. In accordance with the *cut*

off frequency, PCR is increased monotonically. PCR reaches 100% at the cut off frequency of 3445 Hz. Therefore, the first to the third formant frequency have to be maintained their frequency components. Also it may say that 0 to 3443 Hz of frequency components is mandatory for voice recognitions. Thus it is concluded that cut off frequency has to be set more than 3445 Hz at least.

According to the investigation of the frequency component analysis and formant detections, most of voice sounds have the formant frequencies for the first to third frequencies within the range of 3445 Hz. Therefore, nonlinear equalizing multiplier is better to enhance the frequency components for the first to third formants in particular. The experimental results with the aforementioned voice input experiments shows that 0 to more than 8000 Hz of frequency components are required for a good PCR. Also 8162 Hz cut off frequency would be better for both noise suppressions and keeping a good PCR.

IV. CONCLUSION

Mobile device based personalized equalizer for improving hearing capability of human voices in particular for elderly persons is proposed. Through experiments, it is found that the proposed equalizer does work well for improving hearing capability by 2 to 55 % of the voice recognition success ratio.

According to the investigation of the frequency component analysis and formant detections, most of voice sounds have the formant frequencies for the first to third frequencies within the range of 3445 Hz. Therefore, the nonlinear equalizing multiplier is better to enhance the frequency components for the first to third formants, in particular. The experimental results with the voice above input experiments show that 0 to more than 8000 Hz of frequency components are required for a good PCR. Also, 8162 Hz cut off frequency would be better for both noise suppressions and keeping a good PCR.

ACKNOWLEDGMENT

The authors would like to thank all the volunteers of saga University students who participated to the experiments.

REFERENCES

- [1] Bentler Ruth A., Duve , Monica R. (2000). "Comparison of Hearing Aids Over the 20th Century". *Ear & Hearing* 21 (6): 625–639. doi:10.1097/00003446-200012000-00009.
- [2] Bentler, R. A.; Kramer, S. E. (2000). "Guidelines for choosing a self-report outcome measure". *Ear and hearing* 21 (4 Suppl): 37S–49S. doi:10.1097/00003446-200008001-00006. PMID 10981593. edit

- [3] Jack Katz; Larry Medwetsky; Robert Burkard; Linda Hood (2009). "Chapter 38, Hearing Aid Fitting for Adults: Selection, Fitting, Verification, and Validation". *Handbook of Clinical Audiology* (6th ed.). Baltimore MD: Lippincott Williams & Wilkins. p. 858. ISBN 978-0-7817-8106-0.
- [4] K. Sickel, Shortest Path Search with Constraints on Surface Models of In-ear Hearing Aids 52. *IWK, Internationales Wissenschaftliches Kolloquium (Computer science meets automation Ilmenau 10. - 13.09.2007) Vol. 2 Ilmenau : TU Ilmenau Universitätsbibliothek 2007, pp. 221-226*
- [5] K. Sickel et al., Semi-Automatic Manufacturing of Customized Hearing Aids Using a Feature Driven Rule-based Framework *Proceedings of the Vision, Modeling, and Visualization Workshop 2009* (Braunschweig, Germany November 16–18, 2009), pp. 305-312
- [6] Dave Fabry, Hans Mülder, Evert Dijkstra (November 2007). "Acceptance of the wireless microphone as a hearing aid accessory for adults". *The Hearing Journal* 60 (11): 32–36. doi:10.1097/01.hj.0000299170.11367.24.
- [7] Hawkins D (1984). "Comparisons of speech recognition in noise by mildly-to-moderately hearing-impaired children using hearing aids and FM systems". *Journal of Speech and Hearing Disorders* 49 (4): 409. doi:10.1044/jshd.4904.409.
- [8] Ricketts T., Henry P. (2002). "Evaluation of an adaptive, directional-microphone hearing aid". *International Journal of Audiology* 41 (2): 100–112. doi:10.3109/14992020209090400.
- [9] Lewis M Samantha, Crandell Carl C, Valente Michael, Horn Jane Enrietto (2004). "Speech perception in noise: directional microphones versus frequency modulation (FM) systems". *Journal of the American Academy of Audiology* 15 (6): 426–439. doi:10.3766/jaaa.15.6.4.
- [10] Exemption from Preemption of State and Local Hearing Aid Requirements; Applications for Exemption, Docket No. 77N-0333, 45 Fed. Reg. 67326; Medical Devices: Applications for Exemption from Federal Preemption of State and Local hearing Aid Requirements, Docket No. 78P-0222, 45 Fed. 67325 (Oct. 10, 1980).

AUTHORS PROFILE



Kohei Aarai He received BS, MS and PhD degrees in 1972, 1974 and 1982, respectively. He was with The Institute for Industrial Science and Technology of the University of Tokyo from April 1974 to December 1978 and also was with National Space Development Agency of Japan from January, 1979 to March, 1990. During from 1985 to 1987, he was with Canada Centre for Remote Sensing as a Post Doctoral Fellow of National Science and Engineering Research Council of Canada. He moved to Saga University as a Professor in Department of Information Science on April 1990. He was a councilor for the Aeronautics and Space related to the Technology Committee of the Ministry of Science and Technology during from 1998 to 2000. He was a councilor of Saga University for 2002 and 2003. He also was an executive councilor for the Remote Sensing Society of Japan for 2003 to 2005. He is an Adjunct Professor of University of Arizona, USA since 1998. He also is Vice Chairman of the Commission-A of ICSU/COSPAR since 2008. He wrote 33 books and published 500 journal papers.

Iris Compression and Recognition using Spherical Geometry Image

Rabab M. Ramadan

College of Computers and Information Technology University of Tabuk Tabuk, KSA

Abstract—this research is considered to be a research to attract attention to the 3D iris compression to store the database of the iris. Actually, the 3D iris database cannot be found and in trying to solve this problem 2D iris database images are converted to 3D images just to implement the compression techniques used in 3D domain to test it and give an approximation results or to focus on this new direction in research. In this research a fully automated 3D iris compression and recognition system is presented. We use spherical based wavelet coefficients for efficient representation of the 3D iris. The spherical wavelet transformation is used to decompose the iris image into multi-resolution sub images. The representation of features based on spherical wavelet parameterization of the iris image was proposed for the 3D iris compression system. To evaluate the performance of the proposed approach, experiments were performed on the CASIA Iris database. Experimental results show that the spherical wavelet coefficients yield excellent compression capabilities with minimal set of features. Haar wavelet coefficients extracted from the iris image was found to generate good recognition results.

Keywords—3D Iris Recognition; Iris Compression; Geometry coding; Spherical Wavelets

I. INTRODUCTION

Biometric identification is the process of associating an identity to the input biometric data by comparing it against the enrolled identities in a database [1]. To design and implement robust systems capable of mass deployment, one needs to address key issues, such as human factors, environmental conditions, system interoperability, and image standard [2]. The iris, the colored portion of the eye surrounding the pupil, contains unique patterns which are prominent under near-infrared illumination. These patterns remain stable from a very young age, barring trauma or disease, allowing accurate identification with a very high level of confidence. Commercial iris systems are used as access to secure facilities or other resources, even Criminal/terrorist identification. The enrollment of an individual into a commercial iris system requires capturing one or more images from a video stream [3].

The question arises how to store and handle the acquired sensor data. Typically, the database for such system does not contain actual iris images, but rather it stores a binary file that represents each enrolled iris (the template). Most commercial iris systems today use the Daugman algorithm [4-6]. The recognition system used the template as the input to its process and the iris image is discarded to speed up the recognition process and decrease the storage requirements of the system. From the other point of view, if the data have to be transferred via a network link to the respective location, a minimization of

the amount of data must be taken into account. The problem here is that a template alone cannot allow the recreation of the iris image from that it is derived, while the original iris imagery is still valuable for research.

A lot of researches concern on the recognition system which depends on the template of the iris image extracted from the original image. In this paper, the attention is transferred to the iris compression.

This research is considered to be a research to attract attention to the 3D iris compression to store the database of the iris. Actually, the 3D iris database cannot be found and in trying to solve this problem 2D iris database images are converted to 3D images just to implement the compression techniques used in 3D domain to test it and give an approximation results or to focus on this new direction in research. These results may encourage researchers to establish a new 3D iris database image to benefit from all techniques in 3D domain.

Geometry image is an image used to remesh an arbitrary surface onto a completely regular structure [7]. One important use for such a representation is shape compression, the concise encoding of surface geometry [8]. Geometry images can be encoded using traditional image compression and decompression algorithms, such as wavelet-based coders. The mesh-based spherical scheme more natural for coding geometry, and provide good reconstruction of shape detail at very low bit budgets [9].

In this paper, we detail how the geometry image is used to compress the 3D iris images. The 3D iris image is mapped to the spherical parameterization domain then the geometry image is obtained as a color image and a surface. Finally, the spherical based wavelet coefficient are computed for efficient representation and compression of the 3D iris image.

The rest of this paper is organized as follows: overview of related work in 3D image compression will be in section II. Section III contains the overview of image preprocessing stage including segmentation and normalization. Spherical geometry image is discussed in section IV. Section V reports the experimental results. Finally, section VI contains the conclusion of this paper.

II. RELATED WORK

A major advance in the field of iris recognition results from the expiration of two patents [10]. The first one is the pioneer patent dealing with the general idea of the iris recognition process. It was developed by the ophthalmologists Flom and

Safir (1987) and it expired in 2005. The second one, developed by the professor John Daugman (1994), was used to protect the iris-code approach and expired in 2011.

Flom and Safir first proposed the concept of automated iris recognition in 1987 [11]. Since then, some researchers worked on iris representation and matching and have achieved great progress [12], [13], [14], [15].

The iris recognition process starts with the segmentation of the iris ring. Further, data is transformed into a double dimensionless polar coordinate system, through the Daugman's Rubber Sheet process. Regarding the feature extraction stage, existing approaches can be roughly divided into three variants: phase-based [16], zero-crossing [17] and texture analysis methods [18]. Dauman [16] used multi-scale quadrature wavelets to extract texture phase-based information and obtain an iris signature with 2048 binary components. Boles and Boashash [19] calculated a zero-crossing representation of one-dimensional (1-D) wavelet transform at various resolution levels of a concentric circle on an iris image to characterize the texture of the iris. Wildes et al. [20] represented the iris texture with a Laplacian pyramid constructed with four different resolution levels and used the normalized correlation to determine whether the input image and the model image are from the same class. Tisse et al. [21] analyzed the iris characteristics using the analytic image constructed by the original image and its Hilbert transform. Emergent frequency functions for feature extraction were in essence samples of the phase gradient fields of the analytic image's dominant components [22], [23]. Similar to the matching scheme of Daugman, they sampled binary emergent frequency functions to form a feature vector and used Hamming distance for matching. Park et al. [24] used a directional filter bank to decompose an iris image into eight directional subband outputs and extracted the normalized directional energy as features. Iris matching was performed by computing Euclidean distance between the input and the template feature vectors.

Kumar et al. [25] utilized correlation filters to measure the consistency of iris images from the same eye. The correlation filter of each class was designed using the two-dimensional. In [26], Hong and Smith proposed the octave band directional filter banks which are capable of both directional decomposition and an octave band radial decomposition. Finally, in the feature comparison stage, a numeric dissimilarity value is produced, which determines the subject's identity. Here, it is usual to apply different distance metrics (Hamming [16], Euclidian [27] or weighted Euclidian [28]), or methods based on signal correlation [20]. Many image compression and representation methods depend on Gabor analysis or phase information, which are two important components in IrisCode. Daugman demonstrated that Gabor filters are effective for image compression [26]. Behar et al. showed that images can be reconstructed from localized phase [29].

This research is considered to be a research to attract attention to the 3D iris compression to store the database of the iris. Actually, the 3D iris database cannot be found and in trying to solve this problem 2D iris database images are converted to 3D images just to implement the compression

techniques used in 3D domain to test it and give an approximation results or to focus on this new direction in research. These results may encourage researchers to establish a new 3D iris database image to benefit from all techniques in 3D domain. Geometry images and Spherical representations are used in the compression algorithm.

The construction of a geometry image involves parametrizing a given surface onto a planar domain, and resampling the surface geometry on a regular domain grid. The original work [30] heuristically cuts an arbitrary surface into a disk using a network of cut paths, with $2g$ loops for a genus g surface. The resulting cut surface is mapped onto a square using a stretch-minimizing parametrization to reduce under sampling.

For shapes with high genus or long extremities, forcing the whole surface to map into a square can introduce high distortion. To mitigate this, we can instead cut the surface into several pieces to produce a multi-chart geometry image [31]. The challenge is to join these piecewise regular charts into a watertight surface.

For genus-zero models, a geometry image may be constructed via spherical parametrization [32], which does not require any a priori surface cuts. The spherical domain is unfolded into a square using a simple cut with elegant boundary symmetries. These boundary symmetries permit the construction of a smooth (C1) polynomial surface, and the regular control grid structure lets the surface be evaluated entirely within the GPU rasterization pipeline [33]. In addition, a spherical geometry image can be compressed using traditional image wavelet Geometry images for static objects can be generalized to geometry videos for animated shapes [34]. Excellent survey of the various 3D mesh compression algorithms has been given by Alliez and C. Gotsman in [34, 30]. The recent development in the wavelet transforms theory has spurred new interest in multi-resolution methods, and has provided a more rigorous mathematical framework. Wavelets give the possibility of computing compact representations of functions or data. Additionally, wavelets are computationally attractive and allow variable degrees of resolution to be achieved. All these features make them appear as an interesting tool to be used for efficient representation of 3D objects.

3D Face recognition is one of the imperative applications calling for compact storage and rapid processing of 3D meshes. Face recognition based on 3D information is not a new topic. It has been extensively addressed in the related literature since the end of the last century [35-40]. Further surveys of the state-of-the-art in 3D face recognition can be found in [36, 37]. Spherical representations permit to efficiently represent facia surfaces and overcome the limitations of other methods towards occlusions and partial views. In our previous work [41], an innovative fully automated 3D face compression and recognition system is presented. We use spherical based wavelet coefficients for efficient representation of the 3D face. The spherical wavelet transformation is used to decompose the face image into multi-resolution sub images. To the best of our knowledge, the representation of 3D iris point clouds as spherical signals for iris recognition has however not been investigated yet. We therefore propose to take benefit of the

spherical representations in order to build an effective and automatic 3D iris recognition system.

III. IRIS IMAGE PREPROCESSING

Image processing techniques can be employed to extract the unique iris pattern from a digitised image of the eye, and encode it into a biometric template, which can be stored in a database. This biometric template contains an objective mathematical representation of the unique information stored in the iris, and allows comparisons to be made between templates. When a subject wishes to be identified by an iris recognition system, their eye is first photographed, and then a template created for their iris region. This template is then compared with the other templates stored in a database until either a matching template is found and the subject is identified, or no match is found and the subject remains unidentified [42]. There are four main stages of an iris recognition and compression system. They are, image preprocessing, feature extraction and template matching [43], and compression algorithm.

A. Image preprocessing

The iris image is to be preprocessed to obtain useful iris region. Image preprocessing contains, iris localization that detects the inner and outer boundaries of iris [44], [45] and iris normalization, in this step, iris image is converted from Cartesian coordinates to Polar coordinates. In this paper, We are not focusing on the segmentation instead we are interested in iris compression hence we have used the existing algorithms [42] for image preprocessing normalization feature extraction and segmentation but focusing only on iris compression and matching algorithm. Figure 1 shows the output of the segmentation process using Masek algorithm.

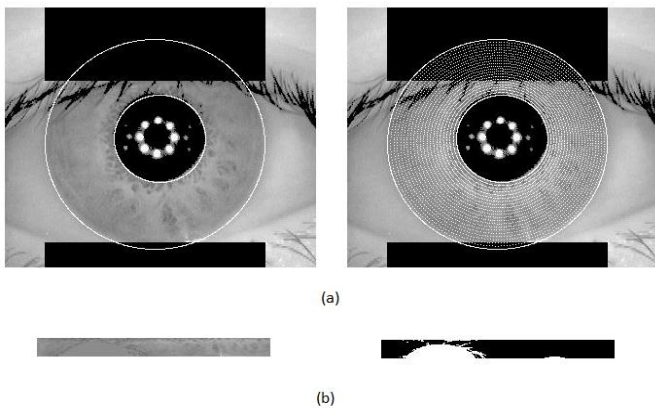


Fig. 1. Example the output of the segmentation process using Masek algorithm. (a) Automatic segmentation of an iris image from the CASIA database. Black regions denote detected eyelid and eyelash regions. (b) Illustration of the normalization process (polar array – noise array)

B. Feature Extraction

Feature extraction is the process of getting the iris features, Wavelet transform is used for this purpose.

C. Template Matching

Template matching compares the user template with templates from the database using a matching algorithm. The matching metric will give a measure of similarity between two

iris templates. Finally, a decision with high confidence level is made through matching methods to identify whether the user is an authentic or imposter.

D. Compression Algorithm

Geometry image and spherical wavelet transform will be used for the compression algorithm as shown in the next section. Figure. 2 shows the stages of iris compression algorithm.

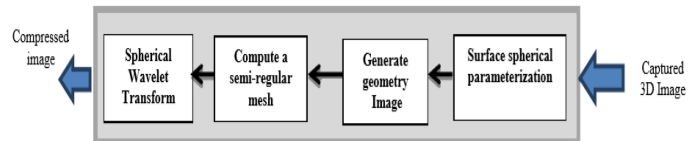


Fig. 2. Stages of iris compression algorithm

IV. SPHERICAL GEOMETRY IMAGE

Surfaces in computer graphics are commonly represented using irregular meshes. While such meshes can approximate a given shape using few vertices, their irregularity comes at a price, since most mesh operations require random memory accesses through vertex indices and texture coordinates. Also, filter kernels must handle arbitrary mesh neighborhoods, and techniques like morphing, level-of-detail (LOD) control, and compression are complicated. As an alternative, we have introduced the geometry image representation, which captures shape using a completely regular sampling, i.e. a 2D grid of (x,y,z) values [46]. The benefits of uniform grids are often taken for granted. Grids allow efficient traversal, random access, convolution, composition, down-sampling, and compression.

A. Spherical Parameterization

Geometric models are often described by closed, genus-zero surfaces, i.e. deformed spheres. For such models, the sphere is the most natural parameterization domain, since it does not require cutting the surface into disk(s). Hence the parameterization process becomes unconstrained [47]. Even though we may subsequently resample the surface signal onto a piecewise continuous domain, these domain boundaries can be determined more conveniently and a posteriori on the sphere. Spherical parameterization proves to be challenging in practice, for two reasons. First, for the algorithm to be robust it must prevent parametric “foldovers” and thus guarantee a 1-to-1 spherical map. Second, while all genus-zero surfaces are in essence sphere-shaped, some can be highly deformed, and creating a parameterization that adequately samples all surface regions is difficult. Once a spherical parameterization is obtained, a number of applications can operate directly on the sphere domain, including shape analysis using spherical harmonics, compression using spherical wavelets [46, 48], and mesh morphing [49].

Given a triangle mesh M , the problem of spherical parameterization is to form a continuous invertible map $\phi: S \rightarrow M$ from the unit sphere to the mesh. The map is specified by assigning each mesh vertex v a parameterization $\phi^{-1}(v) \in S$. Each mesh edge is mapped to a great circle arc, and each mesh triangle is mapped to a spherical triangle bounded by these

arcs. To form a continuous parameterization ϕ , we must define the map within each triangle interior. Let the points $\{A, B, C\}$ on the sphere be the parameterization of the vertices of a mesh triangle $\{A' = \phi(A), B' = \phi(B), C' = \phi(C)\}$. Given a point $P' = \alpha A' + \beta B' + \gamma C'$ with barycentric coordinates $\alpha + \beta + \gamma = 1$ within the mesh triangle, we must define its parameterization $P = \phi^{-1}(P')$. Any such mapping must have distortion since the spherical triangle is not developable.

B. Geometry Image

A simple way to store a mesh is using a compact 2D geometry images. Geometry images was first introduced by Gu et al. [46, 50] where the geometry of a shape is resampled onto a completely regular structure that captures the geometry as a 2D grid of $[x, y, z]$ values. The process involves heuristically cutting open the mesh along an appropriate set of cut paths. The vertices and edges along the cut paths are represented redundantly along the boundary of this disk. This allows the unfolding of the mesh onto a disk-like surface and then the cut surface is parameterized onto the square. Other surface attributes, such as normals and colors, are stored as additional 2D grids, sharing the same domain as the geometry, with grid samples in implicit correspondence, eliminating the need to store a parameterization. Also, the boundary parameterization makes both geometry and textures seamless. The simple 2D grid structure of geometry images is ideally suited for many processing operations. For instance, they can be rendered by traversing the grids sequentially, without expensive memory-gather operations (such as vertex index dereferencing or random-access texture filtering). Geometry images also facilitate compression and level-of-detail control. Figure 3 presents geometric representation of the iris image.

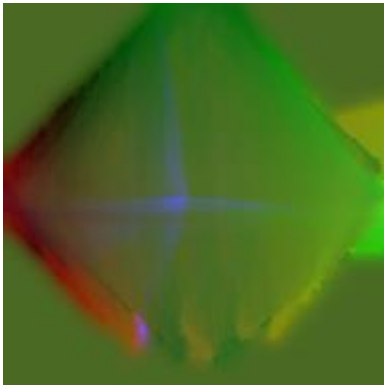


Fig. 3. Geometric representation of the iris image

C. Wavelet Transform

- Haar Transform:

Geometry images are regularly sampled 2D images that have three channels, encoding geometric information (x, y and z) components of a vertex in R^3 [50]. Each channel of the geometry image is treated as a separate image for the wavelet analysis. The Haar wavelet transform has been proven effective for image analysis and feature extraction. It represents a signal by localizing it in both time and frequency domains. The Haar wavelet transform is applied separately on each channel creating four sub bands LL, LH, HL, and HH where each sub

band has a size equal to 1/4 of the original image. The LL sub band captures the low frequency components in both vertical and horizontal directions of the original image and represents the local averages of the image. Whereas the LH, HL and HH sub bands capture horizontal, vertical and diagonal edges, respectively. In wavelet decomposition, only the LL sub band is used to recursively produce the next level of decomposition. The biometric signature is computed as the concatenation of the Haar wavelet coefficients that were extracted from the three channels of the geometry image.

- Spherical Wavelets:

To be able to construct spherical wavelets on an arbitrary mesh, this surface mesh should be represented as a multi-resolution mesh, which is obtained by regular 1:4 subdivision of a base mesh [51, 52, 53]. A multi-resolution mesh is created by recursive subdivision of an initial polyhedral mesh so that each triangle is split into four “child” triangles at each new subdivision

Denoting the set of all vertices on the mesh before the j th subdivision as $K(j)$ a set of new vertices $M(j)$ can be obtained by adding vertices at the midpoint of edges and connecting them with geodesics. Therefore, the complete set of vertices at the $j+1$ th level is given by $K(j+1) = K(j) \cup M(j)$. Consequently, the number of vertices at level j is given by: $10 \cdot 4^j + 2$. This process is presented in Figure 4 (a)-(d) where the iris image is shown at 4 different subdivision levels.

In this research, we use the discrete bi-orthogonal spherical wavelets functions defined on a 3-D mesh constructed with the lifting scheme proposed by Schröder and Sweldens [51, 52, 53, 54]. Spherical wavelets belong to second generation wavelets adapted to manifolds with non-regular grids. The main difference with the classical wavelet is that the filter coefficients of second generation wavelets are not the same throughout, but can change locally to reflect the changing nature of the surface and its measure.

They maintain the notion that a basis function can be written as a linear combination of basis functions at a finer, more subdivided level. Spherical wavelet basis is composed of functions defined on the sphere that are localized in space and characteristic scales and therefore match a wide range of signal characteristics, from high frequency edges to slowly varying harmonics [52, 55].

The basis is constructed of scaling functions defined at the coarsest scale and wavelet functions defined at subsequent finer scales. If there exist N vertices on the mesh, a total of N basis functions are created, composed of scaling functions and where N_0 is the initial number of vertices before the base mesh is subdivided. An interpolating subdivision scheme is used to construct the scaling functions on the standard unit sphere S denoted by $\phi_{j,k}$. The function is defined at level j and node $k \in k(j)$ such that the scaling function at level j is a linear combination of the scaling function at level j and $j+1$. Index j specifies the scale of the function and k is a spatial index that specifies where on the surface the function is centered. Using these scaling functions, the wavelet $\psi_{-(j,m)}$ at level j and node $m \in M(j)$ can be constructed by the lifting scheme.

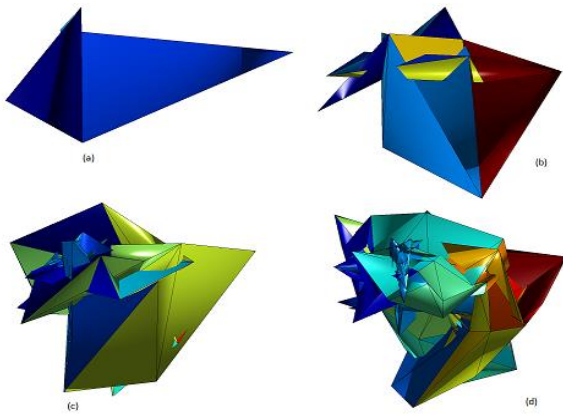


Fig. 4. Visualization of recursive partitioning of the iris mesh at different subdivision levels. (a) Initial icosahedron (scale 0). (b) Single partitioning of icosahedron (scale 1). (c) Two recursive partitioning of icosahedron (scale 2). (d) Three recursive partitioning of icosahedron (scale 3)

A usual shape for the scaling function is a hat function defined to be one at its center and to decay linearly to zero. As the j scale increases, the support of the scaling function decreases. A wavelet function is denoted by $\psi_{j,k} : S \rightarrow R$. The support of the functions becomes smaller as the scale increases. Together, the coarsest level scaling function and all wavelet scaling functions construct a basis for the function space L^2 :

$$L^2 = \{\varphi_{0,k} | k \in N_0\} \cup \{\psi_{j,m} | j \geq 0, m \in N_{j+1}\} \quad (1)$$

A given function $f: S \rightarrow R$ can be expressed in the basis as a linear combination of the basis functions and coefficients

$$f(x) = \sum_k \lambda_{0,k} \varphi_{0,k}(x) + \sum_{0 \leq j} \sum_m \gamma_{j,m} \psi_{j,m}(x) \quad (2)$$

Scaling coefficients $\lambda_{0,k}$ represent the low pass content of the signal f , localized where the associated scaling function has support; whereas, wavelet coefficients $\gamma_{j,m}$ represent localized band pass content of the signal, where the band pass frequency depends on the scale of the associated wavelet function and the localization depends on the support of the function. Figure 5 (a)-(g) presents the spherical wavelets of the iris image.

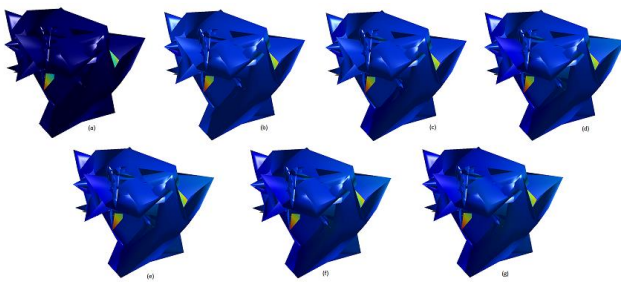


Fig. 5. Spherical wavelet transform of iris image. (a) using 5% of wavelet coefficients (b) using 10% of wavelet coefficients (c) using 20% of wavelet coefficients (d) using 40% of wavelet coefficients (e) using 60% of wavelet coefficients (f) using 80% of wavelet coefficients (g) Using all coefficients

V. EXPERIMENTAL RESULTS

The CASIA-IrisV4 data base was used to evaluate the performance of the proposed system. CASIA-IrisV4 is said to be an extension of CASIA-IrisV3 and contains six subsets. It

contains a total of 54,601 iris image from more than 1,800 genuine subject and 1,000 virtual subjects. All iris images are 8 bit gray-level JPEG files. In our experiment CASIA-Iris-Interval and CASIA-Iris-Lamp will be used.

A. Iris Recognition

In this experiment, CASIA-Iris-Interval contains 249 subjects. Only 99 subjects will be included in this experiment. For each one only 7 images for each eye is taken. The total number of classes is 198 which have 1386 images. 2-dimensional Haar wavelet transform is applied to the templates of the iris images which have dimension of $(20 * 480)$ for each image. Each application of the Haar wavelet decomposition reduces the size of the image to $\frac{1}{4}$ of its original size so the input to the K-fold cross validation method is a pattern of $(10 * 240)$ features.

K-fold cross-validation is a statistical method used to evaluate the performance of a learning algorithm [9]. In K-fold cross validation, the input data is divided into k nearly equal subsets. K iterations are performed. In each iteration, one of the k subsets is considered the test set while the other $k-1$ subsets are put together to form a training set. The output is the average error across all k trials.

The average recognition rate is 94% is achieved in this experiment. This result confirms that iris recognition is a reliable and accurate biometric technology. But as mentioned before, the iris recognition is not the objective of this research. We want to focus on 3D iris compression image which will be discussed in the next experiments.

B. Iris compression

In this experiment, the algorithm is applied to two sets from CASIA Iris-V4, CASIA-Iris-Interval and CASIA-Iris-Lamp. The input image is converted to 3D image then generate the geometry image. After this, a semi-regular mesh from a gim file is computed. Finally, the spherical wavelet transform on the mesh is computed. The total number of the features after computing wavelet transform is 774 features by keeping only the biggest coefficients. Different percentages of these coefficients were tested and each time the inverse wavelet transform was used to reconstruct the iris image. Figure 6 (a)-(g) shows the reconstructed images for the iris using different percentages of wavelet coefficient. These figure shows us that there is no visually difference between the original image and the corresponding reconstructed images.

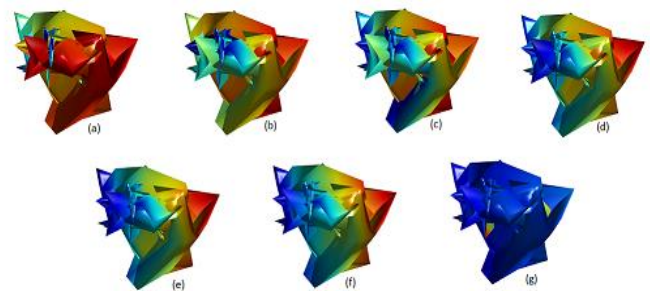


Fig. 6. Wavelet approximation of iris image. (a) using 2% of wavelet coefficients (b) using 5% of wavelet coefficients (c) using 10% of wavelet coefficients (d) using 20% of wavelet coefficients (e) Using all coefficient

To evaluate the quality of the reconstructed iris image, the Normalized Error (NE) and Normalized Correlation (NC) were used to. NE is given as follows:

$$NE = \frac{\|x-y\|}{\|x\|} \quad (3)$$

Where X is the original image and Y is the reconstructed image. i.e. NE is the norm of the difference between the original and reconstructed signals, divided by the norm of the original signal. The NC is given:

$$NC = \frac{\sum_{i=1}^M \sum_{j=1}^N X(i,j)Y(i,j)}{\sum_{i=1}^M \sum_{j=1}^N X(i,j)X(i,j)} \quad (4)$$

Where MxN is the size of the image. The NE and the NC values of the reconstructed images are presented in Table () for the different wavelet subsets.

TABLE I. NE AND NC FOR VARIOUS WAVELET SUBSETS FOR IRIS IMAGE FROM CASIA-IRIS-INTERVAL SUBSET

Percentage	5%	10%	20%	40%	60%	80%	100%
NE	0.477	0.1662	0.0912	0.0664	0.0517	0.0446	0.0311
Nc	0.6165	0.9278	0.9614	0.9671	0.977	0.9795	0.9979
No. of coefficient	39	77	155	310	464	619	774

TABLE II. NE AND NC FOR VARIOUS WAVELET SUBSETS FOR IRIS IMAGE FROM CASIA-IRIS-LAMP SUBSET

Percentage	5%	10%	20%	40%	60%	80%	100%
NE	0.3593	0.0411	0.0275	0.0210	0.0166	0.0130	0.0107
Nc	0.7318	0.9757	0.9959	1	0.9980	0.9973	0.9993
No. of coefficient	39	77	155	310	464	619	774

The NE and NC values indicate that the reconstructed images are the very similar to the original image. In the case of using only 20 % of the wavelets coefficients, the relative error of reconstruction is 9%. The reconstructed signal retains approximately 96.14% of the energy of the original signal while the number of coefficient is only 155.

VI. CONCLUSION

In this paper an innovative approach for 3D iris compression and recognition based on spherical wavelet parameterization was proposed. First. The iris image is to be preprocessed to obtain useful iris region. Image preprocessing contains, iris localization that detects the inner and outer boundaries of iris and iris normalization, in this step, iris image is converted from Cartesian coordinates to Polar coordinates. We are not focusing on the segmentation instead we are interested in iris compression hence we have used the existing algorithms for Masek. Next, the spherical wavelet features were extracted which provide a compact descriptive biometric signature. Spherical representation of iris permits effective dimensionality reduction through simultaneous approximations. The dimensionality reduction step preserves the geometry information, which leads to high performance matching in the reduced space. Multiple representation features based on spherical wavelet parameterization of the iris image

were proposed for the 3D iris compression and recognition. The database CASIA was utilized to test the proposed system. Experimental results show that the spherical wavelet coefficients yield excellent compression capabilities with minimal set of features. Furthermore, it was found that Haar wavelet coefficients extracted from the templet of the iris yield good recognition results.

ACKNOWLEDGEMENTS

The authors would like to acknowledge financial support for this work from the Deanship of Scientific Research (DSR), University of Tabuk, Tabuk, Saudi Arabia, under grant no. 0024/1435.

REFERENCES

- [1] A. Jain, A. Ross, and S. Prabhakar, "An Introduction to Biometric Recognition," IEEE Transactions on Circuits and Systems for Video Technology, vol. 14, no. 1, pp. 4–20, January 2004.
- [2] Rakshit, Soumyadip; Monro, Donald M., "An Evaluation of Image Sampling and Compression for Human Iris Recognition," Information Forensics and Security, IEEE Transactions on , vol.2, no.3, pp.605,612, Sept. 2007 doi: 10.1109/TIFS.2007.902401
- [3] Ives, R.W.; Bishop, D.A.D.; Yingzi Du; Belcher, C., "Effects of image compression on iris recognition performance and image quality," Computational Intelligence in Biometrics: Theory, Algorithms, and Applications, 2009. CIB 2009. IEEE Workshop on , vol., no., pp.16,21, March 30 2009-April 2 2009
- [4] J. Daugman "How iris recognition works," IEEE Trans. on Circuits and Systems for Video Technology., Vol. 14, No. 1, pp. 21-30.
- [5] J. G. Daugman, "High confidence visual recognition of persons by a test of statistical independence," IEEE Trans. Pattern Analysis and Machine. Intelligence, vol. 15, no. 11, pp. 1148 1161, Nov. 1993.
- [6] J. G. Daugman, "The importance of being random: Statistical principles of iris recognition," Pattern Recognition, vol. 36, no. 2, pp. 279–291, Feb. 2003.
- [7] Gu, Xianfeng, Steven J. Gortler, and Hugues Hoppe. "Geometry images." ACM Transactions on Graphics (TOG) 21.3 (2002): 355-361.
- [8] Hoppe, Hugues, and Emil Praun. "Shape compression using spherical geometry images." Advances in Multiresolution for Geometric Modelling. Springer Berlin Heidelberg, 2005. 27-46.
- [9] Blum, Avrim, Adam Kalai, and John Langford. "Beating the hold-out: Bounds for k-fold and progressive cross-validation." Proceedings of the twelfth annual conference on Computational learning theory. ACM, 1999.
- [10] J. Daugman, "Statistical richness of visual phase information: Update on recognizing persons by iris patterns," Int. J. Comput. Vis., vol. 45, pp. 25–38, 2001.
- [11] L. Flom and A. Safir, "Iris Recognition system," U.S. Patent 4 641 394, 1987.
- [12] R. Johnson, "Can iris patterns be used to identify people?," Chemical and Laser Sciences Division LA-12 331-PR, Los Alamos Nat. Lab., Los Alamos, CA, 1991.
- [13] K. Bae, S. Noh, and J. Kim, "Iris feature extraction using independent component analysis," in Proc. 4th Int. Conf. Audio- and Video-Based Biometric Person Authentication, 2003, pp. 838–844.
- [14] J. Daugman, "Biometric personal identification system based on iris analysis," U.S. Patent 5 291 560, 1994.
- [15] R.Wildes, J. Asmuth, S. Hsu, R. Kolczynski, J. Matey, and S. McBride, "Automated, noninvasive iris recognition system and method," U.S. Patent 5 572 596, 1996.
- [16] J. G. Daugman, "Phenotypic versus genotypic approaches to face recognition," in Face Recognition: From Theory to Applications. Heidelberg: Springer-Verlag, 1998, pp. 108–123.
- [17] W. Boles and B. Boashash, "A human identification technique using images of the iris and wavelet transform," Signal Processing, IEEE Transactions on, vol. 46, no. 4, pp. 1185–1188, April 1998.

- [18] R. P. Wildes, "Iris recognition: an emerging biometric technology," Proceedings of the IEEE, vol. 85, no. 9, pp. 1348–1363, September 1997.
- [19] W. Boles and B. Boashash, "A human identification technique using images of the iris and wavelet transform," IEEE Trans. Signal Processing, vol. 46, pp. 1185–1188, Apr. 1998.
- [20] R. Wildes, J. Asmuth, G. Green, S. Hsu, R. Kolczynski, J. Matey, and S. McBride, "A machine-vision system for iris recognition," Mach. Vis. Applic., vol. 9, pp. 1–8, 1996.
- [21] C. Tisse, L. Martin, L. Torres, and M. Robert, "Person identification technique using human iris recognition," in Proc. Vision Interface, 2002, pp. 294–299.
- [22] T. Tangsukson and J. Havlicek, "AM-FM image segmentation," in Proc. IEEE Int. Conf. Image Processing, 2000, pp. 104–107.
- [23] J. Havlicek, D. Harding, and A. Bovik, "The multi-component AM-FM image representation," IEEE Trans. Image Processing, vol. 5, pp. 1094–1100, June 1996.
- [24] C. Park, J. Lee, M. Smith, and K. Park, "Iris-based personal authentication using a normalized directional energy feature," in Proc. 4th Int. Conf. Audio- and Video-Based Biometric Person Authentication, 2003, pp. 224–232.
- [25] B. Kumar, C. Xie, and J. Thornton, "Iris verification using correlation filters," in Proc. 4th Int. Conf. Audio- and Video-Based Biometric Person Authentication, 2003, pp. 697–705.
- [26] P. Hong and M. I. T. Smith, "An octave-band family of nonredundant directional filter banks", IEEE proceedings of ICASSP, vol. 2, pp.1165-1168, 2002.
- [27] Y. Huang, S. Luo, and E. Chen, "An efficient iris recognition system," in Proceedings of the First International Conference on Machine Learning and Cybernetics, China, November 2002, pp. 450–454.
- [28] L. Ma, T. Tan, Y. Wang, and D. Zhang, "Efficient iris recognition by characterizing key local variations," Image Processing, IEEE Transactions on, vol. 13, no. 6, pp. 739–750, June 2004
- [29] J. Behar, M. Porat, and Y.Y. Zeevi, "Image Reconstruction from Localized Phase," IEEE Trans. Signal Processing, vol. 40, no. 4, pp. 736-743, Apr. 1992.
- [30] GU, X., GORTLER, S., AND HOPPE, H. 2002. Geometry images. ACM SIGGRAPH 2002, pp. 355-361.
- [31] SANDER, P., WOOD, Z., GORTLER, S., SNYDER, J., AND HOPPE, H. 2003. Multi-chart geometry images. Eurographics Symposium on Geometry Processing 2003, pp. 146-155.
- [32] PRAUN, E., AND HOPPE, H. 2003. Spherical parametrization and remeshing. ACM SIGGRAPH 2003, pp. 340-349.
- [33] LOSASSO, F., HOPPE, H., SCHAEFER, S., AND WARREN, J. 2003. Smooth geometry images. Eurographics Symposium on Geometry Processing 2003, pp. 138-145.
- [34] BRICEÑO, H., SANDER, P., MCMILLAN, L., GORTLER, S., AND HOPPE, H. 2003. Geometry videos: A new representation for 3D animations. ACM Symposium on Computer Animation 2003, pp. 136-146.
- [35] M. H. Mahoor and M. Abdel-Mottaleb, "Face recognition based on 3D ridge images obtained from range data," Pattern Recognition, Vol. 42, pp. 445 – 451, 2009.
- [36] K.W. Bowyer, K.Chang, and P. Flynn, "A survey of approaches and challenges in 3D and multi-modal 3D + 2D face recognition," Computer Vision and Image Understanding, Vol. 101, No.1, pp. 1-15, 2006.
- [37] A.F. Abate, M. Nappi, D. Riccio and G. Sabatino, "2D and 3D face recognition: A survey," Pattern Recognition Letters, Vol. 28, pp. 1885-1906, 2007.
- [38] K. I. Chang, K. W. Bowyer and P. J. Flynn, "Multiple nose region matching for 3D face recognition under varying facial expression," IEEE Transactions on Pattern Analysis and Machine Intelligence, Vol. 28, pp. 1695-1700, 2006.
- [39] G. Günlü and H. S. Bilge, "Face recognition with discriminating 3D DCT coefficients," The Computer Journal, Vol. 53, No. 8, pp. 1324-1337, 2010.
- [40] L. Akarun, B. Gokberk, and A. Salah, "3D face recognition for biometric applications," In Proceedings of the European Signal Processing Conference, Antalya, 2005.
- [41] Ramadan, Rabab M., and Rehab F. Abdel-Kader. "3D Face Compression and Recognition using Spherical Wavelet Parametrization." International Journal of Advanced Computer Science and Applications (IJACSA) 3.9 (2012).
- [42] Masek, Libor. Recognition of human iris patterns for biometric identification. Diss. Master's thesis, University of Western Australia, 2003.
- [43] Kulkarni, S. B., R. S. Hegadi, and U. P. Kulkarni. "Improvement to libor masek algorithm of template matching method for iris recognition." Proceedings of the International Conference & Workshop on Emerging Trends in Technology. ACM, 2011.
- [44] Kevin W. Boyer, Karan Hollingsworth and Patrick J. Flynn. Image understanding for iris biometric: A survey Computer Vision and Image Understanding 110 (2), 281-307, May 2008.
- [45] Richard Yew Fatt Ng, Yong Haur Tay and Kai Ming Mok. An Effective segmentation method for iris recognition system, The Institution of Engineering and Technology, 2008, PP-548 to 553
- [46] P. Alliez and C. Gotsman, "Shape compression using spherical geometry images," In Proceedings of the Symp. Multi-resolution in Geometric Modeling, 2003.
- [47] Praun and H. Hoppe, "Spherical parameterization and remeshing," in ACM SIGGRAPH 2003, pp. 340–349, 2003.
- [48] L. Pastor, A. Rodriguez, J. M. Espadero, and L. Rincon, "3D wavelet-based multi-resolution object representation," Pattern Recognition, Vol. 34, pp. 2497-2513, 2001.
- [49] M. Alexa, "Recent advances in mesh morphing," Computer Graphics Forum, Vol. 21, No. 2, pp. 173-196, 2002.
- [50] X. Gu, S. J. Gortler and H. Hoppe, "Geometry images," ACM SIGGRAPH, pp. 355-361, 2002.
- [51] P. Schröder and W. Sweldens, "Spherical wavelets: Efficiently representing functions on a sphere," In Proceedings of Computer Graphics (SIGGRAPH 95), pp. 161-172, 1995.
- [52] P. Schröder and W. Sweldens, "Spherical wavelets: Texture processing," in Rendering Techniques, New York, 1995, Springer Verlag.
- [53] P. Schröder and W. Sweldens, "Spherical wavelets: efficiently representing functions on a sphere," In Proceedings of Computer Graphics (SIGGRAPH 95), pp. 161-172, 1995.
- [54] S. Campagna and H.-P. Seidel. Parameterizing meshes with arbitrary topology. In H.Niemann, H.-P. Seidel, and B. Girod, editors, Image and Multidimensional Signal Processing' 98, pp. 287-290, 1998.
- [55] P. Yu, P. Ellen Grant, Y. Qi, X. Han, F. Ségonne and Rudolph Pienaar, "Cortical surface shape analysis based on spherical wavelets," IEEE Transactions on Medical Imaging, Vol. 26, No. 4, pp. 582-597, 2007.

AUTHORS PROFILE

Rabab Mostafa Ramadan attended Suez Canal University, Port-Said, Egypt majoring in Computer Engineering, earning the BS degree in 1993. She graduated from Suez Canal University, Port-Said, Egypt with a MS degree in Electrical Engineering in 1999. She joined the Ph.D. program at Suez Canal University, Port-Said, Egypt and earned her Doctor of Philosophy degree in 2004. She worked as an Instructor in the Department of Electric Engineering (Computer division), Faculty of Engineering, Suez Canal University. From 1994 up to 1999, as a lecturer in Department of Electric Engineering (Computer division), Faculty of Engineering, Suez Canal University. From 1999 up to 2004, and as an assistant Professor in Department of Electric Engineering (Computer division), Faculty of Engineering, Suez Canal University. From 2004 up to 2009. She is currently an Assistant professor in Department of Computer Science, College of Computer & Information Technology, Tabuk University, Tabuk, KSA. Her current research interests include Image Processing, Artificial Intelligence, and Computer Vision.

Gram–Schmidt Process in Different Parallel Platforms

(Control Flow versus Data Flow)

Genci Berati

Tirana University, Department of Mathematics
Tirane, Albania

Abstract—Important operations in numerical computing are vector orthogonalization. One of the well-known algorithms for vector orthogonalisation is Gram–Schmidt algorithm. This is a method for constructing a set of orthogonal vectors in an inner product space, most commonly the Euclidean space R^n . This process takes a finite, linearly independent set $S = \{b_1, b_2, \dots, b_k\}$ vectors for $k \leq n$ and generates an orthogonal set $S_1 = \{o_1, o_2, \dots, o_k\}$. Like the most of the dense operations and big data processing problems, the Gram–Schmidt process steps can be performed by using parallel algorithms and can be implemented in parallel programming platforms. The parallelized algorithm is dependent to the platform used and needs to be adapted for the optimum performance for each parallel platform. The paper shows the algorithms and the implementation process of the Gram –Schmidt vector orthogonalisation in three different parallel platforms. The three platforms are: a) control flow shared memory hardware systems with OpenMP, b) control flow distributed memory hardware systems with MPI and c) dataflow architecture systems using Maxeler Data Flow Engines hardware. Using as single running example a parallel implementation of the computation of the Gram –Schmidt vector orthogonalisation, this paper describes how the fundamentals of parallel programming, are dealt in these platforms. The paper puts into evidence the Maxeler implementation of the Gram–Schmidt algorithms compare to the traditional platforms. Paper treats the speedup and the overall performance of the three platforms versus sequential execution for 50-dimensional Euclidian space.

Keywords—Gram-Schmidt Algorithm; Parallel programming model; OpenMP; MPI; Control Flow architecture

I. INTRODUCTION

Classifications of parallel programming paradigms are mostly related to the hardware architectures.

The paradigms of parallel programming can be divided generally into two categories: process communicates [1] and problem decomposition [2].

Process communication is correlated to the instruments by which parallel processes communicate and share sources to each other. The most common forms of process interaction are shared memory and message passing between processes. Shared memory is an efficient instrument for passing data between programs by accessing that same shared memory. Algorithms may run on a single processor in sequential or on multiple separate processors in sequential way or in parallel. In shared memory model, parallel tasks share a global address

space which they read and write to asynchronously. In shared memory systems the code can create threads each of them can access the same variable in parallel.

Message passing is a concept from computer science related mostly with distributed memory architectures for the parallel programming platforms that is used extensively in the design and implementation of modern software applications; it is very important for some models of concurrency and object-oriented programming. In a message passing model, parallel tasks exchange data and communicate through passing messages to one another. Either shared or distributed can be based Control Flow [3] Von Newman traditional architecture.

The paper deals with three different programming platforms (OpenMP, MPI and Maxeler). These three platforms can be grouped in two different architectures, in Control Flow (OpenMP and MPI) and Data Flow (Maxeler) architectures. These two different computing architectures are compared and analyzed in this paper by choosing a typical dense operations and big data problem which is the Gram – Schmidt process.

Is chosen Gram Schmidt classic algorithm for a 50-dimensional inner product space. The algorithm has operations rising in a significant progression from step to step. If we have a set $S_1 = \{o_1, o_2, \dots, o_n\}$ of orthogonal vectors as basis for the inner product space L , then we can express any vector of space L as a linear combination of the vectors in S_1 :

Let us have an arbitrary basis $\{b_1, b_2, \dots, b_n\}$ for an n -dimensional inner product space L . The Gram-Schmidt algorithm constructs an orthogonal basis $\{o_1, o_2, \dots, o_n\}$ for L . In our paper we take the arbitrary basis $\{b_1, b_2, \dots, b_{50}\}$ for an 50-dimensional inner product space L and after performing the Gram-Schmidt algorithm into a sequential machine platform, OpenMP platform, MPI platform and Maxeler controlflow machine we then constructs an orthogonal basis $\{o_1, o_2, \dots, o_n\}$ for L each time. The paper intends to compare the performance of the parallel platforms and to measure the speedup for each platform. The characteristics of the algorithms regards to the number of nested loops and the numbers of operations for iteration will define the best platform to recommend.

The reason why is selected the Gram – Schmidt algorithm is the time complexity. This algorithm complexity is $O(n^3)$. The operations in each iteration of the process rise progressively, so it is of large interest to study the behavior in different parallel programming platforms.

II. GRAM-SCHMIDT ALGORITHM

To obtain an orthonormal basis for an inner product space L , we use the Gram-Schmidt algorithm to construct an orthogonal basis. For \mathbb{R}^n with the Eukclidean inner product (dot product), we of course already know of the orthonormal basis $\{(1, 0, 0, \dots, 0), (0, 1, 0, \dots, 0), \dots, (0, \dots, 0, 1)\}$. For more abstract spaces, however, the existence of an orthonormal basis is not obvious. The Gram-Schmidt algorithm is powerful in that it not only guarantees the existence of an orthonormal basis for any inner product space, but actually gives the way of construction of such a basis.

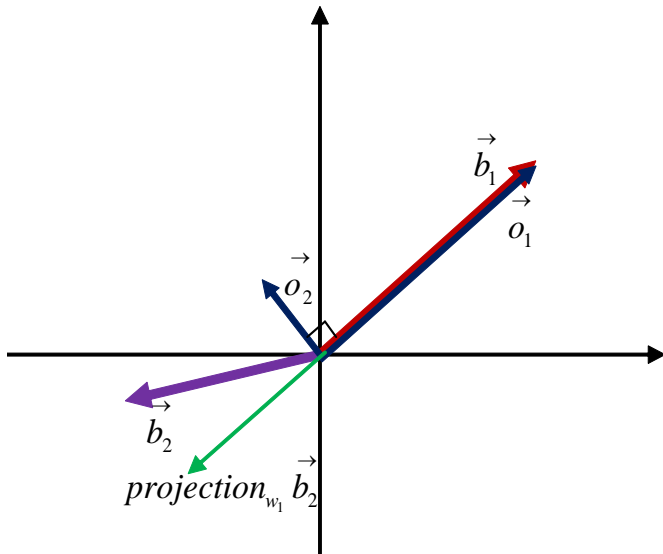


Fig. 1. Graphic representation of the Gram – Schmidt orthogonalisation

The Gram – Schmidt algorithm can be expressed in n steps to be performed. The algorithm steps are:

- 1 for $i = 1$ to n
- 2 $v_i = a_i$
- 3 for $i = 1$ to n
- 4 $r_{ii} = \|v_i\|$
- 5 $q_i = v_i / r_{ii}$
- 6 for $j = i + 1$ to n
- 7 $r_{ij} = q_i \cdot v_j$
- 8 $v_j = v_j - r_{ij} q_i$

This algorithm is implemented in C++ code using Code::Blocks programming platform. This platform is chosen because it is portable to the parallel programming platforms.

III. GRAM – SCHMIDT VECTOR ORTHOGONALISATION ALGORITHM (SEQUENTIAL IMPLEMENTATION)

We implemented the steps mentioned in the previous section in the Code::Blocks¹ with C++ compiler. In our implementation, we take $k=n=50$, where k is the number of the linear independent vectors and n is the dimension of the Euclidian space. The C++ program code of Gram – Schmidt algorithm for a 50 dimensional inner product space, in our example named space L , for $k=50$, looks like:

```
#include <cstdlib>
#include <iostream>
#include <math.h>
using namespace std;
double b[50][50];
double r[50][50], q[50][50];
int main(int argc, char *argv[]) {
    int i, j;
    for (int i=0; i<50; i++)
        for (int j=0; j<50; j++)
            {b [i][j]=rand() % 10;}
    int k;
    for (k=0; k<50; k++){
        r[k][k]=0; // equivalent to sum = 0
        for (i=0; i<50; i++)
            r[k][k] = r[k][k] + b[i][k] * b[i][k]; //rkk = sqr(a0k) + sqr(a1k) + sqr(a2k)
        r[k][k] = sqrt(r[k][k]); //
        cout << endl << "R"<<k<<k<<": " << r[k][k];
        for (i=0; i<3; i++)
            {q[i][k] = b[i][k]/r[k][k];
            cout << "q" <<i<<k<<": " <<q[i][k] << " ";}
        for(j=k+1; j<50; j++)
            {r[k][j]=0; for(i=0; i<50; i++) r[k][j] += q[i][k] * b[i][j];
            cout << endl << "r"<<k <<j<<": " <<r[k][j] <<endl;
            for (i=0; i<50; i++) b[i][j] = a[i][j] - r[k][j]*q[i][k];
            for (i=0; i<50; i++) cout << "b"<<j<<": " << b[i][j]<< " "; }
        system("PAUSE");
    }
    return EXIT_SUCCESS;}
```

Fig. 2. Sequential Gram – Schmidt vector orthogonalisation. Program code in C++ (Code::Blocks)

The average execution time of this sequential algorithm is around 110 seconds. Now let's see in the next session the parallel implementation of this algorithm in OpenMP² parallel platform for C++.

IV. THE GRAM-SCHMIDT VECTOR ORTHOGONALISATION ALGORITHM FOR OPENMP PLATFORM

A parallel program is composed of parallel executing processes. A task-parallel model [4] focuses on processes, or threads of execution. These processes sometimes share the same sources, which emphasizes the need for communication between those processes. Task parallelism is a natural way to express message-passing communication between processing units. It is usually classified as MIMD/MPMD or MISD [5].

A parallel model consists of performing operations on a data set which usually regularly structures in an array. A set of tasks will operate on this data, but independently on separate partitions. In a shared memory system, the data will be accessible to all tasks, but in a distributed-memory system it will divide between memories.

Parallelism is usually classified as SIMD/SPMD (Single Instruction-Multiple Data)/(Single Program-Multiple Data) [6].

¹ Code::Blocks, "A free C, C++ and Fortran IDE".
<http://www.codeblocks.org/>

² OpenMP Specifications. <http://www.openmp.org/blog/specifications>

The systems are categorized into two categories. [7] The systems of the first category were characterized by the isolation of the abstract design space seen by the programmer from the parallel, distributed implementation. In this, all processes are presented with equal access to some kind of shared memory space. In its loosest form, any process may attempt to access any item at any time. The second category considers machines in which the two levels are closer together and in particular, those in which the programmer's world includes explicit parallelism [8]. This category discards shared memory based cooperation in favor of some form of explicit message passing.

A classical shared memory parallel platform is OpenMP. OpenMP (Open Multiprocessing) is an API that supports multi-platform shared memory multiprocessing programming in C, C++ and Fortran programming language. OpenMP³ is an application program interface providing a multi-threaded programming model for shared memory parallelism; it uses directives to extend sequential languages. It consists of a set of compiler directives, library routines, and environment variables that influence run-time behavior.

OpenMP uses a portable, scalable model that gives programmers a simple and flexible interface for developing parallel applications for platforms like a standard desktop computer or supercomputer. After the configuration of the Code::Blocks for OpenMP, we implemented on this platform our algorithm. The code is parallelized for our nested loops as below:

```
#include <cstdlib>
#include <iostream>
#include <math.h>
#include <omp.h>
using namespace std;
double b[50][50];
double r[50][50], q[50][50];
int main(int argc, char *argv[]) {
    int i, j;
    #pragma omp parallel for
    for (int i=0; i<50; i++)
    for (int j=0; j<50; j++)
    {b [i][j]=rand() % 10;}
    int k;
    #pragma omp parallel for
    for (k=0; k<50; k++){
    r[k][k]=0; // equivalent to sum = 0
    for (i=0; i<50; i++)
    r[k][k] = r[k][k] + b[i][k] * b[i][k]; //rkk = sqr(a0k) + sqr(a1k) + sqr(a2k)
    r[k][k] = sqrt(r[k][k]); //
    cout << endl << "R" << k << k << k << " " << r[k][k];
    #pragma omp parallel for
    for (i=0; i<3; i++)
```

```
{q[i][k] = b[i][k]/r[k][k];
cout << "q" << i << k << k << " " << q[i][k] << " ";
for(j=k+1; j<50; j++)
{r[k][j]=0; for(i=0; i<50; i++) r[k][j] += q[i][k] * b[i][j];
cout << endl << "r" << k << j << k << " " << r[k][j] << endl;
for (i=0; i<50; i++) b[i][j] = b[i][j] - r[k][j]*q[i][k];
for (i=0; i<50; i++) cout << "b" << i << j << k << " " << b[i][j] << " "; }}
system("PAUSE");
return EXIT_SUCCESS;}
```

Fig. 3. OpenMP Gram – Schmidt vector orthogonalisation. Program code in C++ (Code::Blocks)

For directive in the code above splits the for-loop, so each thread in the current team handles a different portion of the loop. The main directive used is “#pragma omp parallel for”. This statement is used to open the switch of OpenMP in this algorithm code. Only small changes in C++ sources code are required in order to use OpenMP. So each thread gets a different section of the loop, and they execute their own sections in parallel. We executed this code in the quad core computer where we before executed the sequential algorithm. The average execution time is 30 seconds. Significant speedup is reached for the Gram Schmidt algorithm when we use OpenMP parallel features. By trying this C++ code for OpenMP in PC with different number of cores and the execution time is shown in the table 1, is made a speedup analysis.

V. THE GRAM–SCHMIDT VECTOR ORTHOGONALISATION IN MPI

Message Passing Interface (MPI) is a standardized and portable message-passing system designed. The standard defines the syntax and semantics of a core of library routines useful to a wide range of users writing portable message-passing programs [9] in different programming languages such as Fortran, C, C++ and Java. Message passing this model uses communication libraries to allow efficient parallel programs to be written for distributed memory systems. These libraries provide routines to initiate and configure the messaging environment as well as sending and receiving data packets. Currently, the most popular high-level message-passing system for scientific and engineering applications is MPI (Message Passing Interface)⁴.

We executed the code in a cluster with four computers with the same parameters like the quad core in which we executed the sequential algorithm and OpenMP code. The average time of execution is 22 seconds. The C++ code adopted for using the MPI library for parallelization of our Gram Schmidt vector orthogonalisation algorithm. Both platforms OpenMP and MPI are control flow based architectures. The figure 2 below show the control flow design architecture.

³ OpenMP Specifications. <http://www.openmp.org/blog/specifications/>

⁴ Message Passing Interface. <http://www-unix.mcs.anl.gov/mapi/index.html>

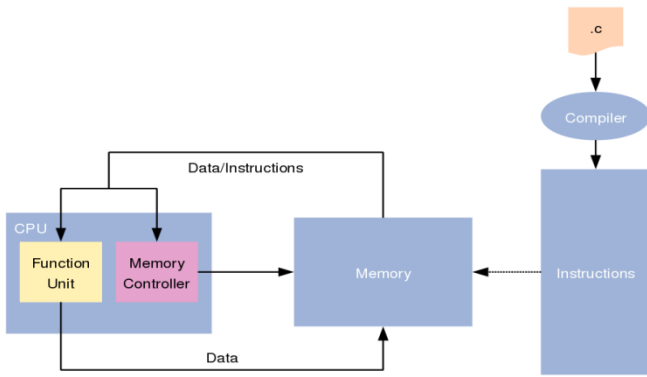


Fig. 4. Control Flow architecture design (source Maxeler)

```
#include <cstdlib>
#include <iostream>
#include <math.h>
#include <mpi.h>
using namespace std;
double b[50][50];
double r[50][50], q[50][50];
int main(int argc, char *argv[]) {
int i, j, rank, nprocs, count, start, stop;
MPI_Init(&argc, &argv);
// get the number of processes, and the id of this process
MPI_Comm_rank(MPI_COMM_WORLD, &rank);
MPI_Comm_size(MPI_COMM_WORLD, &nprocs);
// we want to perform 50 iterations in total. Work out the
// number of iterations to perform per process...
for (int i=0; i<50; i++)
for (int j=0; j<50; j++)
{b [i][j]=rand() % 10;}
int k;
for (k=0; k<50; k++){
r[k][k]=0; // equivalent to sum = 0
for (i=0; i<50; i++)
r[k][k] = r[k][k] + b[i][k] * b[i][k]; //rkk = sqr(a0k) + sqr(a1k) + sqr(a2k)
r[k][k] = sqrt(r[k][k]); //
cout << endl << "R" << k << k << k << " : " << r[k][k];
for (i=0; i<3; i++)
{q[i][k] = b[i][k]/r[k][k];
cout << "q" << i << k << k << " : " << q[i][k] << " , ";}
for(j=k+1; j<50; j++)
{r[k][j]=0; for(i=0; i<50; i++) r[k][j] += q[i][k] * b[i][j];
cout << endl << "r" << k << j << k << " : " << r[k][j] << endl;
for (i=0; i<50; i++) b[i][j] = a[i][j] - r[k][j]*q[i][k];
for (i=0; i<50; i++) cout << "b" << j << k << " : " << b[i][j] << " , "; MPI_Finalize();}}
system("PAUSE");
return EXIT_SUCCESS;}

```

Fig. 5. MPI Gram – Schmidt vector orthogonalisation. Program code in C++ (Code::Blocks)

VI. THE GRAM–SCHMIDT VECTOR ORTHOGONALISATION IN MAXELER

Dataflow architecture [10] is a computer architecture that differs in significant contrasts to the traditional Control Flow - Von Neumann architecture. Dataflow architectures do not have a program counter, or (at least conceptually) the executability and execution of instructions is based on the availability of input arguments to the instructions, so that the order of instruction execution is unpredictable: I. e. behavior is undetermined⁵.

Dataflow machines have been around for more than two decades. Implementation challenges left the technology hidden for many years, but last five years the data flow parallel programming is becoming more and more a technological reality. One of the dataflow machines is the Manchester Dataflow Machine (MDFM) using single-assignment language SISAL. Another successful dataflow machine is Maxeler machine. The Gram – Schmidt algorithm is implemented to the MPC-X Series⁶ machine.

The implementation process of our algorithm includes the adaption of the C++ host code for export to the MPC module. The Data Flow Engine (DFE) part of an accelerated solution itself contains two components: one or more Kernels, responsible for the data computations; and a single Manager, which orchestrates global data movement for the CPUs, DFEs and Kernels+Memory inside. Hence, accelerating an application requires the user to write three program parts: Kernel(s), A Manager, and a CPU application. The Kernel and the Manager is created by writing programs in MaxJ: an extended form of Java adding operator overloading. Using MaxCompiler requires only minimal familiarity with Java. A developer executes a MaxCompiler-based program to produce a “.max file” containing the DFE configuration, meta-data and SLiC functions. The CPU application is compiled and linked with the .max file, SLiC and MaxelerOS, to create the application executable.

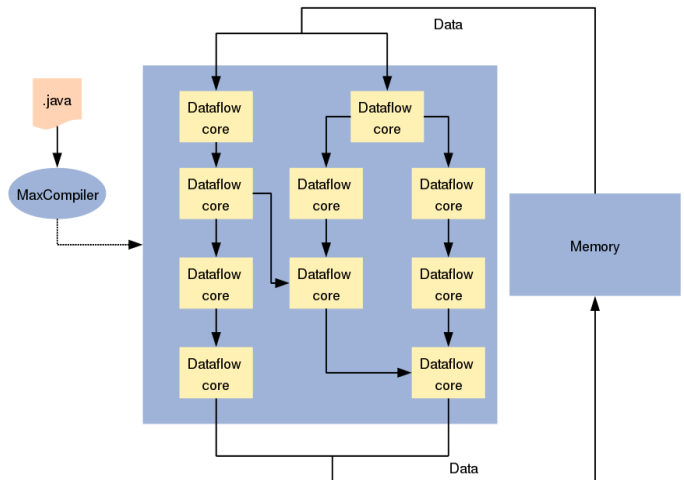


Fig. 6. Data Flow architecture design (source Maxeler)

⁵ http://en.wikipedia.org/wiki/Dataflow_architecture, Retrieved on 21 April 2015

⁶ <https://www.maxeler.com/products/mpc-xseries/>, Retrieved on 20 January 2015.

VII. RESULTS

This paper was dealing the behavior of parallel Gram – Schmidt vector orthogonalization algorithms with respect to OpenMP, MPI and Maxeler platform. The results we found are satisfactory. The number of input data size increased Maxeler gives very good performance. Nevertheless, the performance factor presented here is the execution times and speedup of the implementations for same input data size realized in the parallel programming models.

The speedup achieved by a parallel application varies for different programming models. The models chosen in this paper are only considered from the speedup perspective.

The results of the execution time of the algorithms in three machines are shown in figure 7. In this figure is shown the time in seconds in sequential (column 2) in OpenMP (column 3), MPI (column 4) which are Control Flow based architecture. In the figure 7 is shown also the speedup reached in OpenMP (column 5), speedup reached in MPI (column 6) and the speedup reached in the Maxeler machine (column 7). In Maxeler machine, the speedup is high, but limited and independent to the memory performance.

Memory	(Sequential Program) Execution Time	(OpenMP Program) Execution Time	(MPI Program) Execution Time	Speed up Seq/OpenMP	Speed up Seq/MPI	Speed up Seq/Maxeler
1MB	120	60	55	2.00	2.18	20
2MB	90	28	30	3.21	3.00	20
4MB	70	20	25	3.50	2.80	20
8MB	60	15	23	4.00	2.61	20

Fig. 7. Execution time analysis

VIII. CONCLUSIONS

For Gram – Schmidt vector orthogonalisation the parallel approach demands rethinking algorithms, adaption of the programming approach and environment and underlying hardware. There are a lot of possibilities to effectively create parallel version of the algorithms. To be efficient and to have the optimal performance in algorithm execution is very important to select the proper platform related to the contextual problem. In our example is pretty obvious that the Maxeler technology is the most efficient platform. The Maxeler

machine spends some initial time for transfer from host to DFE, but control time is extremely slow compare to processing time. Data Flow architecture offers significant capabilities to accelerate scientifically numerical computations, such as the Gram – Schmidt vector orthogonalisation. Improvements in Maxeler and bus technology indicate that Data Flow will increase their lead over general purpose processors over the next few years. In this paper is shown that Maxeler machine with its software system are not wedded to von Neumann architectures nor to the von Neumann execution model. Maxeler platform works very well for calculating Gram – Schmidt vector orthogonalisation reaching a significant speedup.

This paper is addressed to the programmers, by providing taxonomy of parallel language designs. They can decide which language to use for contest of their project.

REFERENCES

- [1] Gregory r. Andrews, ACM Computing Surveys, “Paradigms for Process Interaction in Distributed Programs”, Vol 23, No 1, March 1991, page 50-52
- [2] Stephen Boyd, Lin Xiao, and Almir Mutapcic, Notes for EE392o, Stanford University, Autumn, 2003: , “Notes on Decomposition Methods”, page 1
- [3] Micah Beck, Keshav Pingali, Department of Computer Science Cornell University, Ithaca, NY 14853, “From Control Flow To Dataflow”, page 2
- [4] Dounia Khaldi, Pierre Jouvelot, Corinne Ancourt and Francois Irigoien, “ Task Parallelism and Data Distribution: An Overview of Explicit Parallel Programming Languages”, page 10-16
- [5] W, F, McColl, “A General Model of Parallel Computing”, programming research group, Oxford University materials, page 6
- [6] Mark A. Nichols, Howard Jay Siegel, Henry G. Dietz, “Data Management and Control-Flow Aspects of an SIMD/SPMD Parallel Language/Compiler”, page 224-225
- [7] Christoph Kessler, Jörg Keller, “Models for Parallel Computing: Review and Perspectives”, PARS, Mitteilungen, December 2007, ISBN 0177-0454, page 3
- [8] Manar Qamhieh, Serge Midonnet, “Experimental Analysis of the Tardiness of Parallel Tasks in Soft Real-time Systems”, 18th Workshop on Job Scheduling Strategies for Parallel Processing (JSSPP), May 2014, page 5-6
- [9] Board of Trustees of the University of Illinois, “Introduction to MPI”, 2001 page 16
- [10] ARTHUR H. VEEN, Center for Mathematics and Computer Science “Dataflow Machine Architecture”, ACM Computing Surveys, December 1986, Vol. 18, No. 4, December 1986, page 2

A Heuristic Approach for Minimum Set Cover Problem

Fatema Akhter

IEEE student member

Department of Computer Science and Engineering
Jatiya Kabi Kazi Nazrul Islam University Trishal,
Mymensingh-2220, Bangladesh

Abstract—The Minimum Set Cover Problem has many practical applications in various research areas. This problem belongs to the class of NP-hard theoretical problems. Several approximation algorithms have been proposed to find approximate solutions to this problem and research is still going on to optimize the solution. This paper studies the existing algorithms of minimum set cover problem and proposes a heuristic approach to solve the problem using modified hill climbing algorithm. The effectiveness of the approach is tested on set cover problem instances from OR-Library. The experimental results show the effectiveness of our proposed approach.

Keywords—Set Cover; Greedy Algorithm; LP Rounding Algorithm; Hill Climbing Method

I. INTRODUCTION

For a given set system on a universe of items and a collection of a set of items, Minimum Set Cover Problem (MSCP) [1] finds the minimum number of sets that covers the whole universe. This is a NP hard problem proven by Karp in [2]. The optimization has numerous applications in different areas of studies and industrial applications [3]. The applications include multiple sequence alignments for computational biochemistry, manufacturing, network security, service planning and location problems [4]–[7].

Several heuristics and approximation algorithms have been proposed in solving the MSCP [8]. Guanghai Lan et al. proposed a Meta-RaPS (Meta-heuristic for Randomized Priority Search) [9]. Fabrizio Grandoni et al. proposed an algorithm based on the interleaving of standard greedy algorithm that selects the min-cost set which covers at least one uncovered element [10]. Amol Deshpande et al. [11] proposed an Adaptive Dual Greedy which is a generalization of Hochbaums [12] primal-dual algorithm for the classical Set Cover Problem.

This paper studies some popular existing algorithms of MSCP and proposes a heuristic approach to solve MSCP using modified hill climbing method. Within our knowledge, the same approach for MSCP of this paper has not been yet reported. Although this work implements two popular algorithms, Greedy Minimum Set Cover [14] and Linear Polynomial Rounding (LP) algorithm [15] to find solutions to MSCP, this work does not focus on the strength and weakness of the algorithms. The proposed approach starts with an initial solution from Greedy approach and LP rounding and then the result is optimized using modified hill climbing technique. The

computational results shows the effectiveness of the proposed approach.

The rest of the paper is organized as follows: Section II describes the preliminary studies for proposed approach. Section III describes the proposed algorithm for MSCP. Section IV presents the experimental results. Section V provides the conclusion and future work.

II. BACKGROUND THEORY AND STUDY

This section briefly describes MSCP and presents some preliminary studies. This includes Greedy Algorithm, LP Rounding Algorithm, Hill Climbing Algorithm and OR Library of SCP instances.

A. Minimum Set Cover Problem

Given a set of n elements $U = [e_1, e_2, \dots, e_n]$ and a collection $S = \{S_1, S_2, \dots, S_m\}$ of m nonempty subsets of U where $\bigcup_{i=1}^m S_i = U$. Every S_i is associated with a positive cost $c(S_i) \geq 0$. The objective is to find a subset $X \subseteq S$ such that $\sum_{S_i \in X} c(S_i)$ is minimized with respect to $\bigcup_{S_i \in X} S_i = U$.

B. Minimum k -Set Cover Problem

An MSCP (U, S, c) is a k -set cover problem [13] if, for some constant k , it holds that $|S_i| \leq k, \forall S_i \in S$ represented as (U, S, c, k) . For an optimization problem, x^{OPT} presents an optimal solution of the problem where $OPT = f(x^{OPT})$. For a feasible solution x , the ratio $\frac{f(x)}{OPT}$ is regarded as its approximation ratio. If the approximation ratio of a feasible solution is upper-bounded by some value k , that is $1 \leq \frac{f(x)}{OPT} \leq k$, the solution is called an k -approximate solution.

C. Greedy Minimum Set Cover Algorithm

Data: Set system $(U, S), c : S \rightarrow Z^+$

Input: Element set $U = [e_1, e_2, \dots, e_n]$, subset set $S = \{S_1, S_2, \dots, S_m\}$ and cost function $c : S \rightarrow Z^+$

Output: Set cover X with minimum cost

Algorithm 1 Greedy MSCP

```

1: procedure GREEDY( $U, S, c$ ) ▷ Set system  $\{U, S\}$  and
   cost function,  $c(S)$ 
2:    $X \leftarrow \varnothing$ 
3:   while  $\sum_{i \in X} X_i \neq U$  do ▷ Continue until  $X = U$ 
4:     Calculate cost effectiveness,  $\alpha = \frac{c(S)}{|S-X|}$  for every
     unpicked set  $\{S_1, S_2, \dots, S_m\}$ 
5:     Pick a set  $S$ , with minimum cost effectiveness
6:      $X \leftarrow X \cup S$ 
7:   end while
8:   return  $X$  ▷ Output  $X$ , minimum number of subsets
9: end procedure
  
```

D. LP Rounding Algorithm

The LP formulation [15] of MSCP can be represented as

$$\begin{aligned}
 & \text{Minimize:} \\
 & \sum_{i=1}^m c_i \times X_i \\
 & \text{Subject To:} \\
 & \sum_{i:e \in S_i} X_i \geq 1 \quad \forall e \in U \\
 & X_i \leq 1 \quad \forall e \in \{1, 2, \dots, m\} \\
 & X_i \geq 0 \quad \forall e \in \{1, 2, \dots, m\}
 \end{aligned} \tag{1}$$

Algorithm 2 LP Rounding MSCP

```

1: procedure LPROUND( $U, S, c$ )
2:   Get an optimal solution  $x^*$  by solving the linear
   program for MSCP defined in Equation 1.
3:    $X \leftarrow \varnothing$ 
4:   for each  $S_j$  do ▷ Continue for all members of  $S$ 
5:     if  $x_j^* \geq \frac{1}{j}$  then
6:        $X \leftarrow X \cup S_j$ 
7:     end if
8:   end for
9:   return  $X$  ▷ The minimum number of sets
10: end procedure
  
```

E. Hill Climbing Algorithm

Hill climbing [16] is a mathematical optimization technique which belongs to the family of local search. It is an iterative algorithm that starts with an arbitrary solution to a problem, then attempts to find a better solution by incrementally changing a single element of the solution. If the change produces a better solution, an incremental change is made to the new solution, repeating until no further improvements can be found.

F. OR Library

OR-Library [17] is a collection of test data sets for a variety of Operations Research (OR) problems. OR-Library was originally described in [17]. There are currently 87 data files for SCP. The format is

Algorithm 3 Hill Climbing Algorithm

```

1: Pick a random point in the search space.
2: Consider all the neighbors of the current state.
3: Choose the neighbor with the best quality and move to
   that state.
4: Repeat 2 through 4 until all the neighboring states are of
   lower quality.
5: Return the current state as the solution state.
  
```

a) number of rows (m), number of columns (n)
b) the cost of each column $c(j), j = 1, 2, \dots, n$

For each row $i (i = 1, \dots, m)$: the number of columns which cover row i followed by a list of the columns which cover row i .

III. PROPOSED ALGORITHM

This work modified the conventional hill climbing algorithm for set cover problem. To avoid the local maxima problem, this work introduced random re-initialization. For comparisons, greedy algorithm and LP rounding algorithm are used to find the initial state for the modified hill climbing algorithm. The evaluation function for the modified hill climbing algorithm is described below.

A. Problem Formulation

- **Input:** $N = |U|$, $U = [e1, e2, \dots, en]$, $M = |S|$, $S = \{S1, S2, \dots, Sm\}$, $c = \{c1, c2, \dots, cm\}$
- **Output:**
 - 1) Minimum number of sets, $n(X) = |X|$.
 - 2) List of minimum number of Sets, $X = \{X_1, X_2, \dots, X_{n(X)}\}$.
- **Constraint:** Universality of X must hold, that is $\sum_{i \in X} X_i = U$.
- **Objective:**
 - 1) Minimize the number of sets, X .
 - 2) Minimize the total cost, $c(X)$.

B. OR Library MSCP Formulation

The formulation of MSCP for OR Library is given below.

- 1) Let $M^{m \times n}$ be a 0/1 matrix, $\forall a_{ij} \in M_{ij}, a_{ij} = 1$ if element i is covered by set j and $a_{ij} = 0$ otherwise.
- 2) Let $X = \{x_1, x_2, \dots, x_n\}$ where $x_i = 1$ if set i with cost $c_i \geq 0$ is part of the solution and $x_i = 0$ otherwise.

Minimize:

$$\sum_{i=1}^n x_i \times c(x_i)$$

Subject To:

$$\begin{aligned}
 1 & \leq \sum_{i=1}^n x_i \times a_{ij} \quad j \in \{1, 2, \dots, m\} \\
 x_i & \geq 0 \quad \forall x_i \in \{0, 1\}
 \end{aligned} \tag{2}$$

C. Proposed Algorithm

This section describes our proposed algorithm for MSCP. The algorithm finds an initial solution and then optimizes the result using modified hill climbing algorithm.

IV. EXPERIMENTAL RESULTS AND DISCUSSIONS

This section presents the computational results of the proposed approach. The effectiveness of the proposed approach is tested on 20 SCP test instances obtained from Beasley’s OR Library. These instances are divided into 11 sets as in Table I, in which Density is the percentage of nonzero entries in the SCP matrix. All of these test instances are publicly available via electronic mail from OR Library.

The approach presented in this paper is coded using C on an Intel laptop with speed of 2.13 GHz and 2GB of RAM under Windows 7 using the codeblock,version-13.12 compiler. Note here that this study presented here did not apply any kind of preprocessing on the instance sets received from OR-Library. This paper did not report the CPU times or running time of the algorithm as they vary machine to machine and compiler to compiler.

TABLE I: Test instance details

Problem Set	Number of instances	Number of rows(m)	Number of columns(n)	Range of cost	Density %
4	10	200	1000	1-100	2%
5	10	200	2000	1-100	2%
6	5	200	1000	1-100	5%
A	5	300	3000	1-100	2%
B	5	300	3000	1-100	5%
C	5	400	4000	1-100	2%
D	5	400	4000	1-100	5%
NRE	5	500	5000	1-100	10%
NRF	5	500	5000	1-100	20%
NRG	5	1000	10000	1-100	2%
NRH	5	1000	10000	1-100	5%

A. Experimental Results of Weighted SCP

Table II presents the experimental results for the proposed approach for weighted SCP instances. The first column represents the name of each instance. The optimal or best-known solution of each instance is given in the 2nd column. The 3rd and 4th column represent the solution found using greedy and LP rounding approach. The 5th and 6th column represent the solutions found in [5] and [7]. The last two columns contain the result found using proposed approach, started from greedy approach and LP rounding approach respectively.

B. Experimental Results of Unweighted SCP

Table III presents the experimental results of the proposed approach for unweighted SCP instances. This paper used the same 20 instances of weighted SCP and made them unweighted by replacing the weights to 1 on these instances. The first column represents the name of each instance. The optimal or best-known solution of each instance is given in the 2nd column. The 3rd and 4th column represent the solution found using greedy and LP rounding approach. The 5th and 6th column represent the solutions found in [18] and [19]. The last two columns contain the result found using proposed approach, started from greedy approach and LP rounding algorithm respectively.

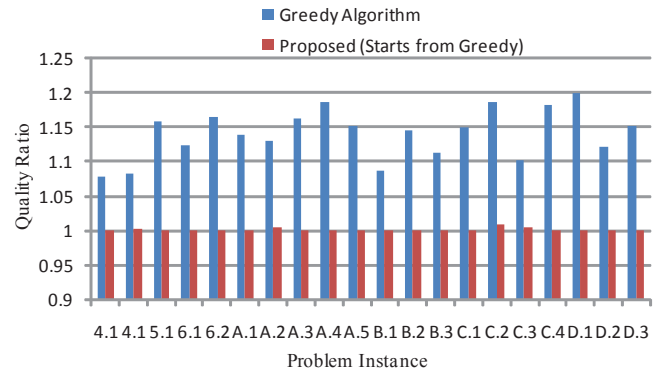


Fig. 1: Quality ratio of weighted problem instances for Greedy and Proposed Algorithm.

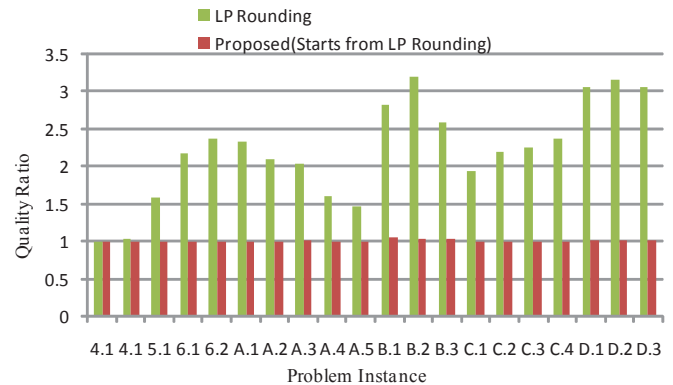


Fig. 2: Quality ratio of weighted problem instances for LP Rounding and Proposed Algorithm.

C. Result Summary

Summary: The optimal solution presented in Table II and Table III are taken from [7]. The quality of a solution derived by an algorithm is measured by *Quality Ratio* which is defined as a ratio of the *derived solution* to the *optimal solution*. The *quality ratio* for each instance for conventional greedy algorithm, LP rounding and Proposed algorithms, presented in this work are shown in Fig. 1, 2, 3 and 4. The figures show the ratio values, plotted as histogram for every instance, presented in this work.

$$Quality\ Measure\ Ratio = \frac{Derived\ Solution}{Optimal\ Solution} \quad (3)$$

Another popular quality measurement reported in literature is called *GAP* which is defined as the percentage of the *deviation of a solution* from the *optimal solution* or *best known solution*. The summarized results, in terms of average quality and average GAP, for weighted set covering instances are presented in Table IV. For unweighted set covering instances it is represented in Table V.

Algorithm 4 Proposed Algorithm

- 1: Preparation: In this step, elements of Universal set U , subsets of sets S and cost c of each set are taken as inputs.
- 2: Initial Solution: This step finds a solution X using *Greedy method* and *LP Rounding algorithm* of MSCP. X is considered the initial state for hill climbing optimization step. This study uses both the solutions and further optimizes for comparisons.
- 3: Hill Climbing Optimization: This Phase uses modified hill climbing algorithm and optimizes the cost of set cover problem.
- 4: Find the cost $c(X)$ from X . ▷ Initial best found cost, $c(X)$
- 5: Keep this (X) as the best found sets. ▷ Initial best found set, X
- 6: Calculate $R = n(S) \times n(U)$ ▷ number of elements, $n(U) = |U|$, number of subsets, $n(S) = |S|$
- 7: **for** M times of R **do** ▷ Here M is the *Set Minimization Repetition Factor*
- 8: Randomly select a set X^* from the selected sets. ▷ Random selection of a candidate redundant set
- 9: Mark this set X^* as *Unselected Set*.
- 10: **if** $X - X^* = U$ **then** ▷ Check whether the universality constraint holds
- 11: Stay with this state and find the cost, C_{new} .
- 12: Replace the best found cost C , with the current cost, C_{new} .
- 13: Remove set X^* from the selected sets, X .
- 14: Go back to step 8
- 15: **end if**
- 16: **for** K times **do** ▷ Here K is the Hill Climbing Repetition Factor
- 17: Randomly select a set Y from the unselected sets, $S - X$
- 18: Mark this set as *Selected*.
- 19: **if** $(X - X^*) \cup Y \neq U$ **then** ▷ Check whether the universality constraint holds
- 20: Go back to step 17
- 21: Find cost C_{new} of $c((X - X^*) \cup Y)$
- 22: **if** $C_{new} \leq C$ **then**
- 23: Replace the best found cost C , with the current cost, C_{new} .
- 24: Enlist Y in the *Selected Sets*.
- 25: Go back to step 17
- 26: **end if**
- 27: **end if**
- 28: **end for**
- 29: **end for**
- 30: Return best found list of sets X and minimum number of sets $n(X)$.

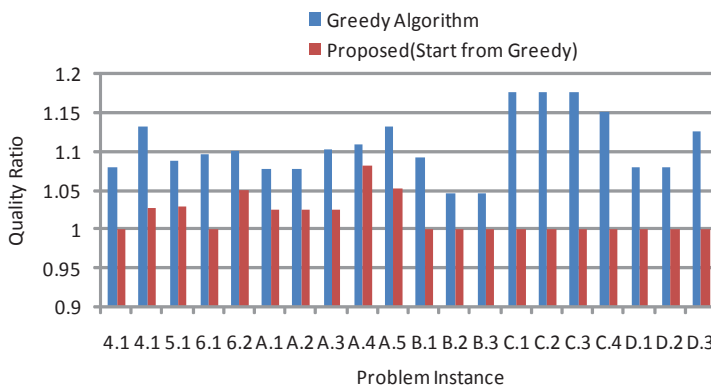


Fig. 3: Quality ratio of unweighted problem instances for Greedy and Proposed Algorithm.

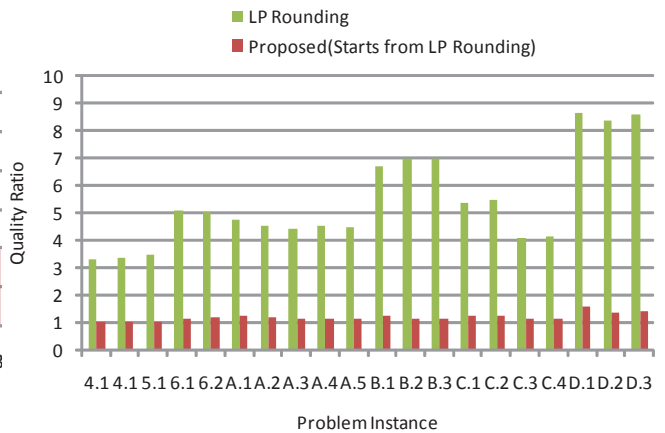


Fig. 4: Quality ratio of unweighted problem instances for LP Rounding and Proposed Algorithm.

$$GAP = \frac{\text{Derived Solution} - \text{Optimal Solution}}{\text{Optimal Solution}} \times 100\% \quad (4)$$

The proposed algorithm presented in this paper used conventional greedy algorithm and LP-Rounding Algorithm as initial solution. Then with the modified hill climbing method,

these results are further optimized. Table IV and Table V compare the proposed heuristic approach to the original greedy approach and LP Rounding algorithm.

In Table IV, the average quality ratio and average GAP of original greedy are 1.14 and 14.10 respectively for weighted SCP while for proposed approach they are 1.00 and 0.09.

TABLE II: Experimental Results for Weighted SCP

Instance number	Optimal Solution	Greedy Algorithm	LP Rounding	[5] (Meta-RaPS)	[7] (Descent Heuristic)	Proposed Algorithm	
						Start from Greedy	Start from LP Rounding %
4.1	429	463	429	429	433	429	429
4.10	514	556	539	514	519	515	514
5.1	253	293	405	253	265	253	255
6.1	138	155	301	138	149	138	138
6.2	146	170	347	146	156	146	147
A.1	253	288	592	253	258	253	255
A.2	252	285	531	252	262	253	253
A.3	232	270	473	232	243	232	235
A.4	234	278	375	234	240	234	234
A.5	236	272	349	236	240	236	236
B.1	69	75	196	69	72	69	73
B.2	76	87	243	76	79	76	79
B.3	80	89	207	80	84	80	84
C.1	227	261	442	227	237	227	229
C.2	219	260	484	219	230	221	221
C.3	243	268	551	243	249	244	245
C.4	219	259	523	219	229	219	221
D.1	60	72	184	60	64	60	61
D.2	66	74	209	66	68	66	68
D.3	72	83	221	72	77	72	74

TABLE III: Experimental Results for Unweighted SCP

Instance number	Optimal Solution	Greedy Algorithm	LP Rounding	[18] (Tabu Search)	[19] Local Search for SCP	Proposed Algorithm	
						Start from Greedy	Start from LP Rounding %
4.1	38	41	125	38	38	38	38
4.10	38	43	127	38	38	39	39
5.1	34	37	117	35	34	35	34
6.1	21	23	107	21	21	21	23
6.2	20	22	101	21	20	21	23
A.1	39	42	186	39	39	40	47
A.2	39	42	176	39	39	40	46
A.3	39	43	172	39	39	40	44
A.4	37	41	167	38	37	40	41
A.5	38	43	170	38	38	40	43
B.1	22	24	147	22	22	22	27
B.2	22	23	154	22	22	22	25
B.3	22	23	154	22	22	22	25
C.1	40	47	214	43	43	40	49
C.2	40	47	220	44	43	40	49
C.3	40	47	163	43	43	40	45
C.4	40	46	165	43	43	40	45
D.1	25	27	216	25	25	25	39
D.2	25	27	209	25	25	25	34
D.3	24	27	206	25	24	24	33

TABLE IV: Average quality ratio and GAP for the Weighted Set Covering Problem

Algorithm	Average Quality Ratio	Average GAP
Greedy Algorithm	1.14	14.10
Proposed (greedy initial solution)	1.00	0.09
LP Rounding	2.22	122.57
Proposed (LP initial solution)	1.01	1.48

TABLE V: Average quality ratio and GAP for the Unweighted Set Covering Problem

Algorithm	Average Quality Ratio	Average GAP
Greedy Algorithm	1.11	10.66
Proposed (greedy initial solution)	1.02	1.58
LP Rounding	5.41	441.06
Proposed (LP initial solution)	1.18	17.6

The average quality ratio and average GAP of LP rounding are 2.22 and 122.57 respectively for weighted SCP while for proposed approach they are 1.01 and 1.48. It is clearly visible that original greedy and LP Rounding are deviated from the

optimal solution by a high degree where proposed approach hardly deviates from the optimal solution.

In Table V, the average quality ratio and average GAP of original greedy are 1.11 and 10.66 respectively for unweighted SCP while for proposed approach they are 1.02 and 1.58. The average quality ratio and average GAP of LP rounding are 5.41 and 441.06 respectively for unweighted SCP while for proposed approach they are 1.18 and 17.6. It is clearly visible that original greedy and LP Rounding are highly deviated from the optimal solution where proposed approach hardly deviates from the optimal solution.

V. CONCLUSION AND FUTURE WORK

This paper studies the existing approaches of MSCP and proposes a new heuristic approach for solving it. Appropriate theorems and algorithms are presented to clarify the proposed approach. The experimental results are compared with the existing results available in literature which shows the effectiveness of the proposed approach. This approach is tested only on OR-Library in this work. In future this approach will be

tested on some other libraries of SCP like *Airline and bus scheduling problems* and *Railway scheduling problems*. The proposed algorithm can also be tested in another popular NP hard problem called *Vertex Cover Problem*.

ACKNOWLEDGEMENT

The author would like to express her greatest gratitude to the anonymous reviewers for their constructive feedback and critical suggestions that helped significantly to elicit the utmost technical attribute of this research work.

REFERENCES

- [1] G. Gens and E. Levner, "Complexity of approximation algorithms for combinatorial problems: a survey," ACM SIGACT News, vol. 12, no. 3, pp. 52-65, Fall 1980.
- [2] R. M. Karp, "Reducibility among combinatorial problems," Springer US, pp. 85-103, March 1972.
- [3] T. M. Chan, E. Grant, J. Knemann and M. Sharpe, "Weighted capacitated, priority, and geometric set cover via improved quasi-uniform sampling," Proceedings of the twenty-third annual ACM-SIAM symposium on Discrete Algorithms, pp. 1576-1585, SIAM, January 2012.
- [4] F. C. Gomes, C. N. Meneses, P. M. Pardalos and G. V. R. Viana, "Experimental analysis of approximation algorithms for the vertex cover and set covering problems," Computers and Operations Research, vol. 33, no. 12, pp. 3520-3534, December 2006.
- [5] G. Lan, G. W. DePuy and G. E. Whitehouse, "An effective and simple heuristic for the set covering problem," European Journal of Operational Research, vol. 176, no. 3, pp. 1387-1403, February 2007.
- [6] L. Ruan, H. Du, X. Jia, W. Wu, Y. Li and K.-I Ko "A greedy approximation for minimum connected dominating sets," Theoretical Computer Science, vol. 329, no. 1, pp. 325-330, December 2004.
- [7] N. Bilal, P. Galinier and F. Guibault, "A New Formulation of the Set Covering Problem for Metaheuristic Approaches," International Scholarly Research Notices, pp.1-10, April 2013.
- [8] Y. Emek and A. Rosen, "Semi-streaming set cover," Automata, Languages, and Programming, pp. 453-464, Springer Berlin Heidelberg, July 2014.
- [9] G. Lan, G. W. DePuy and G. E. Whitehouse, "An effective and simple heuristic for the set covering problem," European journal of operational research, vol. 176, no. 3, pp. 1387-1403, February 2007.
- [10] F. Grandoni, A. Gupta, S. Leonardi, P. Miettinen, P. Sankowski and M. Singh, "Set covering with our eyes closed," SIAM Journal on Computing, vol. 42, no. 3, pp. 808-830, May 2013.
- [11] A. Deshpande, L. Hellerstein and D. Kletenik, "Approximation algorithms for stochastic boolean function evaluation and stochastic submodular set cover," Proceedings of the Twenty-Fifth Annual ACM-SIAM Symposium on Discrete Algorithms, pp. 1453-1467, SIAM, January 2014.
- [12] F. A. Chudak, M. X. Goemans, D. S. Hochbaum and D. P. Williamson, "A primaldual interpretation of two 2-approximation algorithms for the feedback vertex set problem in undirected graphs," Operations Research Letters, vol. 22, no. 4, pp. 111-118, May 1998.
- [13] F. Colombo, R. Cordone and G. Lulli, "A variable neighborhood search algorithm for the multimode set covering problem," Journal of Global Optimization, pp. 1-20, August 2013.
- [14] V. Chvatal, "A greedy heuristic for the set-covering problem," Mathematics of operations research, vol. 4, no. 3, pp. 233-235, August 1979.
- [15] B. Saha and S. Khuller, "Set cover revisited: Hypergraph cover with hard capacities," Automata, Languages, and Programming, pp. 762-773, Springer Berlin Heidelberg, July 2012.
- [16] K. J. Lang, "Hill climbing beats genetic search on a boolean circuit synthesis problem of koza's," Proceedings of the Twelfth International Conference on Machine Learning, pp. 340-343, June 2014.
- [17] J. E. Beasley, "OR-library: distributing test problems by electronic mail," Journal of the Operational Research Society, vol. 41, no. 11, pp. 1069-1072, November 1990.
- [18] G. Kinney, J. W. Barnes and B. Colleti, "A group theoretic tabu search algorithm for set covering problems," Working paper, online available at <http://www.me.utexas.edu/barnes/research/>, 2004.
- [19] N. Musliu, "Local search algorithm for unicast set covering problem," Springer Berlin Heidelberg, pp. 302-311, June 2006.
- [20] B. Yelbay, S. I. Birbil and K. Bulbul, "The set covering problem revisited: an empirical study of the value of dual information," European Journal of Operational Research, September 2012.